Technische Universität München
Fakultät für Elektrotechnik und Informationstechnik
Fachgebiet Energiewandlungstechnik

Potential Analysis of Electrical Drive Trains According to Application Requirements

Jörg Johannes Kammermann

Vollständiger Abdruck der von der Fakultät für Elektrotechnik und Informationstechnik der Technischen Universität München zur Erlangung des akademischen Grades eines

Doktor-Ingenieurs (Dr.-Ing.)

genehmigten Dissertation.

Vorsitzender:		Prof. Dr.-Ing. Thomas Eibert
Prüfer der Dissertation:	1.	Prof. Dr.-Ing. Hans-Georg Herzog
	2.	Prof. Eric Semail, Ph.D.

Die Dissertation wurde am 17.09.2018 bei der Technischen Universität München eingereicht und durch die Fakultät für Elektrotechnik und Informationstechnik am 05.09.2019 angenommen.

Acknowledgments

Success consists of going from failure to failure without loss of enthusiasm.

Winston Churchill

This research work resulted from my activity at the Institute of Energy Conversion Technology at the Technical University of Munich (TUM) in Germany.

First of all and especially, I would like to thank Univ.-Prof. Dr.-Ing. Hans-Georg Herzog for supervising my thesis and for offering me the possibility to not only investigate on electrical drive trains, but also to support and teach students, to attend and manage several internal and external projects, and to experience interdisciplinary programs. It has been a challenging and often therefore an encouraging time, accompanied by technical, but also nontechnical or interdisciplinary discussions.

Furthermore, I would like to thank the second examiner Univ.-Prof. Eric Semail, from Arts et Métiers ParisTech, L2EP in Lille, France, for participating in the examination board and for the very constructive and helpful discussions prior to the submission.

Without the support and the cooperation within the team of research associates, this work in its present form would not have been possible. The working atmosphere was always comparable to a big family and therefore, I would like to thank all my current and former colleagues of the last years at the Institute. My special thanks goes to Dr.-Ing. Igor Bolvashenkov, for the very refreshing private and technically supporting conversations. Last but not least, I would like to thank Sabine Prucker, the secretary and the heart of the Institute, who has always been taking care of us.

Additionally, I would like to thank the students who contributed master's theses, bachelor's theses, or reports to this research work. Every single contribution is comparable to a mosaic completing the big picture. For test reading and their valuable comments on the first version of this work, I owe great appreciation to Dr.-Ing. Patrick Osswald, Dr.-Ing. Tom P. Giovanazzi, and Garth Dowie.

Finally, I would like to warmly thank my close family and also my friends, but especially my wife Anja for her patience and boundless support throughout the whole working period.

In conclusion, I am very thankful to be accompanied by the mentioned group of persons, whether in private or business context. Without these people, the implementation of this work would not have been possible.

Jörg Kammermann

Munich, September 2018

Abstract

The electrification of vehicles is progressing and is applied to different vehicles types. The main reasons for electrifying vehicles are well-known advantages, for instance the reduction of emissions and noise during operation, the increase of efficiency, and the increase of reliability. Additionally, taking into account the high requirements on electric propulsion components for safety-critical systems regarding reliability or the strict limitations on the installation space and weight of the system – especially for aircraft applications –, the correct choice of design features within the drive train is decisive. Obviously, this presents a certain complexity of parameters when trying to solve the task, due to interdependencies between different engineering domains.

This thesis targets a methodology for selecting components for an electric drive train at an early stage of a project, based on special application requirements. Here, the conventional helicopter model EC135 serves as application example, which defines the boundary conditions and requirements for the selection process. The hierarchical system approach, supported by regression analysis and multi-state reliability Markov models, is presented in order to assess the overall application system. The stepwise iteration of these methods enables evaluating appropriate components and their respective topologies.

The solution space within this research work and hence the basis for comparison is characterized by the permanent synchronous machine and the induction machine. The machine is supplied by power electronics, where a six-pulse-bridge inverter and an H-bridge inverter are opposed to each other. The interface between the two drive train components is specified by the number of phases (here: from three to eleven), which is one of the important parameters being in focus for the assessment. The energy storage and auxiliary components are excluded from the assessment. This comparison results in the conclusion that the nine-phase permanent magnet synchronous machine is recommended, whereas the two conventional inverter topologies are not applicable – especially referring to the requirements on fault tolerance and reliability –, since the obtained reliability values result in exceeding 10^{-9} failures per hour.

Therefore, alternative drive train concepts are presented, which finally are auspicious for a realistic application to the helicopter. On the one hand, multilevel inverter topologies are compared based on Markov models. The cascaded H-bridge inverter supplying nine galvanically separated phases within the permanent magnet synchronous machine turns out to comply with the reliability constraints; the obtained reliability value is 10^{-12} failures per hour. On the other hand, a drive train, based on hydrogen and a fuel cell as energy source, is evaluated by means of power and energy densities taking the EC135 as platform. Hence, the available installation space enables an application of the hydrogen-based drive train. In contrary, the weight reserves are tight; nevertheless, this kind of drive train is realizable assuming current technology.

Kurzfassung

Die Elektrifizierung von Fahrzeugen schreitet voran und wird auf immer mehr unterschiedliche Fahrzeugvarianten ausgeweitet. Die Hauptgründe für die Elektrifizierung der Fahrzeuge basieren auf den bekannten Vorteilen, wie beispielsweise die Reduzierung der Emissions- und Lärmbelastung im Betrieb, die Steigerung des Wirkungsgrads und die Erhöhung der Zuverlässigkeit. Um den hohen Anforderungen sicherheitskritischer Systeme – vor allem in der Luftfahrt – gerecht zu werden, ist die korrekte Wahl der Entwurfskriterien im Antriebsstrang entscheidend. Speziell die Anforderungen hinsichtlich Zuverlässigkeit, Gewicht und Bauraum des Systems sind als kritisch einzustufen. Aufgrund der Wechselwirkungen zwischen verschiedenen Ingenieursdisziplinen bringt diese Aufgabe eine gewisse Komplexität der Parameter mit sich.

Die vorliegende Arbeit zielt darauf ab, gerade in der Anfangsphase eines Projekts, eine Methodik zur Auswahl von Komponenten für einen elektrischen Antriebsstrang zu entwickeln. Hierzu wird das konventionelle Helikoptermodell EC135 als Anwendungsplattform herangezogen, was die Randbedingungen und Anforderungen für die Komponentenauswahl festlegt. Ein hierarchischer Systemansatz, eine Regressionsanalyse und Multi-State-Markov-Reliability-Modelle werden vorgestellt und verwendet, um das Gesamtsystem zu analysieren. Die schrittweise Iteration dieser Methoden ermöglicht es, passende Komponenten und entsprechende Topologien zu bewerten.

Der Lösungsraum dieser Arbeit beinhaltet sowohl die permanenterregte Synchronmaschine als auch die Asynchronmaschine. Die Maschine wird von einer Leistungselektronik versorgt, wofür anfangs Halb- und Vollbrücken-Umrichtertopologien gegenübergestellt werden. Die Schnittstelle der beiden Antriebsstrangkomponenten wird durch die Anzahl der Stränge (hier: drei bis elf) charakterisiert. Die Strangzahl stellt somit eine essenzielle Größe des Vergleichs dar. Der Energiespeicher und zusätzliche Komponenten werden vernachlässigt. Die Analyse resultiert in der Empfehlung einer neunsträngigen permanenterregten Synchronmaschine, wohingegen sich die Umrichtertopologien bezogen auf die Zuverlässigkeitsanforderungen als nicht anwendbar erweisen, da die berechneten Zuverlässigkeitswerte den geforderten Wert von 10^{-9} Ausfällen pro Stunde überschreiten.

Daher werden alternative Antriebsstrangkonzepte vorgestellt, die letztendlich vielversprechend für eine realistische Anwendung im Helikopter sind. Auf der einen Seite werden Multilevel-Umrichtertopologien durch Markov-Modelle miteinander verglichen. Der kaskadierte H-Brücken-Umrichter, der die neun galvanisch getrennten Maschinenstränge versorgt, erfüllt die Anforderungen hinsichtlich der Zuverlässigkeit. Es werden 10^{-12} Ausfälle pro Stunde unterschritten. Auf der anderen Seite wird ein Antriebskonzept für den EC135 basierend auf Wasserstoff und Brennstoffzellen mit Hilfe von Leistungs- und Energiedichten untersucht. Dabei zeigt sich, dass die Implementierung dieses Konzepts bezüglich des verfügbaren Bauraums möglich ist, im Gegensatz dazu aber die Gewichtsreserven eher knapp bemessen sind.

Résumé

L'électrification des véhicules progresse et s'adapte de plus en plus à plusieurs types de véhicule. Les raisons principales de l'électrification des véhicules se justifient par des avantages notoirement connus : par exemple la réduction des émissions et du bruit pendant l'opération, l'augmentation de l'efficacité et l'amélioration de la fiabilité. En outre, le choix correct des critères de conception est décisif pour être à la hauteur des exigences du projet. Notamment dans l'aéronautique, les exigences concernant la fiabilité, le poids et l'espace d'installation sont classés comme critiques. En raison des interdépendances entre les différents domaines de l'ingénierie, une certaine complexité de paramètres apparaît en traitant la tâche.

La présente thèse a pour objet de développer une méthodologie afin de pouvoir déterminer une sélection de composants pour une chaîne cinématique électrique pendant la première phase d'un projet. A cette occasion, l'hélicoptère conventionnel EC135 a été choisi comme plateforme, qui définit les conditions limites et les exigences pour le processus de sélection. Une approche systémique hiérarchique, une analyse de régression et un modèle de Markov avec plusieurs états sont présentés pour analyser le système complet. L'itération progressive des méthodes permet d'évaluer les composants adéquats et les topologies correspondantes.

L'espace de solution de cette recherche contient la machine synchrone à aimants permanents et la machine asynchrone. La machine est fournie par l'électronique de puissance, dont des topologies d'onduleur sur la base de demi-ponts et de ponts complets. L'interface entre les deux composants de la chaîne cinématique électrique est caractérisée par le nombre de phases (ici : trois à onze), qui est un des paramètres les plus importants dans l'analyse. Les réserves énergétiques et les composants supplémentaires ont été exclus de l'évaluation. Les résultats de la comparaison mènent à la recommandation d'utiliser la machine synchrone à aimants permanents à neuf phases, tandis que les topologies d'onduleur s'avèrent inapplicables en ce qui concernent les exigences de fiabilité. Les valeurs de fiabilité excèdent la valeur exigée de 10^{-9} défaillances par heure.

En conséquence, des concepts alternatifs pour la chaîne cinématique électrique sont présentés, ceux-ci étant prometteurs en ce qui concerne l'application réaliste dans l'hélicoptère. D'un côté, les topologies d'onduleur multiniveaux sont comparées grâce aux modèles de Markov. L'onduleur cascadé à ponts en H, qui alimente neuf phases (étant séparées galvaniquement), satisfait les exigences concernant la fiabilité. Cette chaîne cinématique électrique atteint 10^{-12} défaillances par heure. De l'autre côté, un concept d'entraînement sur la base d'hydrogène et les piles à combustible est examiné pour le EC135 en prenant appui sur les densités de puissance et les densités énergétiques. Finalement, les résultats indiquent que la réalisation du concept est faisable quant à l'espace d'installation disponible, mais par contraste les réserves de poids sont comptées concisément.

Contents

List of Figures III

List of Tables V

Nomenclature VII

1 Introduction 1
- 1.1 Application-Based Overview about Vehicle Electrification . . . 2
  - 1.1.1 Road Traffic . . . 3
  - 1.1.2 Ship Traffic . . . 4
  - 1.1.3 Rail Traffic . . . 4
  - 1.1.4 Air Traffic . . . 5
- 1.2 Motivation for an Electrical Drive Train Analysis . . . 6
  - 1.2.1 General Problem Description by Means of the V-Model . . . 6
  - 1.2.2 System Definition and the State of the Art of System Design . . . 8
  - 1.2.3 Demarcation . . . 9
- 1.3 Targets and Work Structure . . . 10

2 Methodology for Potential Analysis of Electrical Drive Trains 11
- 2.1 Dependency of the Design on Targets and Parameters . . . 11
  - 2.1.1 Requirement Distinction between Applications . . . 11
  - 2.1.2 Evaluation of a Complex System . . . 15
- 2.2 Hierarchical System Approach . . . 18
  - 2.2.1 System Level . . . 19
  - 2.2.2 Subsystem Level . . . 19
  - 2.2.3 Unit Level . . . 19
  - 2.2.4 Element Level . . . 19
- 2.3 Torque-Speed Characteristics . . . 20
  - 2.3.1 Limit Cases . . . 20
  - 2.3.2 Overload Conditions Caused by Rare Operating Points . . . 22
  - 2.3.3 Overload Conditions Caused by Failures . . . 22
- 2.4 Weighting Factors for System Parameters . . . 22
- 2.5 Regression Analysis . . . 23
  - 2.5.1 Basics on Regression Analysis . . . 23
  - 2.5.2 Volume and Weight . . . 24
- 2.6 Reliability and the Related Terminologies . . . 26
- 2.7 Markov Chains . . . 28
  - 2.7.1 Basics on Continuous-Time Markov Chains . . . 28
  - 2.7.2 Results of Differential Equations . . . 31
  - 2.7.3 Implementation of Automatic Calculation . . . 32
  - 2.7.4 Multi-State System Markov Models for Reliability Assessment . . . 32

2.8 Conclusion for the Potential Analysis . . . 36

3 Solution Space of Drive Train Components 39
3.1 Electrical Machines and Their Characteristics . . . 39
3.1.1 Different Machine Types . . . 39
3.1.2 Failure Cases . . . 41
3.2 Power Electronics and Their Characteristics . . . 42
3.2.1 Converter Design . . . 43
3.2.2 Failure Cases . . . 44
3.3 Solution Space: Electrical Drive Train . . . 46
3.3.1 Number of Phases as Degree of Freedom . . . 46
3.3.2 Failure Cases . . . 47

4 Application of the Potential Analysis to an Electrical Helicopter 49
4.1 Key Parameters of the Electrical Helicopter . . . 50
4.1.1 Volume and Weight . . . 50
4.1.2 Reliability and Fault Tolerance . . . 51
4.1.3 Flight Scenario . . . 51
4.2 Selection of Components in Electrical Drive Trains . . . 52
4.2.1 Potential Analysis of Electrical Machine Types . . . 52
4.2.2 Potential Analysis of Converter Topologies . . . 57
4.2.3 Interdependency of Components . . . 58
4.3 System Evaluation by Means of Multi-State Reliability Markov Models . . . 60
4.3.1 Markov Modeling for the Electrical Machine . . . 61
4.3.2 Markov Modeling for the Drive Train System . . . 63

5 Alternative Drive Train Concepts 69
5.1 Increasing Fault Tolerance by Different Topologies . . . 69
5.1.1 Multilevel Inverter . . . 69
5.1.2 Different Topologies with Multilevel Cascaded H-Bridge Inverter . . . 70
5.1.3 Assessment of Reliability and Fault Tolerance . . . 71
5.2 Hydrogen-Based Drive Train System . . . 76
5.2.1 Fuel Cell . . . 76
5.2.2 Converter . . . 77
5.2.3 Superconducting Electrical Machine . . . 78
5.2.4 Hydrogen Tank . . . 79
5.2.5 Feasibility Assessment for a Fuel Cell Drive Train . . . 81

6 Conclusion 89
6.1 Achieved Targets . . . 89
6.2 Reflection of Critical Aspects and Outlook . . . 90

Bibliography i
Reference List . . . xiv
Own Publications . . . xv
Supervised Student Projects . . . xviii

List of Figures

1.1 Examples for electric road vehicles . . . 3
1.2 Examples for pure electric ship propulsion systems . . . 4
1.3 Examples for electric aircraft . . . 5
1.4 V-model for the system design . . . 7
1.5 Abstract drive train system definition . . . 8

2.1 Differentiation of system requirements . . . 13
2.2 Different possibilities of redundancy . . . 15
2.3 Description of complex systems and influencing factors . . . 17
2.4 Hierarchical system approach applied to electrified vehicles . . . 18
2.5 Physical limits of torque versus speed characteristic . . . 20
2.6 Regression mass characteristics for different machine types . . . 25
2.7 Residuals for the regression equation of the induction machine . . . 25
2.8 General Markov chain with n states and their transitions . . . 29
2.9 Flowchart of automatic Markov model calculation . . . 33
2.10 An exemplary multi-state Markov birth-death model with n states . . . 34
2.11 Theoretical graphical interpretation of the degree of fault tolerance . . . 35
2.12 Bathtub curve and exponential failure probability function . . . 36
2.13 Methodology for the potential analysis . . . 37

3.1 Schematic illustration of the considered machine types . . . 41
3.2 Qualitative fault tree of electrical machines . . . 42
3.3 Different types of power converters . . . 43
3.4 General half- and full-bridge converter structures . . . 44
3.5 Statistics on failures of power electronic components and their causes . . . 45
3.6 System consideration defined by the number and the loss of phases . . . 47

4.1 Provided installation space within the platform being the helicopter EC135 . . . 49
4.2 Comparison of electrical machines regarding efficiency over power density . . . 54
4.3 Regression mass for the nominal power and nominal rotational speed . . . 54
4.4 Statistical failure distribution for electrical machines . . . 56
4.5 Failure simulation for six-pulse-bridge and H-bridge converter topology . . . 57
4.6 Reliability reduction due to an increase of the machine's number of phases . . . 59
4.7 Markov models for machines with a different number of phases . . . 62
4.8 Development of the electrical machines' failure probabilities over time . . . 62
4.9 Markov model for the overall drive train system . . . 65
4.10 Reliability and failure probability functions . . . 66
4.11 Results from the overall drive train Markov model . . . 67

5.1 17-level CHB inverter structure for one phase . . . 71
5.2 Different connection topologies using CHB inverters . . . 72

5.3 Markov model for one phase of the CHB inverter topologies 73
5.4 Markov models for drive train with CHB inverter for two topologies 74
5.5 Results from the overall drive train Markov model using CHB 75
5.6 Conceptual illustration of the components of a fuel-cell-based drive train . . . 76
5.7 Comparison of surface ratio to radius ratio between spherical and cylinder . . 80
5.8 Sankey diagram for the fuel cell system 81
5.9 Power chain for the fuel-cell-based drive train 82
5.10 Total system mass for a range of the fuel cell efficiency from 0.45 to 0.65 . . . 84
5.11 Total system volume for a range of the fuel cell efficiency from 0.45 to 0.65 . . 84
5.12 Power response of the different energy supply devices 86
5.13 Total system mass (a) and volume (b) including ultracapacitors 88

List of Tables

1.1 Distribution of electric vehicles by country 2

2.1 Electrical machine types used for electric cars summarized by manufacturer . 12
2.2 Requirements for electric vehicles 14
2.3 Qualitative weighting factors for different vehicle types 23
2.4 Transition matrix influenced by transition types and loop types 31

3.1 Number of components for different topologies of power electronics 45

4.1 Key parameter of the EC135 and the requirements 50
4.2 Quantitative weighting factors for the comparative analysis 53
4.3 Comparison of electrical machines for aircraft applications 56
4.4 General assessment of remaining power in failure case 60
4.5 Failure probabilities of the electrical machine 62
4.6 Reliability values for the system components 63
4.7 Failure probabilities of the overall drive train 67

5.1 Number of components and FIT values for the CHB topology 73
5.2 Failure probabilities of the drive train using multilevel inverter 75
5.3 Gravimetric and volumetric power densities for two fuel cell types 77
5.4 Gravimetric and volumetric power densities for the power electronics 78
5.5 Gravimetric and volumetric power densities for HTS machine and gearbox . . 79
5.6 Gravimetric and volumetric energy densities for two tank geometries 81
5.7 Resulting weight and volume for a one-hour flight scenario 83
5.8 Additional weight and volume for different ultracapacitor types 87

Nomenclature

The nomenclature is divided into acronyms, Greek letters, and Roman letters. Within the acronyms, the lower case entries are used as indices throughout the thesis. All *italic* entries, as well as Greek letters, represent variables.

Acronyms

AC	Alternating current
ADAC	German automobile club (Allgemeiner Deutscher Automobil-Club e.V.)
AEA	All electric aircraft
batt	Battery
cap	Capacitor
CHB	Cascaded H-bridge
CTMC	Continuous-time Markov chain
CTOL	Conventional take-off and landing
DOFT	Degree of fault tolerance
DC	Direct current
di	Diode
DTMC	Discrete-time Markov chain
EC135/H135	Helicopter model from Airbus Helicopters (formerly Eurocopter)
EM	Electrical machine
EV	Electric vehicle
FC	Fuel cell
FIT	Failure in time
FMEA	Failure mode and effects analysis
FTA	Fault tree analysis
HTS	High temperature superconducting
IM	Induction machine (asynchronous machine)
MEA	More electric aircraft
MTBF	Mean time between failure
MTOW	Maximum take-off weight
MTTF	Mean time to failure
MTTR	Mean time to repair

MSS-MM	Multi-state system Markov model
oc	Open-circuit
pcb	Printed circuit board
PE	Power electronics
PSM	Permanent magnet synchronous machine
SAR	Search and rescue (flight mission)
semi	Semiconductor
sc	Short-circuit
SOR	Sum of row
TCI	Theme-Centered Interaction
UC	Ultracapacitor
VTOL	Vertical take-off and landing

Greek Letters

Δt	Step width
κ	Auxiliary variable
λ	Failure rate
λ_{ij}	Transition probability from state i to j
τ	Tangential stress
ω	Angular velocity

Roman Letters

A	Surface
a	Fitting factor
A_{sys}	System availability
A_{cyl}	Surface of a cylinder
A_{sph}	Surface of a spherical
c_{err}	Variable for error correction
D_δ	Bore diameter
$f(x;a)$	Function depending on x and a
F_{tot}	Total force acting on the rotor surface
h_{cyl}	Height of a cylinder
i	Control variable
$\boldsymbol{I}$	Identity matrix
i_{g}	gear transmission ratio
j	Control variable
k	Control variable
K_{w}	Weighting factor
l_{i}	Ideal length of the machine

m	Number of phases
$\boldsymbol{M}$	Transition intensity matrix
m_r	Mass obtained by regression
m_EM	Mass of electrical machine
n	Rotational Speed
n_m	Mechanical speed
n_n	Nominal speed
P	Power
p	Number of pole pairs
$\boldsymbol{P}_\lambda$	Transition probability matrix
$P(t)$	Failure probability function dependent on the time t
$P_\mathrm{EM,loss}$	Power losses of the electrical machine
$P_\mathrm{FC,loss}$	Power losses of the fuel cell
P_m	Mechanical power
P_n	Nominal power
$P_\mathrm{PE,loss}$	Power losses of the power electronics
P_PSM	Failure probability of the permanent magnet synchronous machine
$R(t)$	Reliability function dependent on the time t
r_cyl	Radius of a cylinder
r_sph	Radius of a spherical
S_i	Switch number i
T	Torque
t	Time
T_max	Maximum torque
T_n	Nominal torque
V	Volume
V_cyl	Volume of a cylinder
V_DC	DC supply voltage
V_rotor	Rotor volume
V_sph	Volume of a spherical
$\vec{y}_0$	Initial vector

1 Introduction

Within the last decade, due to political orientations in different countries and new technological developments, electric vehicles have become more and more attractive for research institutes, industries, and ultimately for society. Nowadays, it is a continuity issue, which is discussed back and forth in the media, not least because of companies, such as "Tesla, Inc." or many others. This is also the reason why the electrification of cars is of high interest. Moreover, feasibility is increasingly demonstrated, such as the consideration of range and charging time – two of society's main refutations. However, the price of electric cars does not meet society's requirements. Additionally, the charging infrastructure and the contradiction between power and range are yet thought to be a big challenge.

Therefore, different countries offer financial incentives regarding purchase and maintenance of electric vehicles (EV). Thus, political initiatives and benefits for "e-drivers" are strongly being discussed in order to increase the number of electric vehicle sales. The companies themselves are trying to change the customer's attitude towards electrification of daily transportation, by means of free charging, additional services, or guaranties. Just to mention a few incentives, some countries, such as Norway or China, pay one-time benefits for the purchase of an EV for private, but also commercial use. For instance, the USA and Germany, grant tax reductions or exemptions partially depending on battery size or CO_2 emissions. Cities, such as Barcelona (Spain) or Paris (France), introduced reduced toll and parking fees or even provide free parking or charging. In China, the purchase of a license plate for cars in general costs around 8,000 euros, whereas for EVs it is free of charge and the waiting time gets reduced.

Taking in international discussion and contracts, the following numbers can help to visualize a future trend perspective. Table 1.1 displays the distribution of electric vehicles per country at the beginning of 2016 compared to the desired number of electric vehicles in 2020 based on statistical surveys [97, 166]. Up until the beginning of 2016, around 1.3 million electric cars were counted in use worldwide, 550,000 more than 2014 [166]. The accomplished amount shows a certain difficulty in reaching the desired number of electric vehicles for every listed country until 2020, even though the growth rate for most of the countries is approximately 70 % on the previous year. Nevertheless, it also accentuates the high demand for electric drive trains in cars.

However, cars are not the only type of electric vehicles, even though these are most commonly talked about in the media and society. In other disciplines – such as electric aircraft, ships, or trains – hybrid or pure electric traction drives are already in use for many years. Nowadays, different projects, such as "Clean Sky", "Clean Sky 2", "ZeroCat", or others, have signed up to the European Union's emission reduction plans, set up in the "Europe 2020 Strategy" from 2010 and in 2011's "Energy Efficiency Plan". The project "Horizon 2020" further shows the European interest in leading technologies to achieve the reduction plans and to save the intercontinental competitiveness.

Table 1.1: Distribution of electric vehicles by country of use at the beginning of 2016 opposed to the desired number of electric vehicles in 2020 based on [97, 166].

country	status of 2016	politically desired in 2020	accomplished
USA	409,820	3,000,000	13.7 %
China	306,650	11,900,000	2.6 %
Japan	129,730	2,000,000	6.5 %
France	76,070	2,000,000	3.8 %
Germany	55,250	1,000,000	5.5 %
Canada	16,990	1,400,000	1.2 %

However, building electric vehicles is not a new idea. The first section provides an overview about the history of vehicle electrification tracing back to the year 1838/39 [18, 37, 116]. Then, the motivation for an electrical drive train analysis will be explained, followed by the state of the art regarding electrical drive trains. Finally, the targets and the structure of this work will be presented.

1.1 Application-Based Overview about Vehicle Electrification

The first documented electric vehicle was a boat for 12 passengers constructed by B. S. Jacobi in 1838 which had paddle wheels to navigate the Neva river in Saint Petersburg [18, 116]. Already in 1879, Werner Siemens introduced the first functioning electric train which was followed by an electric tram only two years later [127]. Gustav Trouvé built the first ready-to-use electric road vehicle in 1881, which was followed by another small electrically driven boat in 1882 and a battery powered balloon in 1883 [37, 56, 131, 153]. These applications were the first documented applications being electrified. Since then, years have passed by and driven by new technological evolutions few electrified vehicles have been developed further or newly invented. More detailed technical information and illustrations are to be found in [127, 153], where Ernest H. Wakefield describes the "History of the Electric Automobile". For whatever reason, either political, social, or technical, – several arguments exist for each aspect – it has taken more than a century to bring electrification to reality, as well as to global society, and it will be a continuously ongoing process during the next decades or even longer.

Today many electrical drive trains have already been applied to all kind of vehicles, among them cars, trains, scooters, ships, aircraft, and utility vehicles [115], or new electrical transportation systems have been invented. Therefore, the next subsections show different fields of application considering electric propulsion systems, which means road, ship, rail, and air traffic. They provide a brief overview about a few examples of already completed and planned projects within vehicle electrification. It details the evolution of the electrification of vehicles during the last decade and scrutinizes the future promising developments.

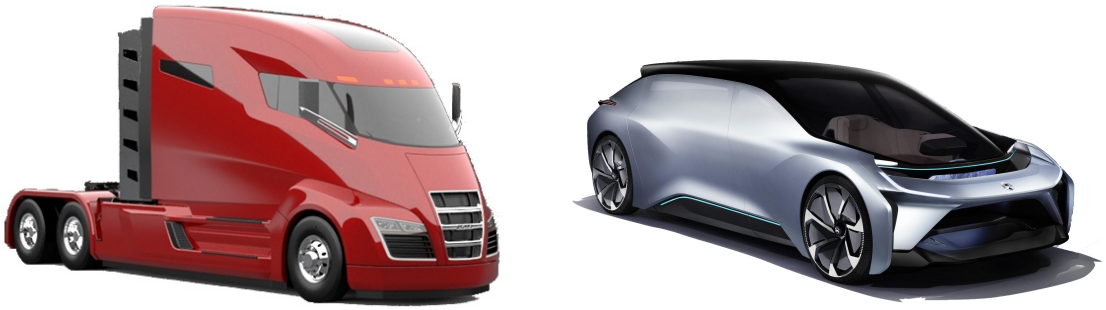

(a) (b)

Figure 1.1: Examples for electric road vehicles. In (a) the truck "Nikola One" [109] is shown, whereas (b) illustrates the "NIO EVE" [110], one of the passenger car concepts.

1.1.1 Road Traffic

One of the most commonly known fields of electrification is road traffic. Within the last several years, media reported about full or hybrid electrical road vehicles, such as cars, scooters, trucks, buses, or utility vehicles. Due to the climate discussion, every car manufacturer is trying to push onto the market with an electric car version. A varied range between small city cruisers and high performance sports cars are already present on streets all over the world. Vehicle fleets are an especially good platform for electrification, which is for instance demonstrated by "La Poste" in France, having today one of the largest electric fleet in the world.

Realized projects out of the last years show the increasing technical progression within the electrification of all kind of vehicles. As example of such projects concerning utility vehicles, the hybridization of a dump truck of approximately 500 tons from 2013, which is driven by a drive train consisting of numerous electrical machines [134]. As well as electric tractors which have already been developed and constructed [115]. Already several years ago, electric scooters have been very popular in Asian megacities and their popularity is skyrocketing in the rest of the world. Furthermore, this trend does not spare cargo transportation. The "Nikola One" in Figure 1.1a is set up as a purely electrically driven truck supplied by lithium-ion battery pack of 320 kWh and a 300 kW fuel cell [109].

The commonly mostly known application is the electrical passenger car, since it is publicly discussed in the media. Beside the popular car manufacturers, a lot of new companies and start-ups try to establish an electric car with higher practicability, higher range, or higher performance. Autonomous drive is one of the currently discussed topics, especially considering legal issues. The "NIO EVE" is only one concept for future electric road vehicles [110] and is here mentioned as a representative for all other companies heading towards autonomous electric vehicles. An illustration of this autonomous car is provided in Figure 1.1b. In some cities, such as Monaco – to mention only one example –, first autonomous test buses are running around the city centers. Hence, the electrification of road vehicles compared to other vehicle types is already broadly developed and the future trend is leading to an increasing proportion of electric vehicles worldwide on the streets.

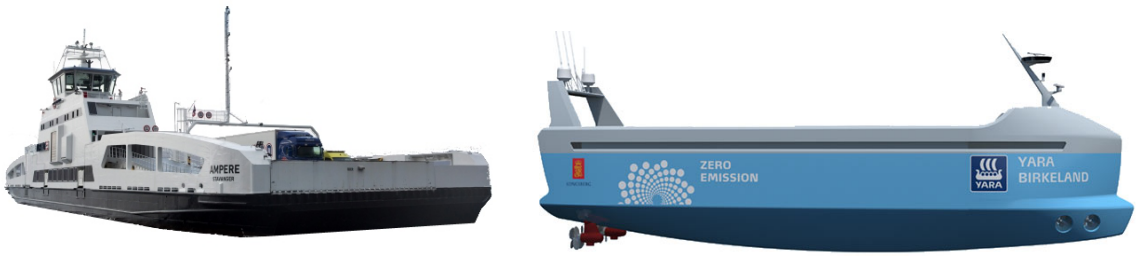

(a) (b)

Figure 1.2: Examples for pure electric ship propulsion systems. The already operating electric ferry "Ampere" is displayed in (a) [135] and the container ship concept "YARA Birkeland" in (b) [76].

1.1.2 Ship Traffic

Considering water traffic, ships were the first electrified vehicles and have been electrified for almost two centuries, as mentioned earlier. Submarines have also been equipped with electrical drive trains for approximately the last century. Nowadays, not only the smaller passenger boats, but huge ships, such as ferries, icebreakers, container ships, and others have been or are becoming more and more (partially or fully) electrified. The first electric ferry "ZeroCat 120", also called "Ampere", carrying persons and vehicles across the Sognefjord in Norway started its operation in 2015 [135]. Figure 1.2a shows the "Ampere". Adding to this, the propulsion system of icebreakers, namely for instance the Finnish "Polaris", is also electrical. The needed energy is produced by diesel and gas power plants. Furthermore, an example for a container ship is the autonomous pure electric "YARA Birkeland", which will be produced in Norway. The first delivery is planned for 2018, whereas the autonomous application is planned for 2020 [76]. A conceptual illustration can be seen in Figure 1.2b. This shows that also water traffic is progressing with electrification of their drive systems in attempt to increase efficiency and decrease pollution. Going back to land, rail traffic is another example where electrification takes place.

1.1.3 Rail Traffic

Rail is also one of most commonly known electrically driven vehicle types. Although in many countries a high proportion of the railway network is supplied by diesel locomotives, the grids are more and more electrified. Usually, the trains are then mains-operated via overhead lines and therefore do not need any energy storage; hence, it is not a real mobile application. However, for rural areas, which are not that frequently supplied, the construction of an overhead lines network can be too expensive. In such cases, battery driven trains do already exist, such as the "Electrostar" [20], which enables the electric propulsion for these areas, even though the overhead lines are not installed. These trains could enable a broader electrification without facing cost intensive overhead line constructions. More information also about the history of electrification can be again found in literature, as mentioned earlier. Taking off the ground leads to an increasing electrification trend of air traffic.

(a) (b)

Figure 1.3: Examples for electric aircraft. New air taxiing concepts are presented, namely the "Airbus Pop.Up" in (a) [1] and the "Lilium Jet" in (b) [87].

1.1.4 Air Traffic

The CO_2 discussions of the last years also influence the aircraft industry. The projects are dealing with or have already implemented More Electric Aircraft (MEA), which included more and more electrical systems or various auxiliary actuators into the aircraft in order to improve, for instance, reliability or efficiency of the systems. The Airbus A380, A350, or the Boeing 787 ("Dreamliner") are just a few commonly known examples for MEA. The current movement and investigations, which already started years ago, lead towards All Electric Aircraft (AEA) which also includes the propulsion system to be electric. The first AEA have been realized within the last years, only to mention some conventional take-off and landing (CTOL) jets, such as the "Pipistrel Alpha Electro" or the "Extra 330 LE" which are both supplied by batteries, but also the "Hy4" which gets the energy from fuel cells for the cruise flight and from a battery for the take-off and landing. The basic disadvantage of such aircraft is that for take-off and landing runways are required. Therefore, different concepts are dealing with vertical take-off and landing (VTOL), as known from helicopters. The "Volocopter", the "Ehang 184", or the "Pop.Up" are examples for this type of aircraft. The "Pop.Up" concept combines a road vehicle with an aircraft, having separated ground and air modules, and can be seen in Figure 1.3a [1]. Other concepts try to team the advantages of a VTOL aircraft with the efficiency benefit of conventional airplanes during cruise flight. The "Lilium Jet", which can be seen in Figure 1.3b, realized a first unmanned prototype in 2017 and by 2025, the first air taxi is said to be in operation [87]. The "Ehang 184", "Pop.Up", and "Lilium Jet" are planned to establish air taxiing within an economically affordable extent.

Taking into account the variety of the today's differing application cases, it becomes obvious that there is a need for electrical drive trains dependent on a huge variety of requirements. Therefore, new system approaches are required in order to investigate optimal drive train topologies considering a wide range of requirements and possibilities. This widely spread application range also leads to broader power and torque ranges, which need to be provided by the drive train. Hence, the next section covers the system design of electrical drive trains, defines and explains the fundamental problem, and imbeds it into a system design process. The last paragraph demarcates the topic based on actual and fundamental publications.

1.2 Motivation for an Electrical Drive Train Analysis

Technical and political developments along with new technologies or materials in the area of electric power engineering empower research regarding electrification of drive train systems. The main reasons for electrification are the well-known advantages; the reduction of emissions and noise, the increase of efficiency, and the increase of reliability are just some examples among others. The automotive industry is one of the most common fields where drive train electrification has been executed and this is one such example for the constant need of electrical drive trains for specific applications, such as aforementioned in section 1.1.

Therefore, this constant demand of electrical drive trains asks for the appropriate selection of drive train components and an optimal system with respect to application requirements. However, having optimal components does not necessarily mean to have the optimal system and an electric drive train has to be considered as one such system. Thus, it is necessary to examine the whole system – including the interdependency between the components – and not only each component on its own. Therefore, a methodology will be presented within this work in order to evaluate possible drive train configurations according to the application requirements based on a system-oriented approach.

For the electrification of vehicle propulsion systems, the requirements are defined in advance of a project, whereas the single components are not yet determined. In this case, it is difficult to choose the single drive train components, since only the system information exists at this point. Additionally, taking into account the high requirements on electric propulsion systems regarding reliability and fault tolerance, or the strict limitations on the installation space and weight of the system, the correct choice of design features within the drive train is extremely important. Obviously, a certain complexity of parameters appears trying to solve the task, due to interdependencies between different engineering domains.

1.2.1 General Problem Description by Means of the V-Model

The present work can be built on the V-model [50] shown in Figure 1.4. It provides a basis in order to show the fundamental idea of the work, the positioning within the system design, and the basic problem, which triggered the research within the design of electrical drive trains for traction applications.

Product development processes are characterized by a certain complexity. The development of electrical drive trains also contains a variety of parameters, which needs to be managed. In general, the V-model is, besides many others, one of several possible process models to deal with complex processes, which was originally used for software development [12].

In addition, it has already been successfully used and therefore adapted by different disciplines in varying applications, such as industrial engineering [58] or mechatronic systems [50, 70, 148]. The ‘V’ stands for verification or validation and the model is characterized by a sequential execution of steps, requiring each phase to be accomplished before the next phase begins.

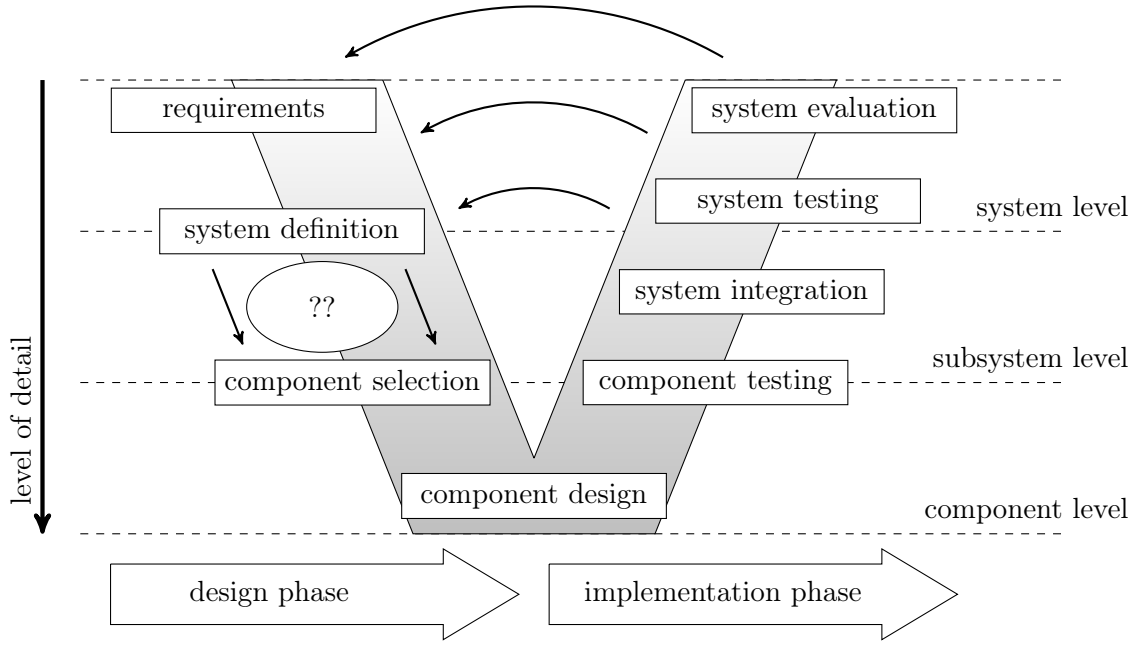

Figure 1.4: V-model for the system design on the macro-level based on [50, 58, 103]. The left top-down path is often skipped by jumping directly from the requirements to the component design.

The V-model was extended to an iterative process, since – according to Gausemeier and Möhringer [50] – mechatronic systems usually cannot be produced within one macro-cycle. This means, the development process runs through the macro-cycle several times while increasing the product maturity or the cycle can be interrupted in order to step back for an improvement of the previous step. However, the repetition of the cycle is time consuming and some steps are not precisely defined yet.

Therefore, in [103], where the model is used for the development of electric drives, Moiszi et al. complemented the right bottom-up path by a hardware-in-the-loop test bench. Many other research works focused on the bottom-up path, including component design, testing, measurements, and evaluation on a system level [141]. Höhn et al. described the starting point of a project defining three steps [58]. Projects always need a problem to be solved, which defines the targets. Thus, the identification of a problem is the first step, followed by the second, the problem evaluation, and the third step, the problem description. These steps usually are realized or specified by a specification sheet.

However, the left top-down path is often skipped quickly, starting from *requirements* and jumping over to the *component design*, without realizing a selection process containing hard criteria. Compared to Moiszi et al. [103], the gap should be closed between *system definition* and *component selection* in the top-down path, shown in Figure 1.4. Until now, publications hardly define a procedure to run through the selection process starting from the system definition and ending with the component selection. It is indispensable to define a solution space for the system and to examine an adequate choice of the components from the system perspective. Here only low detailed component information is given, whereas the system parameters need to be defined.

1.2.2 System Definition and the State of the Art of System Design

Hence, the *system definition* is a crucial aspect and will be covered within this part to define the starting point of this work. As aforementioned, this research deals with electrical drive trains. The term drive train describes the traction drive including the *electrical machine* (EM) and the *power electronics* (PE), which can be seen in Figure 1.5. The drive train is considered to be a direct drive. Thus, no gearbox is used, which means that the machine's output power and rotational speed are equal to the mechanical power and rotational speed which are required by the application. Furthermore, the drive is fully electrified, which means that only a pure electric drive is taken into account and no hybrid or range extender alternative. The gray faded box in Figure 1.5 defines the abstract system, with the terminals on the left for the connection to an energy storage device, such as a battery or a fuel cell. On the right, the shaft as mechanical connection to the application is illustrated. Both components – the electrical machine and the power electronics – are connected by a to-be-defined number of phases; conventionally three phases are used.

The design process of electrical machines has been described step by step in different works, such as [119]. Since those processes are usually based on known initial parameters, it is possible to follow the described procedure to obtain the final component design. Nevertheless, it is necessary to decide which component types are suitable before starting the design process. At this point almost no key parameters are yet determined or still need optimization iterations, such as number of phases, number of pole pairs, and others [119]. Reichert et al. [122] briefly describes the selection process for components within the electrical drive train based on predefined or existing components, whereas works are missing which cover the selection of the appropriate component features at an early stage of a design process. Typically, the first step is to evaluate the needed forces for an application and then to translate them to torque and speed requirements [38, 51, 123]. These requirements lead to energy demands by taking application scenarios into account. Hence, the drive train can be designed based on force and time issues.

However, what is the procedure of choosing the right drive train configuration? In general, two possibilities exist for the selection of drive train components (EM or PE) for special application cases. 'Selection' here means, to choose the working principle of the electrical machine, e.g. synchronous or induction machine, or to choose the appropriate topology of power electronics. On the one hand, the appropriate component can be selected due to the experience of engineers, which may result in only taking one aspect into account for the comparison and the decision. On the other hand, it is possible to design every single type of

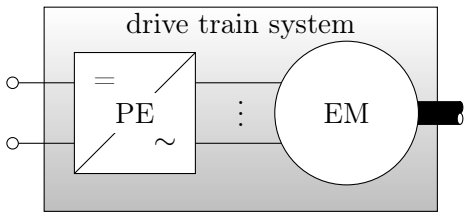

Figure 1.5: Abstract drive train system definition. For mobile applications, a DC-voltage is transformed to an AC-voltage by the DC-AC-converter (PE) which supplies the electrical machine (EM) having multiple phases.

component, such as mentioned in [37, 44, 100, 156], simulate their operating behavior, and finally select the optimal component. Since this procedure needs an enormous amount of time, it is hence necessary to develop a method taking care of selection criteria and the requirements of applications at an early stage. This is especially true in the field of safety-critical drive trains for mobile applications, where there is a need for methods considering the selection of components and design of the system topology at an early stage based on the system requirements.

1.2.3 Demarcation

At the Technical University of Munich (TUM) in Germany, the Institute of Energy Conversion Technology covers the research fields *electrical machines*, *electrical systems*, and *electrical automotive technology*.

This work bases on works that have been accomplished within the area of reliability and is connected to the publication of Bolvashenkov [15]. It provides the first step of component and topology comparison at an early stage of a project and is framed by research works of Bücherl [24], Thanheiser [141], and Meyer [100] covering the methods considering scaling and drive train optimization, efficiency mapping, and the preliminary design of electrical machines, respectively.

Current component technologies within the field of electrical machine design or the power electronics are not covered by this work, but can be found in the publications by Hecker [57], Willerich [160], Lahlou [19], and Filusch [43]. Apart from the institute, machine comparison in general or for special applications can be found for instance published by Finken [44], Wang [157], or Ganev [48]. Additionally, the detailed design and the control of multiphase machines, as well as fault detection methods, have been conducted for instance by Bennett [5], Bianchi [6], Duran [34], Levi [82], and Semail [132].

Pertaining to the system analysis, Reupold [123] also covered the solution space analysis for drive trains, where a possibility to assess electric drive train components in order to use them in electric cars is presented. However, a reliability assessment is not included, which is indispensable for an overall assessment of safety-critical applications.

As mentioned within the target description, this thesis examines the reliability of drive train systems at an early design stage which means that failure probabilities of the system's components are needed. These values will be taken from Ermolin [40] and Mecrow [98]. Considering reliability or system assessments in literature, Wang [155] for instance describes the reliability process for existing renewable energy systems based on methods, such as Markov modeling or fault tree analysis (FTA). Another example for a system analysis was presented by Graebener [52]. Both examples evaluate existing component designs in order to select the appropriate components or topology, in contrary to the target of this work to evaluate components and topologies without a finalized component design at an early stage.

Once the selection process is completed, the components can be designed in detail. Although this step will not be a part of this work, the design process for electrical machines follows the selection process. The design of machines is covered in other works, such as [100], where the basis was set up for a machine design tool, which was created at the Institute of Energy Conversion Technology and which is presented in [P12].

Hence, this work was established at the Institute of Energy Conversion Technology based on the context of publicly funded projects in cooperation with industry, where the idea and motivation for this research work was born. Within these projects, other PhD theses were created covering the design of components, such as the electrical machine in [30], [80], or [121], only to mention a few of them.

Finally, this work was accomplished on the basis of supervised student projects, such as seminar works, reports, and bachelor's and master's theses, where the idea of a potential analysis for traction drives and the respective topics were also expanded. A list of these supervised student projects can be found at the end of the bibliography.

1.3 Targets and Work Structure

This research work is aimed at finding a method for a potential analysis of electrical drive trains for mobile applications at an early stage of a project. Thus, the main drive train topology is fixed – as also described in section 1.2.2 –, whereas the components *electrical machine* and *power electronics* need to be evaluated separately, as well as the interdependency between those two components. This approach generates an impression about a possible system configuration and finally leads to the most auspicious topologies. Furthermore, it takes into account weighting factors depending on the application case and the corresponding requirements. Therefore, it is necessary to choose significant evaluation criteria – basically efficiency, volume, weight, reliability, and fault tolerance – in order to assess the different drive train topologies. This thesis does not aim at a detailed description of the system's behavior, but in functional correlations and behavioral patterns. The overall target of finding a methodology can be divided into subtasks, which point out to the main work structure explained below:

- the evaluation of electrical machine types,
- the evaluation of power electronic topologies,
- the evaluation of their interdependency, and
- the selection of the appropriate components and system topologies.

Hence, within this work, the fundamentals are explained in chapter 2, which contains a tool cloud defining a possible methodology in order to assess the electrical drive trains and some definitions on used terms and theory in order to avoid misunderstandings. Chapter 3 describes the solution space of usable components, containing two different types of electrical machines and the appropriate definition of power electronics. Furthermore, the interdependency between the components is shown by means of multiphase drive systems. Then, chapter 4 is dedicated to applying the previously presented methodology to these components and to provide a feasibility check considering a helicopter application based on high requirements. Alternative drive trains are further investigated in chapter 5 in order to find realizable drive train topologies. Finally, all results are concluded in chapter 6, also providing a critical reflection and an outlook on future work.

2 Methodology for Potential Analysis of Electrical Drive Trains

The target to analyze the potential of electrical drive trains asks for different methods depending on the application case and the according requirements. This chapter concludes and explains different methods and combines them into a multipurpose methodology, which is used in this work to evaluate and select possible topologies for a traction drive, whereas it could also be used for industrial drive trains. Only the focus would need to be shifted and the parameters adapted accordingly. Hence, this part covers a variety of methods and the first part describes the dependency of the design on targets and parameters, also varying by applications. Since pursuing only one solution approach at an early stage is less constructive [145], the following different methods or design procedures, which have previously been published or described in relevant literature are combined into a methodology for analyzing electrical drive trains.

2.1 Dependency of the Design on Targets and Parameters

Projects dealing with electrical drive trains for electric vehicles are usually based on hard requirements. Weight or installation space are the most common design factors, especially if the design is based on conversion design, where – in contrast to purpose design – the drive train has to suit a given platform and not only a set of requirements. The system always requires a certain amount of mechanical power P_{m} at a specified nominal speed n_{n}, depending on the transmission ratio. These parameters describe or define the initial situation for drive train design from where all other parameters can be deduced for the system description. They differ in the level of detail given for traction application cases and the focus is different, depending on the specific application case.

2.1.1 Requirement Distinction between Applications

The differences related to the requirements between the aforementioned vehicle types are depicted within this part. Section 1.1 has already shown the different fields of application. Each application often does not use the same technology regarding electrical drive train components, which means for instance that different types of electrical machines are applied for electric cars. Therefore, it is necessary to answer some upcoming questions: Is the same technology preferred because of traditional, political, or technical reasons? Does the preparation of specification sheets affect the choice of technology for electrical drive trains?

Table 2.1: Summary of electrical machine types – permanent magnet synchronous (PSM) and induction machine (IM) – used for electric cars depicted by manufacturer including the respective year and reference.

manufacturer	machine type	year	reference
Audi	PSM	2011	[2]
BMW	PSM	2013	[11]
Citroën	PSM	2011	[39, 61]
Daimler	PSM	2009	[63]
Hyundai	IM	2013	[64]
Mercedes-Benz	PSM	2010	[99]
Mitsubishi	PSM	2009	[39]
Nissan	PSM	2011	[39]
Peugeot	PSM	2010	[39, 62]
Tesla	IM & PSM	2015	[124]
Toyota	PSM	2016	[39]
VW	PSM	2015	[146]

Traditional or Technical Reason?

Until today, electrical drive trains have hardly been established in aircraft applications, but due to the requirements of torque and weight, the permanent magnet synchronous machine is the preferred machine type in current research studies. For the other mentioned application types of electric vehicles, electrical drive trains have already been implemented. Starting with the electric cars, it can be seen that most manufacturers use permanent magnet synchronous machines, whereas two companies chose the induction machine also to be the optimal option for the same application case. Table 2.1 summarizes a collection of different manufactures of electric cars and specifies the types of electrical machine, which are used in their electric cars. Apparently, only those two machine types are practically used for cars, also mentioned by Tschöke [145]. Focusing on ship propulsion, permanent magnet synchronous machines and induction machines are used. Synchronous machines can be found especially being used in conventional ship propulsion systems, whereas at the world exhibition SMM in 2012 the "azipod" traction technologies were presented using the induction machine, where single gondolas are placed outside of the main body of the ship. [18]

The same approach can be seen for trains. Both machine types can be found during the last decades of high speed train, normal train, and subway production. It seems to be dependent on the manufacturer, but also the country, where the trains are used. For instance, "Bombardier Inc." typically uses induction machines, but permanent magnet synchronous machines in Sweden. The German high-speed train ICE uses induction machines, as well as the Japanese Shinkansen or the French TGV, whereas the TGV-POS Eurostar is equipped with permanent magnet synchronous machines. [128, 150]

Finally, the use of electrical machines – whether synchronous or induction machine – seems to be a traditional choice coming from experience and knowledge within a manufacturer. Nevertheless, the choice is dependent on requirements, which need to be collected and weighted.

Preparation of Specification Sheets

At the beginning of technical projects, *specification sheets* are created in order to obtain a certain quantity of requirements. From experience, specification sheets out of former more-or-less comparable projects serve as a basis for current projects, even though requirements do not match adequately. Another procedure to start a project is from scratch, whereas this possibility tends to be time consuming, because all needed parameters have to be calculated before starting the preliminary design. Therefore, requirements from previous specification sheets need to be reevaluated, for instance by first examinations, research works, or simulations. Then, they need to be separated and categorized in *hard requirements*, *soft requirements*, and *degrees of freedom*, as shown in Figure 2.1. Especially for *hard requirements*, which need to be accomplished, it is indispensable to avoid contradictory combinations of parameters leading to iterative design or calculation processes, or even worse, an interruption of the project. *Soft requirements* shall include guiding values, which can be rejected, if necessary. Finally, it is helpful to define the *degrees of freedom* in order to not forget any important parameters being decisive for the final design. Hence, the specification sheet is a crucial part and especially the appropriate categorization of parameters is indispensable for a success of a project and directly linked to a suitable choice of technology.

Furthermore, each application is exposed to different operational conditions based on environmental and target impact. These influences can be defined by the area and purpose of application or by architectural or structural constraints, enabling or disabling the possibility of redundancy. This fact results in diverging requirements that a drive train must comply with and therefore in variable design approaches.

Operational Differences between Applications

In general, the applications differ regarding several parameters. These parameters can be clustered in vehicle performance related-parameters and vehicle design-related parameters, based on operational differences characterizing each application. Table 2.2 shows a brief collection of clustered parameters often requested within a project concerning electric vehicles; however, the collection is not exhaustive. All these parameters depend on the choice of technology and engineering certification standards, which need to be reached, for instance regarding the system's safety. The area of application [101], which is characterized by environmental restrictions, holds a huge impact on design parameters. Additionally, the parameters themselves are interdependent on each other. These two facts limit the performance or vehicle related parameters. More in detail, the impact becomes clearer while focusing on

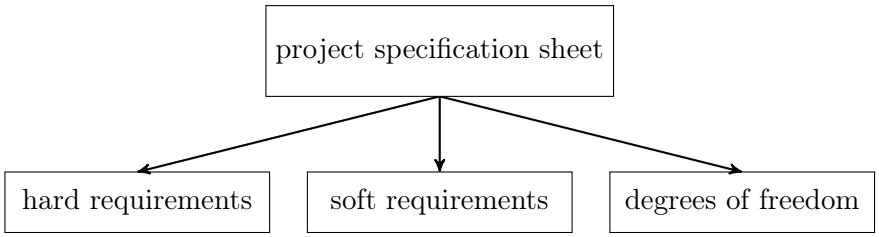

Figure 2.1: Differentiation of system requirements into hard and soft requirements and finally the degrees of freedom to distinguish between indispensable and preferable targets.

Table 2.2: Requirements for electric vehicles. The requirements requested by society can be clustered in performance and vehicle related parameters.

vehicle performance	vehicle design
velocity	geometry
power/torque	weight
acceleration	reliability
efficiency	fault tolerance
operation range	maintenance

the forces which are needed to operate the vehicle system adequately. These forces already include a quantity of environmental parameters, such as wind conditions, ambient temperature, driving surface, slopes, friction, drag, and gravity. These forces enable a first evaluation of maximum and minimum velocity, the required acceleration, climbing ability, and the operation range of a vehicle system. This results in different torque-speed characteristics of the drive train.

Besides, these boundary conditions restrict or allow a conditioning of systems, the use of different cooling techniques, as well as the optimization of volume and weight in order to increase the system performance. The operational time and operational conditions are of special importance. The operational time directly influences the requirement intensity, for instance regarding the amount of needed energy. The correlation with the operation cycle is crucial to assess among others range and reliability. In case of discontinuous and periodic operations, the system can be recharged, maintained, or repaired in case of failure, leading to an increase in reliability or range. In case the system is continuously operated, the requirements are intensified. Focusing on reliability, redundancy can be a possible solution to achieve the required values for continuous operations.

Possibility of Redundancy

All forms of transportation belong to the category of safety-critical or also called life-critical systems, especially considering autonomous vehicles. These are systems where failure can lead to environmental damage, damage to property, or injury and death of people. Safety-critical systems require a high reliability, whereas the values of reliability range from 10^{-9} to 10^{-6} failures per hour depending on the application. This value can be matched by increasing the value by enabling repair – whereas repair for some applications is not suitable – or by providing redundancy. Redundancy describes a technical approach to provide more components or methods than explicitly needed for the operation of the system. These additional parts serve as backup in case of a failure. The system's capability itself of tolerating faults is not considered to be a proper part of the operation [36]. Furthermore, redundancy can be divided into different types, such as structural, functional, and time redundancy. First, *structural redundancy* stands for added components to the system, whereas these components are not necessary for a nominal operation, no matter if they are similar or different compared to the needed components [36]. For instance, enlarging a drive train system with a completely identical drive train system which is not necessary for the required system performance would cause structural redundancy. Moreover, *functional redundancy* can be reached by appending functions or methods being

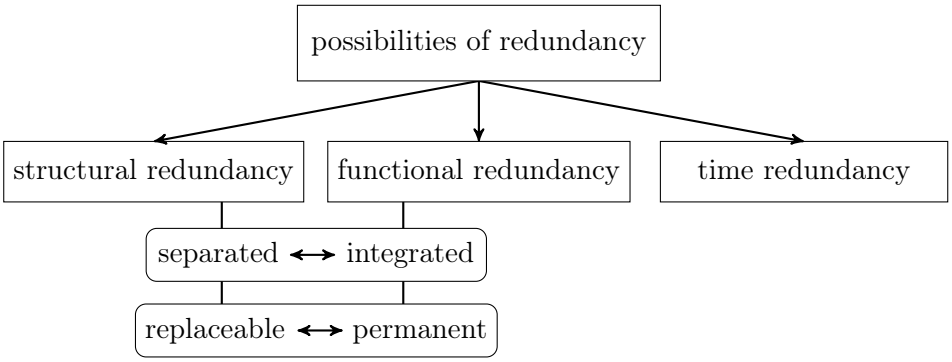

Figure 2.2: Different possibilities of redundancy are depicted including their characteristics for technical systems based on [36] and [P5].

dispensable for the operation, for instance distributing power over several separate components which enables a fail-operational behavior. *Time redundancy* describes the time needed by a system to execute redundancy [36]. This means, that a system needs to provide a certain time before failing completely in order to ensure that redundancy possibilities can be activated or used. Referring to [P5], the different possibilities of redundancy are illustrated in Figure 2.2. The characteristics between structural and functional redundancy are defined by *separated* or *integrated* redundancy and *replaceable* or *permanent* redundancy. Replaceable redundancy, for instance, enables repair. Finally, each kind of redundancy enables the possibility to reach high reliability restrictions within systems [9], whereas it is also possible to combine the different types of redundancy always depending on the constraints of the system.

Based on this distinction and the definition of the appropriate requirements – considering the possibility of redundancy, installation space and weight, and other environmental circumstances –, the evaluation of a complex system can be started.

2.1.2 Evaluation of a Complex System

However, no agreed definition of what constitutes a complex system exists. It is a term used to describe a wide range of systems in different areas of science and contains many different points of views. Complex systems research tries to give insight into how different systems can be expressed in similar ways. This section covers the definition about complex systems and discusses three involved questions in order to approach the meaning of the terminology *complex system*: 'What is a system?', 'What are targets?', and 'What is complexity?'.

What is a system?

In literature, a lot of definitions for the word *system* can be found. Patzak [113] combined the definitions existing back then to the distinction of *elements*, *properties*, and *relationships*, or more technically speaking *correlations*. Hence, on the one hand, a system consists of a certain number of elements, which are characterized by their own properties. On the other hand, the elements are linked to each other by correlations based on the need for compliance with the requirements or targets. This means, components within a system have one common main purpose, which needs to be fulfilled. All these interdependencies are influenced by

environmental circumstances as mentioned in section 2.1.1. Hence, a system can be defined as an arrangement of varying complexity. [113, 114, 125]

What are targets?

One fundamental explanation for project goals was presented by Doran in 1981 [31], who defined SMART objectives. According to this definition, SMART stands for a specific, measurable, assignable, realistic, and time-related description of the objective. Hence, overall and general project goals are split into several targets, which need to be defined in detail, in order to ensure a common understanding of the project procedure. However, the SMART description of targets is only the first step of handling complex systems.

What is complexity?

There are multiple definitions of complexity, as mentioned above, but in general a complex system consists of multiple different parts connected to a causal network. These connections enable an influence from one part to another and such a complex structure makes a prediction about the system's behavior hardly possible. Hence, number and type of connections and the variety, defined by the number and type of elements, can be a specification of complexity [113]. Furthermore, the depth of a structural or functional hierarchy, i.e. the level of detail, often is one very decisive factor for the level of complexity. Mobus and Kalton [102] described one possibility to evaluate complexity by a ratio of the amount of surprise a system causes to the amount of knowledge about a system. Consequently, the quality of information – having a huge impact on the knowledge about a complex system – defines if a system's behavior is surprising or predictable. [102, 149]

According to Mobus and Kalton, the "[...] capacity to understand systems is directly affected by the complexity of those systems" [102]. They state that systems are composed of subsystems and subsystems comprise even smaller subsystems. This procedure leads to a final composition of elements on micro and macro levels or the distinction between more global or more local perspectives. Each level defines the level of detail, but also the level of complexity. The abstraction of the system, the objectives, and the combination of these two aspects carry weight, which are decisive in order to ensure the possibility of understanding the system and to gather knowledge about the components, their behavior, and their interdependencies. [102]

In order to acquire this knowledge, the single components and their system composition have to be identified. Thus, considering electrical systems, one may think that the design of electrical drive trains can be described by physical and mathematical equations and can therefore be calculated easily. This is true for each of the technical components. However, at an early stage of a project, these calculations are not feasible or very time consuming either due to the lack of parameters and detailed information about the project, or due to the increasing number of components.

Hence, the initial phase of assessing a complex system is the important one. Vester [149] defined six mistakes while handling complex systems, of which the tendency to oversteer or tendency to authoritarian behavior are negligible for this consideration and the following four mistakes trace back to the starting point of the project:

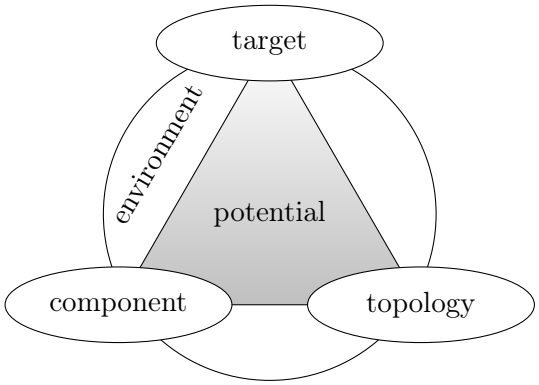

Figure 2.3: Description for complex systems and influencing factors based on [113] and [130]. The potential of a complex system is influenced by each component, the correlation or topology, the environment, and the target of the application.

1. Mistaken or wrong objectives
2. Unlinked situation analysis
3. Irreversible concentration
4. Disregarded side effects

In order to overcome these mistakes, a model based on four factors is proposed. This consideration is based on a model, which was invented by Ruth Cohn [130] linked to Theme-Centered Interaction (TCI) – within the field of the humanities as a psychological approach to work with groups – and is further adapted to technical perspectives of systems and their design. Figure 2.3 illustrates four factors, which have an impact on a system design characterized by several parameters.

The four factors are the *component*, the *topology*, the *target*, and the *environment*. First, the factor *target* defines the overall purpose of a technical system, whereas the special sub-targets are defined in the aforementioned specification sheet. Targets may also be linked to the single subsystems and their properties. These sub-targets highly depend on the solution space of the *components* and also on the *topology*, hence, the correlations between components having different properties. The components are structured and set together in different topologies in order to form a technical system.

The achievability of targets and the choice of components or topologies are highly influenced by the interactions between those three factors and additionally these dependencies are based on environmental circumstances. This means that the *environment* sets the boundaries for different parameters within a system. It demarcates the interfaces to other disciplines or other not considered systems, subsystems, or the frameworks within the overall system [102]. These environmental conditions have to be defined in advance, in order to get the best knowledge about the dependencies of the system on its environment. This factor, beside others, encompasses the field of application, as well as political or social influences. For instance, the discussion about carbon dioxide reduction is only one aspect that could influence the choice of drive train systems and components for traction applications.

Considering all these four factors results in gathering knowledge on the dependencies between the factors. Finally, it allows to assess and to conclude on the *potential* of the system. It also shows that it is a dynamic iterative process to include all four factors to the system assessment, hence to focus alternately on the factors and to ensure that all factors are being taken into account during the potential analysis of electrical drive trains.

System models are representing a complex system including crucial system properties, most likely without capturing the system entirely. At this point, the previously mentioned abstraction is applied. The models can be described by diagrams, mathematical equations, physical dependencies, etc. [102]. Several methods exist to manage or evaluate complex systems by means of abstraction. While the description may not perfectly match reality, it puts an abstract representation of a system into a solvable framework. Taking the explanation of complexity by Mobus and Kalton [102] into account, directly leads to the system's description by a hierarchical system approach, which was previously presented in [P6].

2.2 Hierarchical System Approach

The hierarchical system approach is a useful method in order to describe and to distinguish a system [102], [P6]. Generally, a system can be divided into different levels of detail in order to simplify the consideration of the system at first. The point of view often depends on the previous knowledge about the system, but can also be adapted according to the focus of the system assessment. The mentioned drive train system can be defined by four levels characterizing four different levels of detail, namely *system level*, *subsystem level*, *unit level*, and *component level*, which are displayed in Fig. 2.4. The level of detail considering the description of a system increases from the top level down to the bottom level. The decision, if the hierarchy is applied top-down or bottom-up or if not all of the levels are taken into account, can be made dependent on the targets of the investigation. Furthermore, the target of investigation and especially how it can be pursued, highly depends on how detailed the information about a system at a certain design stage already is.

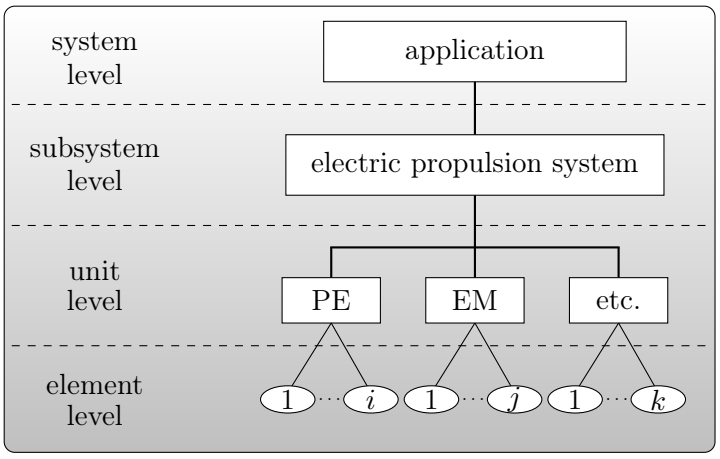

Figure 2.4: Hierarchical system approach applied to electrified vehicles based on [102] and [P6]. The hierarchy consists of four levels, system level, subsystem level, unit level, and element level, which describe the level of detail.

2.2.1 System Level

Starting at the top level of the system consideration, the *system level* describes the functionality of the *application*, which can include information about the distinction between (non)operational and (non)functional times to complete life cycles. Operational means to fulfill the function that the application has to undertake, which means being in action. In contrast, functional implies the system's condition of being ready to use and that a system can be functional during operation or at stand-by. Accordingly, nonfunctional describes the failed state of the system. Furthermore, the environmental circumstances are of interest, as already mentioned in section 2.1. In other words, the system level characterizes the overall application and its surrounding, thus, the internal and external operation conditions leading to an operation scenario, which describes the requirements for power, speed, and time.

2.2.2 Subsystem Level

The *subsystem level* includes the application's subsystems, which need to be evaluated. In general, it can contain more subsystems, whereas in this work the *electric propulsion system* represents the only subsystem. It consists of the interdependency of the included components, which implies the electrical machine and the power electronics. On this level, it is not the single component which is evaluated, but the correlating behavior within the subsystem based on the torque and speed requirements. The possibilities to connect the two components need to be defined according to the system requirements depending on the interfaces, typically the torque and the rotational speed, as well as the duration of each operating point. Additional constraints, such as installation space, volume or weight, and reliability, can be evaluated based on the interaction between the components defining the subsystem.

2.2.3 Unit Level

Within the *unit level*, the focus is set on each component of the to-be-assessed drive train subsystem. As aforementioned, the only components being investigated in this work are the power electronics (PE) and the electrical machine (EM). Of course, other components have to be included in order to get a closer and more detailed assessment of the overall application. However, the number of included or not considered components highly depends on the information available at a specific design stage.

2.2.4 Element Level

The *element level* covers the construction elements of the units. For instance, the electrical machine consists of yoke, teeth, slots, copper windings, end windings, etc., whereas the power electronics contain semiconductors, diodes, capacitors, printed circuit board, cabling, and others. Each of these elements follows its physical rules and possesses its characteristics, such as functional principle, failure rates, etc. This level is definitely the most detailed level where the most accurate results can be obtained, whereas this level also requires the highest amount of accuracy, since a lot of detailed data and the precise implementation need to be known in advance.

Within this work, the *unit level* and the *subsystem level* are covered in order to get an answer on which components and which topologies are possible solutions for the electrification of a drive train. The interfaces for this work are therefore coming from the system and element levels in order to define the constraints of the two inner levels. Consequently, the focus is set on the torque-speed characteristics.

2.3 Torque-Speed Characteristics

Design engineers use torque-speed characteristics for the preliminary design of electrical machines, since all operating points of the machine are supposed to be located beneath the curve. Applications claim certain driving scenarios, including power demand, rotational speed, and time values for the persistence in operational points. Hence, the driving scenarios of the given application restrict the choice of the maximum torque, power, and speed or in other words the nominal operating point of the design curve. These values are characterized by physical limits and dependent on the application requirements. Combining physical limits and the requirements can lead to overload conditions, which can be divided into two overload possibilities; overload conditions caused by rare operating points or failure of components.

2.3.1 Limit Cases

Figure 2.5 illustrates the torque-speed characteristic for controlled electrical machines including operational areas, which are separated or restricted by physical limits. Area (A1) characterizes the partial load operation, which means that the machine is driven in thermally uncritical operating points, since the occurring losses are not resulting in an unacceptable thermal characteristic of the materials. Hence, in this area the machine does not operate at full capacity until reaching the limits of the respective area. On the one hand, increasing the speed leads to the transition to area (A2) corresponding to the field weakening operation of

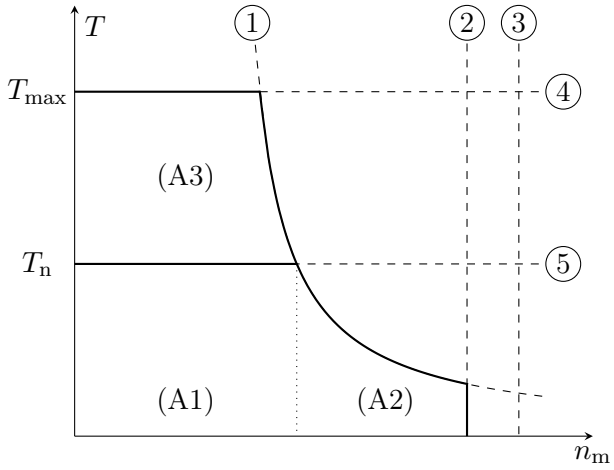

Figure 2.5: Physical limits of torque T versus speed n_m characteristic for controlled electrical machines based on [8]. The numbers 1 to 5 show the physical limits and (A1) to (A3) show the different operational areas, respectively.

the machine. The field weakening characteristic is simplified by an n^{-1} behavior, which is sufficient to explain the general limitations. The size of this area depends on the design of the machine and the definition of the nominal operating point, which defines the transition from constant torque to constant power.

On the other hand, the increase of the torque out of a partial load operation is restricted by limit (5). The decisive parameter for this physical limit is the insulation material and its temperature development, which can be influenced by cooling technologies. Especially the insulation in the slots representing the hot spots of the machine is essential. Thus, an overload operational mode – which comes along with a respective over-temperature – is only possible within the nominal temperature limits of the used insulation material. Exceeding limit (5) leads to an overload operation in area (A3). This operational mode is defined by losses heating up the machine as long as no unacceptable thermal condition of the machine is reached, which provokes a critical damage of the material, such as overheated wires and therefore melting insulation material. Hence, the operating time within this area is limited but also a further increase of the torque is therefore restricted by limit (4). Passing this limit directly leads to the destruction of the machine. Furthermore, coming from this area (A3), the speed is limited by the voltage, since an increase of the power is needed to increase the speed. This is where limit (1) comes into effect.

Limit (1) is defined by the limit value of the voltage for the insulation material, which is used within the slots of the machine. This insulation material aims to avoid short circuits between the windings and needs to withstand the voltage difference between two adjacent windings. The insulation material can be chosen depending on the voltage needed to supply the machine in order to achieve the required performance, which is the typical way of designing the insulation material. Increasing the volume of the insulation material, which would lead to a higher insulation capability as well, results in a lower slot fill factor and hence in a lower electric loading. This is the reason why the insulation material is typically designed for the nominal voltage of the machine. Applying overload by means of higher voltages is not permitted, since the insulation material would be irreversibly damaged in case of exceeding the voltage limit. In order to avoid insulation damage within the machine, the power electronics can be designed for a lower output voltage than the insulation material in the slots is able to resist. [106]

Limit (2) is defined by the output frequency of the inverter driving the machine. This fact plays an important role, especially for high numbers of poles ($2p$), since the electrical frequency increases proportionally by the factor p. This correlation sets the upper rotational speed limit for area (A2) and lowers it electrically. In addition, the rotational speed is mechanically restricted by limit (3). This limit is characterized by the maximum centripetal acceleration of the rotor, which depends on the diameter and the rotational speed [8]. Due to this characteristic, the diameter of the rotor is the decisive factor for high speed machines, whereas the ideal length of the machine is responsible for the torque. In contrast, low speed and high torque machines can therefore also be designed with an increased diameter and a decreased length.

As aforementioned, increasing the torque leads to an overload operating mode (A3) where the machine provides a higher torque than the nominal torque. Within the design of an electrical machine, the overload situations need to be known in order to prevent oversize the machine or to be able to handle the overload conditions. Hence, two different overload causes need to be mentioned, in this case rare operating points and failures.

2.3.2 Overload Conditions Caused by Rare Operating Points

For some applications, rare operating points characterize a special overload condition which is accepted within the operation. Overriding the curb from standstill is only one application example for electric cars or scooters. Hence, these rare operating points are not taken into consideration for the design of the machine, since the thermal time constant is not critical. In contrary, the power electronics need to be designed also based on these short-term operating points, since the currents occurring during overload can damage the semiconductors. Within this work, the overall design of the drive train is not covered and hence, the overload by rare operating points is henceforth neglected.

2.3.3 Overload Conditions Caused by Failures

Other than that, occurring failures can lead to overload conditions. In order to meet the required torque or power after failing components arise, it is possible that other components need to be overloaded. This means, the different fault chains leading to a component or system failure can be derived – for instance from a fault tree – and hence, the power or torque degradation can be defined based on occurring failures. The degradation levels result in the determination whether the requirements are obtained or if overload has to be taken into account in order to comply with the performance requirements.

2.4 Weighting Factors for System Parameters

Based on the system assessment including driving scenarios and the resulting torque-speed characteristics, different parameters need to be evaluated, whereas the consideration of several system parameters requires their classification. System parameters which are commonly evaluated in literature – for instance in [44, 167] – are efficiency, power density, reliability, fault tolerance, repairability, volume, complexity, and cost. The method to use weighting factors is well established, but effective in order to weight parameters within a system, to overcome target conflicts, and especially not to overemphasize parameters of less importance considering a special application. The difference between the various vehicle applications regarding the parameter priority is schematically presented in Table 2.3, previously published in [P4]. Efficiency, reliability, and fault tolerance have a high priority for all applications, based on the requirements regarding the operation range and the fact to be safety-critical applications. Power density and volume are very critical for aircraft, whereas for cars, ships, and trains, the importance is a less crucial aspect. Repairability represents an important factor for all applications except aircraft, since repair of a drive train during the flight is not applicable in contrast to the operating scenarios of the other applications. The complexity differs due to the state of the art of each application. For aircraft, the complexity is not the most relevant parameter, whereas for the other applications the mass production is applied since electrical drive trains are current technology. Finally, costs are very important especially regarding mass production, which is the reason for the increased interest in costs for car, ship, and train. However, within aircraft – a relatively new field of electrification application – costs are not significant, since it targets a feasibility study and cost are irrelevant at this point. The next section presents a first approach to assess the component *electrical machine* at an early stage by means of regression models.

Table 2.3: Qualitative weighting factors for the four different vehicle types, aircraft, car, ship, and train, where '⊘' stands for 'not applicable', '∘' for 'low priority', '+' implies 'medium priority', and '++' represents 'high priority' [P4].

vehicle type	aircraft	car	ship	train
efficiency	++	++	++	++
power density	++	+	+	+
reliability	++	++	++	++
fault tolerance	++	++	++	++
repairability	⊘	++	++	++
volume	++	+	+	+
complexity	∘	+	+	+
cost	∘	++	++	++

2.5 Regression Analysis

Gathering information and data is a crucial process in today's life. With regard to technical systems or components, it can be helpful to collect data of realized devices. Hence, a machine database – including two different machine types existing on the market – was composed within the frame of this work [P13]. First, a brief explanation on the basics of regression will be presented, followed by the regression model for volume and weight of the electrical machine. By means of the database, first tendencies about the use of a machine type for certain applications can be derived. This allows getting an impression about the characteristics and the differences between both types used within this work.

2.5.1 Basics on Regression Analysis

Curve fitting is a well-known approach to analyze data in many scientific fields. Regression models are mathematical functions fitted to these data and can generally be described as

$$y = f(x; a) + c_{\mathrm{err}} \ , \tag{2.1}$$

where a is a factor describing the relation between x and y. The variable x stands for multiple criteria being represented by the variables x_1 to x_i. The variable c_{err} includes the standard deviation to the model, whereas in the case of qualitative data assessment, this correction factor can be neglected. Other than that, it is necessary to define this function in advance and to decide whether it is linear or nonlinear, which can consist of polynomials of single or higher order numbers. Taking into account nontechnical systems, the function, which fits best to the data is chosen, whereas for technical problems this procedure is not physically well-founded and certain functions can be inadequate considering the physical correlations. [27]

2.5.2 Volume and Weight

In order to obtain a physical correlation within the regression model, the dependence of weight and volume on the fundamental equations needs to be derived. Taking into account the tangential stress τ, which depends on the magnetic flux density and the electric loading, multiplied by the cylindrical surface of the rotor, leads to the total force F_{tot} acting on the rotor. The multiplication of the total force by the lever arm, hence, the radius of the rotor, results in the dependence of the torque T on the volume V_{rotor}.

$$F_{\mathrm{tot}} = \tau \cdot 2\pi \cdot \frac{D_\delta}{2} \cdot l_{\mathrm{i}} \tag{2.2}$$

$$T = F_{\mathrm{tot}} \cdot \frac{D_\delta}{2} \tag{2.3}$$

$$\implies \quad T = \tau \cdot 2 \underbrace{\pi \cdot \left(\frac{D_\delta}{2}\right)^2 \cdot l_{\mathrm{i}}}_{=V_{\mathrm{rotor}}} \tag{2.4}$$

Assuming that the volume is proportional to the mass finally results in the direct proportionality between the torque and the mass of the electrical machine.

$$\left.\begin{array}{c} T \sim V_{\mathrm{rotor}} \\ V_{\mathrm{rotor}} \sim m_{\mathrm{EM}} \end{array}\right\} \implies T \sim m_{\mathrm{EM}} \tag{2.5}$$

The mechanical power of electrical machines can be calculated by multiplying the torque and the angular velocity, which is directly proportional to the rotational speed of the machine. This is expressed by

$$P = \omega \cdot T, \text{ where } \omega = 2\pi \cdot n \ . \tag{2.6}$$

The design equations (2.4) and (2.6) finally lead to the regression equation, where the mass can be explained by the ratio of power and rotational speed. The following dependence can be obtained, where a constant factor a is introduced for each machine type; here induction machine and permanent magnet synchronous machine:

$$m_{\mathrm{r}} = a \cdot \frac{P}{n} \tag{2.7}$$

In equation (2.7), the factor a can be determined by fitting a surface to the given values from the machine database. These surfaces are illustrated in Figure 2.6, where the gray surface stands for the induction machine (IM) and the green surface for the permanent magnet synchronous machine (PSM).

The resulting value a for the two machine types is not decisive, since this fitted curve is only usable qualitatively. This means that the prediction of values is hardly realizable by means of this regression function, but for comparison purposes, the obtained equations are usable. This can be shown by the coefficients of determination, which indicate how good the equation fits the provided data [27]. The obtained coefficients of determination for the induction machine and the permanent magnet synchronous machine result in approximately 84 % and 93 %, respectively. The residuals for the induction machine are depicted in Figure 2.7, where the statement can be derived, that the function is well-fitted for lower power values,

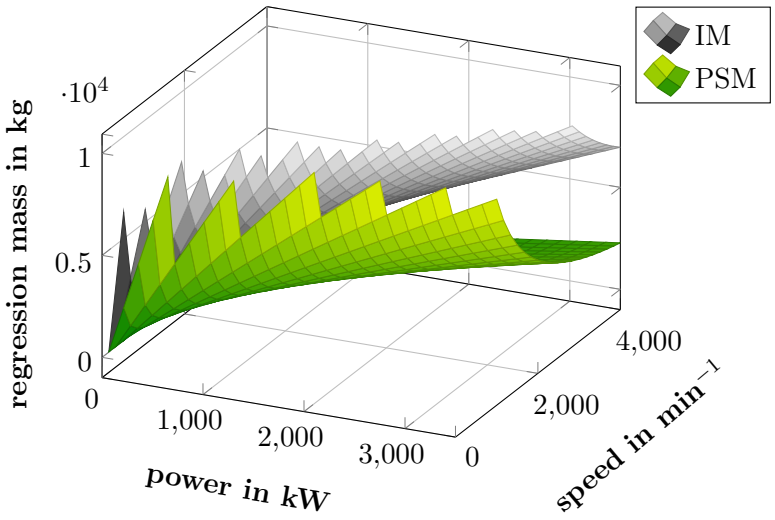

Figure 2.6: Regression mass characteristics for different machine types. The permanent magnet synchronous machine (PSM), displayed in green, results in lower weight than the induction machine (IM), depicted in gray. The regression mass is applied to power and speed based on [P16].

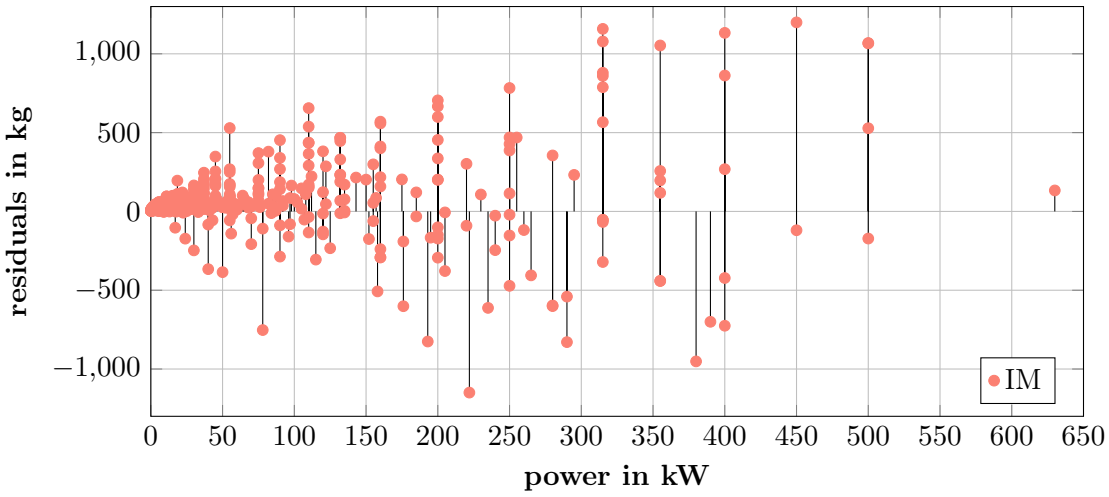

Figure 2.7: Residuals for the regression equation of the induction machine (IM). For lower power values up to 200 kW, the function is well-fitted, whereas the residuals increase with increasing power. Quantitative evaluations are therefore not realistic, but usable for qualitative comparisons.

whereas the residuals increase with an increasing power. The representation of the residuals for the permanent magnet synchronous machine is not shown here, due to the complexity of visualization in three dimensions or the high number of data values. However, the function shows the same behavior – except a few outliers – additionally grouped by speed ranges. Furthermore, the aforementioned constant c_{err} is neglected, although it increases the coefficient of determination for both machines by approximately 1 %. However, physically this constant is not realistic, since the design of a machine, which theoretically requires no speed and no power, would result in weight of the machine different to zero.

In conclusion, with these equations an early statement regarding the weight of the machine becomes possible and the types can be compared. Of course, the validity depends on the minimal and maximal value of the database, since for very high values of the power P and very low speed n, the mass m_{r} reaches infinite values. However, for the range of validity, this result helps to rapidly evaluate the system requirements.

2.6 Reliability and the Related Terminologies

Reliability, fault tolerance, availability, and many other terminologies have become highly important for the evaluation of complete systems [7] and therefore also for the assessment of electrical drive trains. Basically, this topic gains importance due to the increasing number of components whether for redundancy, mechanical, or electrical reasons, such as described in literature and papers, for instance in [114]. There is often a different understanding of the terminologies in discussions about systems' reliability. Reliability is often understood as a comprehensive indicator including a mixture of definitions, such as availability, failure-free operation, fault tolerance, and others. Therefore, this part briefly but clearly defines the different terminologies used within this work. More information about reliability analysis can be found in literature [9].

- In general, *reliability* describes the ability of a device or a system "to perform a required function under stated conditions for a stated period of time" [68]. The reliability values can be determined for an existent item or it has to be predicted, which means considering the design of a device or system regarding "the reliability computed from the observed, assessed, or extrapolated reliabilities of its parts" [68]. In conclusion, *reliability* is the probability of a failure-free operation within a certain amount of time.

- An available system is often mistaken for a reliable system. However, *availability* is a term used for repairable systems, which indicates the time when the system is usable. The value for availability can be calculated from the mean time between failure ($MTBF$) and the mean time to repair ($MTTR$), taking into account the average duration of repair [85].

$$\text{availability:} \quad A_{\mathrm{sys}} = \frac{MTBF}{MTBF + MTTR} \tag{2.8}$$

- In contrast to the $MTBF$ another terminology is the mean time to failure ($MTTF$), where the $MTBF$ is used for repairable and the $MTTF$ for nonrepairable systems [85]. Both variables, as well as the $MTTR$, are given in hours.

- Accordingly, the failure-free operation can be determined by the *failure rate* λ, which is the reciprocal value of the *MTBF* or the *MTTF*, respectively. The failure rate can be visualized by a bathtub curve, which is shown later in Figure 2.12, and hence, it is assumed to be constant during the main lifetime. The constant failure rate is used to define the exponential distribution of the reliability function and consequently, the failure probability function [85].

$$\text{reliability function:} \quad R(t) = \mathrm{e}^{-\lambda t} \tag{2.9}$$

$$\text{failure probability function:} \quad P(t) = 1 - R(t) \tag{2.10}$$

  The reliability function $R(t)$ describes the probability that a system operates without failure in a time range, in contrast to the failure probability function $P(t)$, also called unreliability function [159].

- The *failure probability* describes the probability that a fully functional system experiences a failure within a certain amount of time [36]. The failure probability does not have any unit in contrast to the reliability, as well as the failure rate, which is typically given as failure in time (FIT), defined as the number of failures within the time frame of 10^9 hours.

- *System performance* is an important indicator if the occurring faults can be accepted. It "takes the capacity of different [system] configurations into account" [14]. This means, that after a fault, the remaining system performance can be evaluated depending on the system topology. Then, the decision can be made, whether the remaining performance is sufficient to maintain the service of the assessed system. However, performance does not stand for exclusively for power, but also for any other output unit.

- *Fault tolerance* is another terminology used, describing the ability of tolerating or accepting a defined number of faults within a range of requirements regarding the remaining performance of the system. Vallée et al. [147] even distinguish between reactive and proactive fault tolerance, which differ in the prior knowledge of occurring faults and hence in monitoring and fault detection methods. Within this work, the possibility of proactive fault tolerance is considered, which means to design the system, such that it can suffer a defined number of faults but is still providing the performance needed to run the system adequately.

- *Fault avoidance* is one possibility to increase reliability of a system. This directly leads to detailed component investigations and optimization of those components by means of new materials or new technical developments based on time consuming testing and detailed design approaches [36]. Fault avoidance is not included to this work, hence, the faults occurring within the system need to be accepted and tolerated.

In general, it is noticeable that a safety-critical system can meet the requirements without high reliability, but with high fault tolerance. In other words, a system can be structurally redundant by taking more components – leading to a lower reliability of the sum of components –, but resulting in a higher fault tolerance due to the redundancy. This qualitative statement will be shown later, by a quantitative evaluation regarding the reliability or better fault tolerance. Hence, this system assessment can be conducted by means of the Markovian approach, where the theory is introduced in the next section.

2.7 Markov Chains

The theory of Markov chains, invented by the Russian mathematician Andrey A. Markov (1856–1922), represents a possible mathematical tool to model complex scientific systems proceeding in time steps, i.e. a Markov chain is interested in how those systems evolve over time. Therefore, the Markov chain theory is the basis for the so-called Markov models, which allow to simulate the reliability behavior of technical systems. For instance, Markov models have been already used to investigate on electrical machines, especially regarding fault diagnosis [21, 55, 165]. Generally, Markov chains can be distinguished between two types:

- Discrete-Time Markov Chain (DTMC) and
- Continuous-Time Markov Chain (CTMC).

Whereas DTMC can be calculated by simple matrix multiplication, the CTMC needs to be calculated by a set of differential equations. For traction drive trains, there are no discrete steps, only failure probabilities, and in the following, only the CTMC will be explained in more detail. In case of interest, extensive studies about Markov chains in general, CTMC, DTMC, and building Markov models can be found in other books or publications, such as [14, 26, 53, 59, 86, 111, 138, 163]. Most of the references are formulated very mathematically or just adapted to one special problem. Therefore, the next sections briefly introduce the basics on CTMC, how to build a Markov model including a transition matrix, and how to solve the differential matrix equation in order to simulate a system's behavior. The explanations within the next section are kept as simple as possible – based on [14, 59, 86] –, in order to ensure a simple adaption to other technical systems.

2.7.1 Basics on Continuous-Time Markov Chains

First, the process, which can be calculated due to Markov chains, needs to underlie the *memoryless Markov property*. This means, that – with a given present condition X_k – the past behavior (e.g. X_{k-1}) and the future X_{k+1} are conditionally independent, hence, the past is not important and can be neglected (memoryless). This fact is mathematically expressed in equation (2.11) [14, 86].

$$\begin{aligned} &P(X_{k+1} = j \mid X_k = i, X_{k-1} = i_{k-1}, X_{k-2} = i_{k-2}, \ldots, X_0 = i_0) = \\ &= P(X_{k+1} = j \mid X_k = i) = \lambda_{ij} \quad \text{(transition probability)} \end{aligned} \tag{2.11}$$

A Markov model contains a finite number of states, between two and n, and different transition possibilities (see Figure 2.8). The transitions describe the way from one state to another, whereas it is possible to have forward, backward, and bypass transitions. In the following, they will be distinguished as *short* or *long transitions* and *closed* or *open loop*. A closed loop is a system, in which it is possible to have steps back to previous states, which could mean a possibility of repair for technical systems. In contrast, an open loop describes a system where only progressive transitions to next states are possible, i.e. a system where repair is not feasible or practicable.

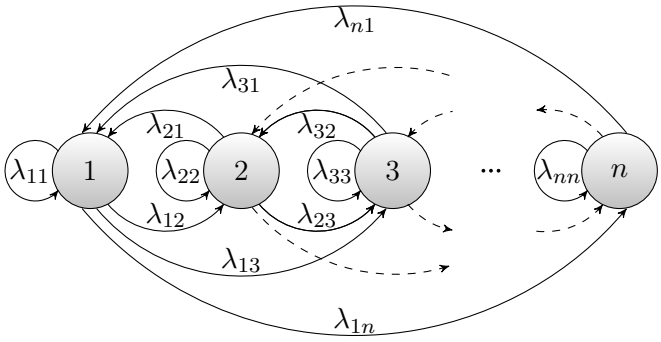

Figure 2.8: General Markov chain with n states and their transitions. In the most general Markov chain, each state can be reached from any other state.

Furthermore, the transitions between states are defined by nonnegative probabilities. These transition probabilities, named λ_{ij} in Figure 2.8 can be summarized in a transition matrix for n states, where each line represents the event probabilities for one state. In addition, the transition probabilities have to be *homogeneous* over time, in other words, they stay constant and never change their value over time [59]. The transition matrix $\boldsymbol{P_\lambda}$ can be written in the form, as follows in equation (2.12).

$$\boldsymbol{P_\lambda} = \begin{pmatrix} \lambda_{11} & \lambda_{12} & \lambda_{13} & \cdots & \lambda_{1n} \\ \lambda_{21} & \lambda_{22} & \lambda_{23} & \cdots & \lambda_{2n} \\ \lambda_{31} & \lambda_{32} & \lambda_{33} & \cdots & \lambda_{3n} \\ \vdots & \vdots & \vdots & \ddots & \vdots \\ \lambda_{n1} & \lambda_{n2} & \lambda_{n3} & \cdots & \lambda_{nn} \end{pmatrix} \tag{2.12}$$

Considering the analysis of technical systems, for example reliability analysis, the transition probabilities can be categorized. They represent:

- failure rates,
- repairs transferring the system from one failure free to another failure free state, and
- repairs, which transfer the system from a failed to an operational state.

In Figure 2.8 it becomes clear that a certain number of states results in a high number of transition probabilities. However, in a real system not every single transition λ_{ij} occurs and hence, can be set to zero. The following four cases can be distinguished for complexity reduction of the matrix.

Case 1: A *closed loop* Markov chain with *short and long* transition steps is the most complex case regarding the transition matrix. It can contain all transition possibilities λ_{ij} depending on the analyzed system. The mathematical expression explains the possibly needed values to calculate such a Markov chain:

$$\lambda_{ij} \neq 0 \quad \forall \quad (i,j) \in \{i, j \in \{1, \ldots, n\} \mid n \in \mathbb{N}\} \tag{2.13}$$

Case 2: If it is an *open loop* system with *short and long* transition steps, the left-handed triangle beneath the diagonal of the matrix can be neglected, hence, set to zero. Consequently, the λ_{ij} on the diagonal and on the right-handed triangle above, need to be filled for calculation:

$$\lambda_{ij} = \begin{cases} \lambda_{ij} & \forall \ \ (i,j) \in \{i, j \in \{1,\dots,n\} \mid j \geq i \wedge n \in \mathbb{N}\} \\ 0 & \text{otherwise.} \end{cases} \tag{2.14}$$

Case 3: For a *closed loop* Markov chain with only *short* transition steps, the matrix can be simplified to the diagonal and both secondary diagonals, whereas all other λ_{ij} are set to zero. In literature, this case is also called birth-death process [22, 154]. The diagonals can be explained mathematically as:

$$\lambda_{ij} = \begin{cases} \lambda_{ij} & \forall \ \ (i,j) \in \{i, j \in \{1,\dots,n\} \mid (j = i \vee j = i \pm 1) \wedge n \in \mathbb{N}\} \\ 0 & \text{otherwise.} \end{cases} \tag{2.15}$$

Case 4: Finally, the less complex matrix is the version with an *open loop* and only *short* transition steps. Here, the complete lower left-handed triangle beneath the diagonal, as well as the triangle above the positive secondary diagonal, can be set to zero. Thus, the λ_{ij} on the diagonal and on the positive secondary diagonal remain for calculation, which is described as:

$$\lambda_{ij} = \begin{cases} \lambda_{ij} & \forall \ \ (i,j) \in \{i, j \in \{1,\dots,n\} \mid (j = i \vee j = i + 1) \wedge n \in \mathbb{N}\} \\ 0 & \text{otherwise.} \end{cases} \tag{2.16}$$

These four cases are visualized by the partly simplified matrices, such as shown in Table 2.4. The reduction of the matrix finally leads to a reduction of differential equations for the Markov model calculations.

Furthermore, each line of $\boldsymbol{P_\lambda}$, including all transition probabilities from one state, needs to sum up to one, since transition events have to take place at continuous time without delay.

$$\sum_{j=1}^{n} \lambda_{1j} = \sum_{j=1}^{n} \lambda_{2j} = \ldots = \sum_{j=1}^{n} \lambda_{nj} = 1 \tag{2.17}$$

Additionally, for building the matrix for a Markov chain, the diagonal of the matrix needs to be defined as follows in equation (2.18). It describes that the value λ_{ii} is the negative sum of the transition rates for one state [59] or in other words that each row needs to sum up to zero.

$$\lambda_{ii} = -\sum_{i \neq j} \lambda_{ij}, \quad i, j \in \{1,\dots,n\} \tag{2.18}$$

Hence, the matrix $\boldsymbol{M}$ – called transition intensity matrix [88] – can be received by the subtraction of the transition matrix $\boldsymbol{P_\lambda}$ and the identity matrix $\boldsymbol{I}$.

$$\boldsymbol{M} = \boldsymbol{P_\lambda} - \boldsymbol{I} \tag{2.19}$$

Table 2.4: Transition matrix influenced by transition types and loop types. Four combination cases can be deduced out of the transition and loop types, which define the complexity of the transition matrix. k equals $(n-1)$ for the sake of clarity.

	short and long transitions	short transitions
closed loop	$\begin{pmatrix} \lambda_{11} & \lambda_{12} & \lambda_{13} & \cdots & \lambda_{1n} \\ \lambda_{21} & \lambda_{22} & \lambda_{23} & \cdots & \lambda_{2n} \\ \lambda_{31} & \lambda_{32} & \lambda_{33} & \cdots & \lambda_{3n} \\ \vdots & \vdots & \vdots & \ddots & \vdots \\ \lambda_{n1} & \lambda_{n2} & \lambda_{n3} & \cdots & \lambda_{nn} \end{pmatrix}$ **Case 1**	$\begin{pmatrix} \lambda_{11} & \lambda_{12} & 0 & \cdots & 0 \\ \lambda_{21} & \lambda_{22} & \lambda_{23} & \ddots & \vdots \\ 0 & \lambda_{32} & \lambda_{33} & \ddots & 0 \\ \vdots & \ddots & \ddots & \ddots & \lambda_{kn} \\ 0 & \cdots & 0 & \lambda_{nk} & \lambda_{nn} \end{pmatrix}$ **Case 3**
open loop	$\begin{pmatrix} \lambda_{11} & \lambda_{12} & \lambda_{13} & \cdots & \lambda_{1n} \\ 0 & \lambda_{22} & \lambda_{23} & \cdots & \lambda_{2n} \\ 0 & 0 & \lambda_{33} & \cdots & \lambda_{3n} \\ \vdots & \ddots & \ddots & \ddots & \vdots \\ 0 & \cdots & 0 & 0 & \lambda_{nn} \end{pmatrix}$ **Case 2**	$\begin{pmatrix} \lambda_{11} & \lambda_{12} & 0 & \cdots & 0 \\ 0 & \lambda_{22} & \lambda_{23} & \ddots & \vdots \\ 0 & 0 & \lambda_{33} & \ddots & 0 \\ \vdots & \ddots & \ddots & \ddots & \lambda_{kn} \\ 0 & \cdots & 0 & 0 & \lambda_{nn} \end{pmatrix}$ **Case 4**

For most applications, the Markov chain describing the appropriate system approaches a final state, at which point the system completely fails. This type of Markov chain is called *absorbing*; contrary to the *ergodic* Markov chain, which is somehow alternating between the states [88]. The extreme type of the ergodic Markov chain is the *irreducible* one, where every state is reachable from every other state, such as generally presented in Figure 2.8. Moreover, the transition probability for all existing transitions is greater than zero. The transitions typically are *homogeneous*, which means that each transition probability stays constant during the calculation. This type of transition is assumed to be sufficient for technical systems being proved in literature, for instance in [85]. In contrast, *inhomogeneous* transitions – which mean changing probabilities over time or probabilities, which differ from the exponential characteristic – lead to semi-Markov models [4], which are not discussed in this work. Another distinction between Markov models is *finite* or *infinite* number of states, where *finite* describes a fixed number of states during calculation and *infinite* a dynamic increase of the number of states, which represents a sudden occurrence of unknown states. The latter is neglected in this work.

2.7.2 Results of Differential Equations

After obtaining the transition intensity matrix $\boldsymbol{M}$, the differential matrix equation (2.20) can be identified in order to calculate the probabilities for each state.

$$\dot{\vec{y}}(t) = \boldsymbol{M} \cdot \vec{y}(t) \tag{2.20}$$

This system of ordinary differential equations can be solved by using Euler's method, based on an initial vector $\vec{y}_0$ and a step width Δt at t_k with $k = [0, n]$:

$$\vec{y}_{k+1} = \vec{y}_k + \Delta t \cdot \boldsymbol{M} \cdot \vec{y}_k \tag{2.21}$$

The resulting values $\vec{y}_{k+1}$ directly characterize the system's behavior over continuous time.

In order to facilitate the calculation of Markov models, a script has been implemented within this work in order to calculate the Markov chains and solve the corresponding differential equations mentioned above.

2.7.3 Implementation of Automatic Calculation

The implementation of an automatic calculation was realized in MATLAB (version R2015a, "The MathWorks, Inc.") and enables a quick simulation of Markov models. The flowchart of the function is shown in Figure 2.9.

At first, the function asks for some input values of the assessed system, such as the number of states, the possibility of repair, and the transition type. Due to these parameters, the matrix with the transition probabilities can be predefined, as mentioned in section 2.7.1.

The next step is the entry of the transition probabilities λ_{ij} for each state. The sum of row (SOR) is checked after each row entry. In case, that the sum of row is not equal to 1, the current row needs to be entered again. As soon as the matrix is filled up appropriately, the algorithm asks for the number of simulation steps and the initial starting vector $\vec{y}_0$, defining the starting probability or in other words defining in which state the calculation starts. Afterwards, the differential equations are solved and the corresponding results are saved in a text file for further data processing or visualization.

2.7.4 Multi-State System Markov Models for Reliability Assessment

Within technical systems or components, the probability for the total system failure is usually the most interesting aspect for the reliability assessment. The binary-state or two-state system is the simplest Markov model, only representing a failure-free operating mode and the failed state of a system. However, it is more significant to evaluate a possible system performance degradation, which can be considered by introducing multiple states in order to represent the degradation levels until the system fails completely [84]. Therefore, one special state arrangement of Multi-State System Markov Models (MSS-MM) is presented – the *birth-death model* –, followed by the explanation how the number of states and the transition probabilities can be determined and what the appropriate transition types are.

Birth-Death Model

A general example for a birth-death model is depicted in Figure 2.10, where n is the absorbing or failed state. The forward connections symbolize the occurrence of faults, whereas the backward connections stand for the possibility to recover. The difference between a repairable and a nonrepairable system or component regarding the Markov model can be seen in the

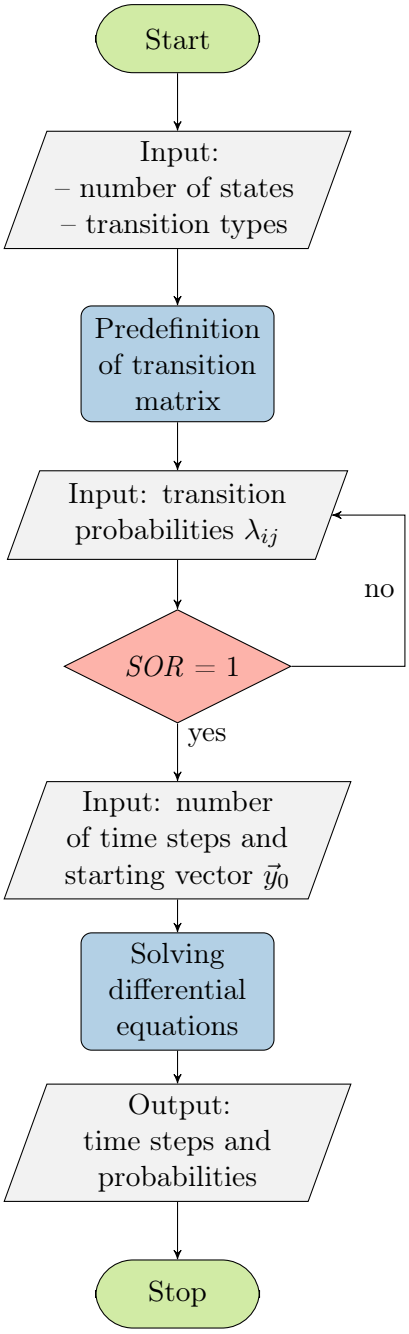

Figure 2.9: Flowchart of automatic Markov model calculation describing each action of the calculation, for instance filling the transition probabilities before the sum of row (SOR) of the matrix is checked.

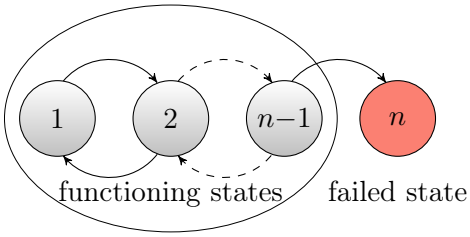

Figure 2.10: An exemplary multi-state Markov birth-death model with n states for the evaluation of a component or a system. The n-th state is an absorbing state, which means total failure, whereas all states from 1 to $(n-1)$ are functioning states.

aforementioned Table 2.4, where **Case 3** describes the repairable and **Case 4** the nonrepairable version. Furthermore, the failure types can be classified by minor and major failures, where minor failures lead to the next state and major failures result in a transition to a state after the next one or even in a transition to the system's death. Figure 2.10 shows only an example for minor failures. In case of a possibility to recover, also the back transitions can be minor or major, of course. [22, 88, 154]

Other extensions of this model have been shown, such as the performance-demand model [88], which can be used mainly for the determination of a system's availability. In this work, it is sufficient to use the typical birth-death model including minor or major failures.

Determination of Number of States and Transitions

In order to use the Markovian approach for the assessment of reliability, the focus needs to be set on the requirements in case of a failure. The approach to determine the number of states and the transitions bases on a method, called degree of fault tolerance, which was presented in [16, 17]. The theoretical graphical interpretation of the degree of fault tolerance is depicted in Figure 2.11, which is based on [88]. This illustration simplifies the explanation how to select the number of states.

Selection of the Number of States: The solid black line in Figure 2.11 represents the performance behavior of the system after the occurrence of critical faults. The steps stand for a thereby involved performance degradation at a certain time t_i. For instance, for $i = 3$ three critical faults occur, which result in the appropriate degradation and the third fault at the time t_3 causes the system's death. The dashed red line is defined by the load level, which is required to operate the system while providing sufficient performance. This means that the fault at the time t_2 already limits the functional operation; hence, the system is not working sufficiently to comply with the requirements.

In other words: In case of an occurring fault, the drive train system suffers a power degradation. So, as long as a system is still able to operate after a certain number of faults and complies with the system requirements, the number of states is determined by the number of degradation levels defined by the maximum acceptable performance reduction. Calculating the amount of degradation per fault and taking into account the required power for operation despite of faults, it is possible to determine the required number of states for the Markov model.

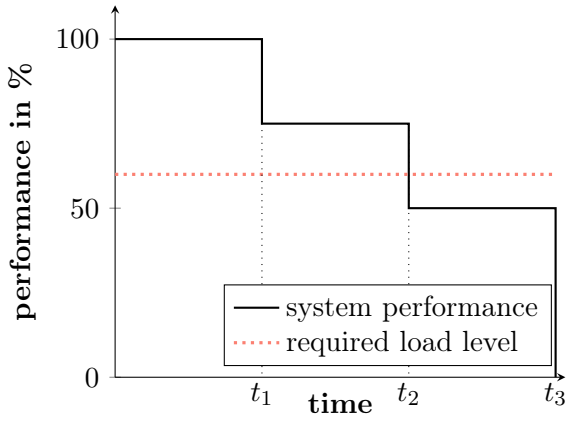

Figure 2.11: The theoretical graphical interpretation of the degree of fault tolerance ($DOFT$) is based on [88], with respect to the possible power degradation of a system.

Determination of the Transition Probabilities: Dependent on the degradation levels, the transition probabilities are defined by the respective faults and their probabilities leading to the performance degradation. The first step is the *identification of all possible faults* within the assessed system. Hence, all units and elements need to be listed and the corresponding faults, which are possible to occur, are collected. Depending on the level of detail, this usually leads to a fault tree analysis (FTA) or a failure mode and effects analysis (FMEA), especially within product development in industry. These procedures are time consuming and failure documentation or the experience of fault occurrence for components or systems is required.

Second, the *distinction between critical and noncritical failures* is important to evaluate the system's behavior after the occurrence of failures and to decide whether a failure needs to be considered for further calculation or not. This is depending on the failure consequences, which are here defined as performance degradation. It means that a failure is noncritical if it is leading to a certain amount of performance degradation but not to a complete system failure, also called fail operational. In contrast, a failure resulting in a performance degradation level – which is not sufficient to run the system – is a critical failure. However, several noncritical faults can finally lead to a critical failure within the system and hence need to be taken into account.

Third, the possibility of *failure recovery* needs to be evaluated regarding its complexity of implementation. This possibility characterizes the transition types, as well as the recovery of degradation in order to repair or renew a system. The possibility of recovery is highly influenced by the available installation space, since failure recovery can be supported by structural redundancy, hence, devices replacing others in case of failure. Furthermore, recovery can be obtained by repairing the failed component, whereas for some applications repair is not applicable.

Fourth, all component faults leading to a certain failure, which is linked to a *performance degradation* are summed up in order to get the first transition probability. The single failure probabilities can be found in literature, as suggested and mentioned later on, or by statistical evaluation of failure protocols of existing electrical actuators. As previously explained, the failure rates are constant and therefore not changing over time while neglecting the aging of the system components. However, the transitions leading to following states change according

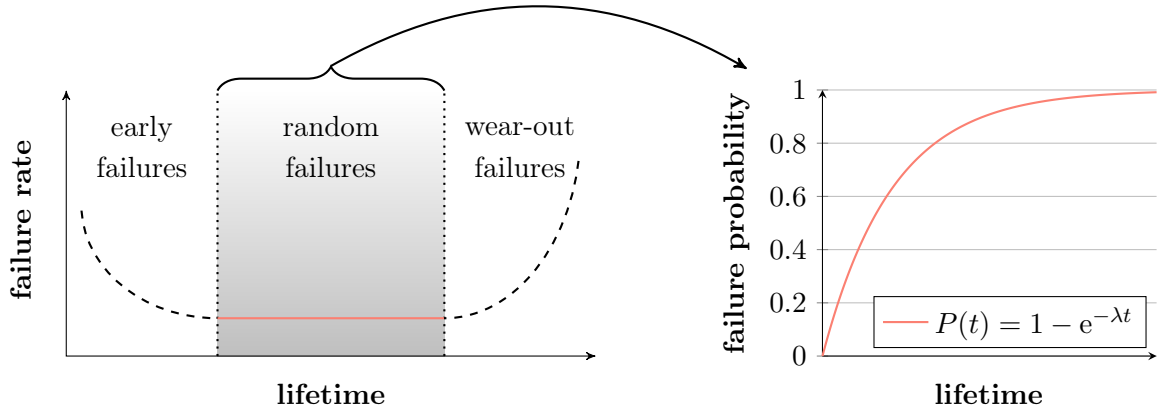

Figure 2.12: Relationship between bathtub curve and exponential failure probability function [85]. The exponential failure probability function $P(t)$ is only valid for the shaded area of the bathtub curve, where the failure rate λ is constant.

to the exponential function compared to the first transition, but still stay constant during the calculation of the model. This means that the constant failure rate is only defined by *random failures* during the lifetime of a system, where *early* and *wear-out failures* are exempted. This is assumed to be a valid approach, since early and wear-out failures must not occur within safety-critical systems; where the components are tested before using and replaced before failing. However, the failure probability evolves over time, since after a failure of a component, all other components have been in operation, and hence the failure probability has to increase, which somehow takes aging into account. This evolution over time is modeled by exponential function depending on the failure rate λ and the lifetime t, as previously mentioned within this chapter. Figure 2.12 – which was taken from [85] and slightly adapted – shows the bathtub curve representing the failure rate over time, and the exponential function, which needs to be applied to obtain the failure probability and hence, the new failure rate.

In conclusion, the Multi-State System Markov Models are helpful to characterize drive train systems, but it becomes clear that the determination of the transition probabilities and the chosen number of states including the definition of each state are the decisive parts in order to start the calculation of the system behavior.

2.8 Conclusion for the Potential Analysis

In chapter 1, the demand of system consideration was explained, whereas the components on its own need to be evaluated before setting up the electrical drive train. Combining the methods presented in this chapter to a methodology leads to the possible structure shown in Figure 2.13. This structure tries to fill the gap between the system definition and the component selection within the V-model, which was previously explained in subsection 1.2.1. The sum or the cloud of methods, which was presented in the previous chapter, is divided into two steps, the *system check* and the *potential analysis*. Chapter 3 is dedicated to describing the solution space for the system check. The evaluation of requirements and the overall potential analysis are presented in chapter 4 and chapter 5, based on the hierarchical system approach.

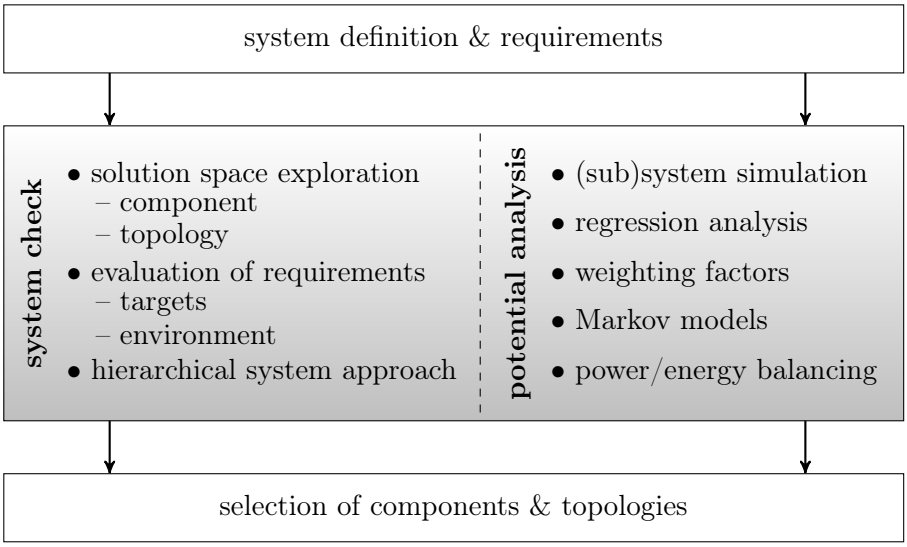

Figure 2.13: Methodology for the potential analysis of electrical drive trains. The step from the system definition and requirements to the component and topology selection can be conducted by means of the sum of presented methods.

3 Solution Space of Drive Train Components

This chapter focuses on the solution space of the drive train components to demarcate possible combinations. As mentioned in chapter 1, only electrical machines and power electronics are considered and they are explained within this chapter. This means that for both components different topologies or types and their characteristics are depicted. Failure cases are presented for the electrical machine and the power electronics, since performance degradation caused by failures needs to be identified. In order to ensure a fair system assessment, the overall definition of the components' interdependencies needs to be set up which signifies the definition of the interface between the components. This interface is represented by varying the number of phases m. Therefore, the configuration of the drive train system and the consideration of decisive failure cases are defined.

3.1 Electrical Machines and Their Characteristics

Electrical machines have been built, investigated, and developed for more than 150 years. Since then, researchers investigated on working principles, materials, and – after the invention of power electronics – control techniques, which have been improved always targeting at increasing torque density and efficiency. The next subsection is dedicated to presenting the further assessed machine types – as can be seen in Figure 3.1 – and to conclude their advantages and disadvantages in a more general way. Additionally, failure cases are highlighted for the electrical machine in order to find the critical faults, which need to be taken into account for assessing drive train systems.

3.1.1 Different Machine Types

Basically, AC electrical machines can be divided into induction machine and synchronous machine. The synchronous machine can be built as permanent magnet, separately excited, or reluctance machine, whereas the induction machine can be carried out as squirrel cage or slip-ring induction machine. However, the slip-ring induction machine and the separately excited synchronous machine [69, 72] are excluded from the analysis, since they require higher maintenance effort due to the slip-rings needed to supply the rotor with current. The slip-rings are characterized by a high abrasion and therefore lower reliability due to contamination.

Furthermore, the application of electrical machines to any vehicle type was shown in chapter 1 and the two different AC machines emerged to be commonly used, which can also be seen in [167]. Therefore, the reluctance machine is disregarded in this work and only the permanent magnet synchronous machine and the induction machine are considered, which are presented in the following paragraphs.

Permanent Magnet Synchronous Machine

At first glance, the stator is basically constructed the same for both machines. The distinction between induction and permanent magnet synchronous machine is defined by the rotor design. An example of the permanent magnet synchronous machine (PSM) is depicted in Figure 3.1a, here realized as a PSM with surface mounted magnets on the rotor, colored in red and green. The type of magnet allocation is not important at this point, since only the working principle and not the design of the electrical machines is considered. The winding in the stator slots is schematically illustrated in blue.

The permanent magnets support the machine with their high energy density. Thus, the PSM provides the highest power density and efficiency at nominal speed compared to other types of electrical machines, which is commonly known in literature and which is shown later within this work. The high efficiency is also the reason for the use of PSM for direct drives without gearbox and low rotational speeds [8]. One further advantage is, that the rotor does not need windings connected to an external rotor excitation, which results in having no rotor copper losses [44, 54, 157]. This means that the machine requires less cooling ending up with a smaller overall volume and weight of the overall drive train.

The basic disadvantage of using permanent magnets is the need for rare-earths which are costly and hence, increase the production costs [44]. However, this fact is not decisive within this work due to the application within the field of safety-critical mobile systems, where the focus is set on fault tolerance and torque density, respectively. Permanent magnets in form of rare-earths are typically used, due to a relatively low magnet volume [8], which makes the PSM auspicious for high torque density or power density applications [157]. The efficiency decreases at higher speeds, but high speeds especially are critical for surface-mounted magnets, since the assembly quality decreases the maximum rotational speed due to centrifugal forces [37]. The permanent magnet synchronous machine is commonly used for high-torque low-speed applications, which is a requirement resulting from direct drives. Hence, it is important to choose a high number of poles in order to reduce the flux per pole [105], which enables an increase of the torque due to the possibility of decreasing the thickness of the yoke.

Induction Machine

The induction machine (IM), which is also known as asynchronous machine, probably is the most commonly used for industrial applications, due to the robustness and comparably low maintenance. Hence, the high reliability is one advantage of the induction machine [54]. Additionally, the noise and vibration characteristic of the machine is better compared to other machines [101]. However, even though the material cost for the machine parts are lower than for other machine types, the bearing characteristic – in order to ensure the necessarily small air gap – leads to increased production costs [44, 101]. In contrast, the complexity regarding the construction is lower than for the permanent magnet synchronous machine. Furthermore, the efficiency decreases at lower speeds, whereas the power decreases at higher speeds, which leads to a limited operation [44, 54]. A schematic illustration for a squirrel cage induction machine is shown in Figure 3.1b, whereas the stator winding is again displayed in blue and the rotor bars of the squirrel cage of the rotor are colored in orange.

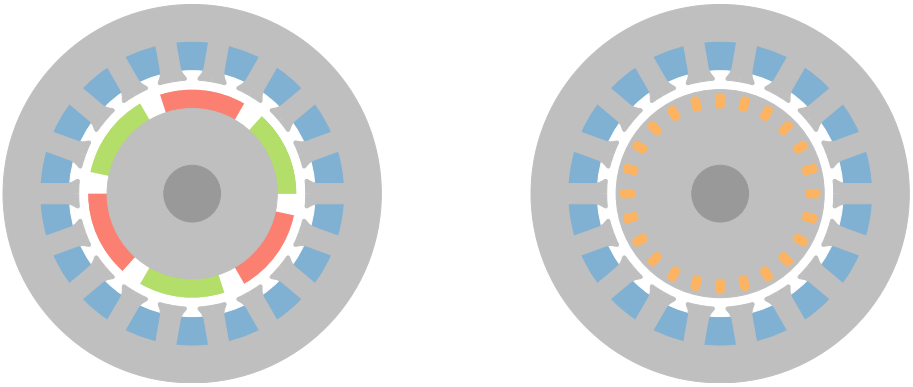

(a) (b)

Figure 3.1: Schematic illustration of the considered machine types. A schematic cross section of a permanent magnet synchronous machine is shown in (a) and an induction machine in (b). Both machines can have the same stator, hence at first glance only the rotor distinguishes the two machine types.

Compared to the permanent magnet synchronous machine with surface mounted magnets, the rotor is slotted and within the slots rotor bars – made of aluminum or copper – are placed. These rotor bars are short-circuited by solid rings on both sides of the rotor, which resembles a cage. A voltage system is induced by the stator field impressing a rotating current in each bar, where always two bars form one winding over the appropriate segment of the rings. The created magnetic rotor field interacts with the stator magnetic field and generates the torque. The stator is supplied by m phases (typically $m = 3$). The stator field is created by windings in the slots of the stator core, which is produced out of laminated steel, where the stator currents are impressed by a voltage provided by an inverter. [8, 157]

For the reliability analysis, the failure cases of both electrical machine types need to be considered. Hence, the next subsection shows these failure cases, as well as the difference between the induction and the permanent magnet synchronous machine.

3.1.2 Failure Cases

The failure cases for an electrical machine are presented in Figure 3.2. The figure shows a qualitative fault tree, which aims at illustrating the common and different faults between the permanent magnet synchronous machine and the induction machine. In general, the main faults within electrical machines are [137]

- winding faults including stator insulation and open-circuited phases,
- bearing faults and mechanical damage of the rotor,
- eccentricity of the rotor,
- damage of the laminated core,
- damage of the rotor bars or end-rings of the IM, and
- damage of the permanent magnets of the PSM.

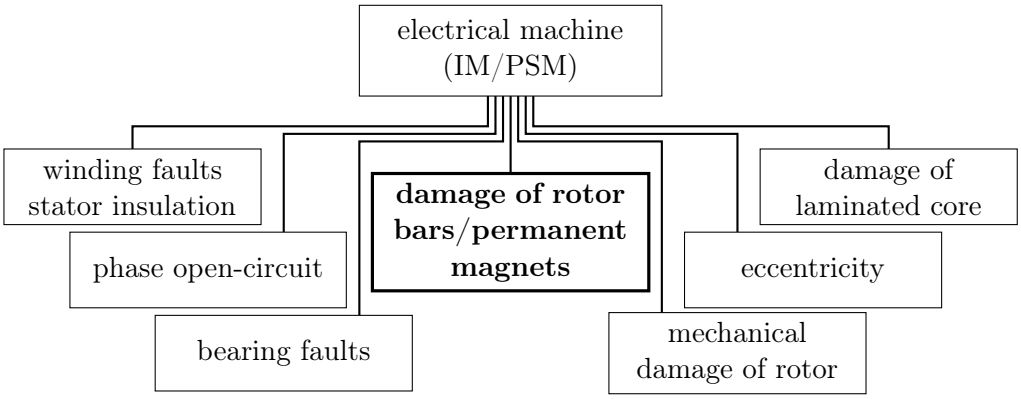

Figure 3.2: Qualitative fault tree of electrical machines. The common and the different faults for induction machine (IM) and permanent magnet synchronous machine (PSM) are summarized based on [137, 162].

The main difference between the two machine types is based on the rotor with a *damage of the rotor bars* or the *permanent magnets*. Each of the faults shown in Figure 3.2 contains its own fault tree heading towards the single material of elements. Based on these illustrations, the previously mentioned fault tree analysis (FTA) and FMEA are conducted especially in industry. These two methods are not taken into account within this work, but the qualitative fault tree serves as illustration to classify the faults of electrical machines. The overall failure rate of the machine can be calculated as the sum of the appropriate single failure rates. Although the same faults, except the rotor related ones, occur for both machine types, the failure rates depend on the power and speed requirements based on the application case. Hence, the evaluation of the appropriate failure probabilities, needed for further calculations, is included in the following chapters.

3.2 Power Electronics and Their Characteristics

Section 3.1 described only one necessary part of electrical drive trains, whereas the component *electrical machine* still requires *power electronics*, which provides the alternating voltages to the machine. Starting from the scratch, Figure 3.3 illustrates a basic overview of converter types or functions.

This research work covers mobile applications, as explained in section 1.1. The AC-AC-converter is typically used for grid connections and is therefore not useful for mobile applications. Rectifiers are also exempted from this work – as recuperation is not considered –, as well as the DC-DC-converter due to the high requirements regarding volume and weight. Drive trains for mobile applications are supplied by DC-sources, such as a battery. Since the aforementioned electrical machines require AC-voltages, only the DC-AC-converter is relevant for the electrical drive train. This is the only converter type being considered for the assessment. Nevertheless, a DC-AC-converter can be implemented based on different topologies, which means regarding the arrangement of the switches or devices in order to supply the stator phases of the machine. Therefore, this section will focus on the different converter designs – based on different arrangements of the switches – and the respective failure cases of the converter.

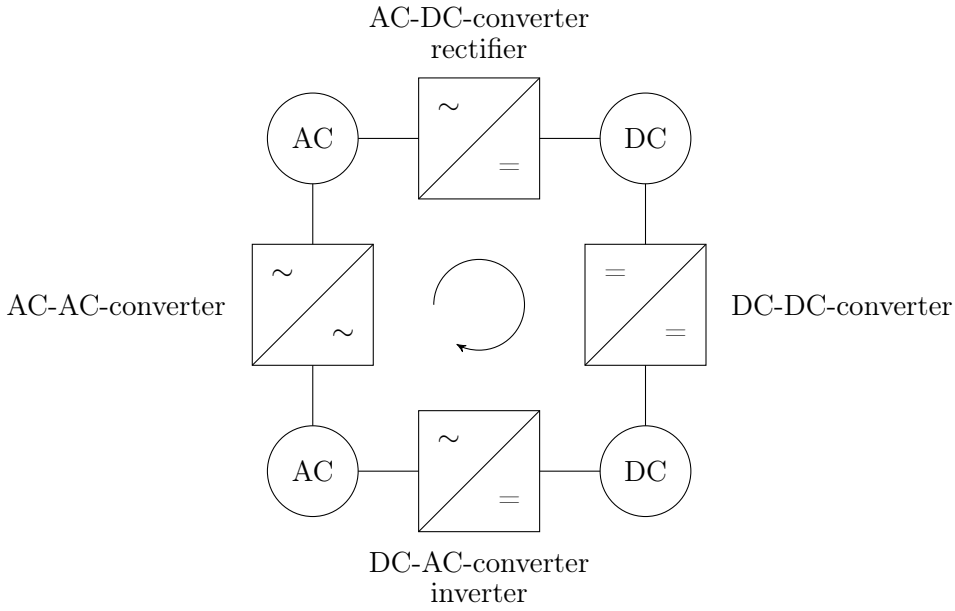

Figure 3.3: Different types of power converters [118]. Each converter type enables the conversion of power, whereas for the consideration within this work, only the DC-AC-converter is relevant for the electrical drive train of mobile applications.

3.2.1 Converter Design

The different arrangement of the switches leads to two converter topologies commonly used in any kind of application – half-bridge and full-bridge topology. Figure 3.4 shows these arrangements schematically, whereas each switch S_i consists of a semiconductor in parallel to a freewheeling diode. Nevertheless, for the first general illustration, the representation by a simple switch is sufficient. Additionally, within this section, the machine's phase is represented by a single inductance instead of a resistance, inductance, and an induced voltage. This is a valid assumption at this point, since the focus is set on the topologies of power electronics and not the physical simulations.

Half-Bridge Converter

Half-bridge converters consist of two semiconductors per phase and with the appropriate control of the switches, a positive or a negative voltage is applied to the phase and therefore produces the needed alternating voltage. Hence, only one switch per half-bridge leg may be closed at the same time in order to avoid a short-circuit of the voltage source. Increasing the number of half-bridge legs results in the same number of possible phases. Figure 3.4a shows an example for the connection of machine phases with m half-bridge legs, where m is the number of phases. Hence, the number of switches needed to realize the half-bridge topology is calculated from the number of phases m times two.

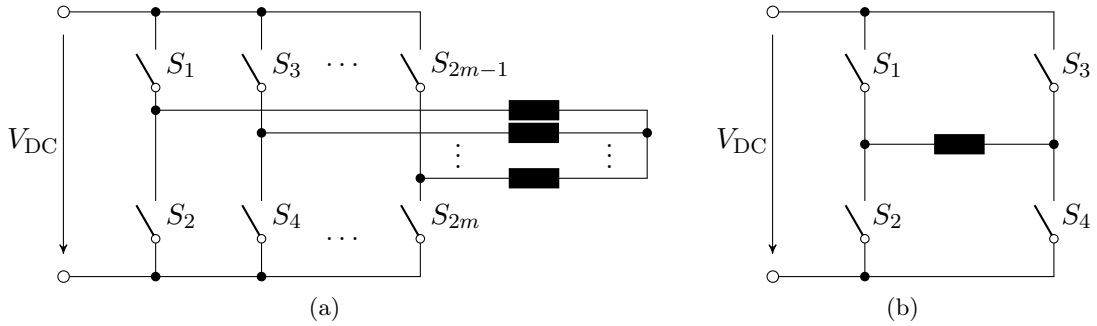

Figure 3.4: General half- and full-bridge converter structures. In (a), a connection of half-bridges for m phases with star connection is shown, whereas (b) illustrates one module for full-bridge topologies, which is used m times to connect to m phases.

Full-Bridge Converter

A full-bridge converter, also called H-bridge, is a topology of two half-bridge legs framing one phase and thus consists of four semiconductors per phase. In order to produce an alternating voltage, the switches are again controlled appropriately by closing the crosswise opposite switches, which are not in the same leg, in a way that no short-circuit is generated. A graphical interpretation of this topology for one phase can be seen in Figure 3.4b. The number of switches is determined by the number of phases m multiplied by four. Additionally, the number of voltage sources equals the number of phases m, as well as the number of capacitors and printed circuit boards.

3.2.2 Failure Cases

The failure cases for the inverters are well-documented in literature, such as in [156], including their statistical distribution. The most probable components to fail are the semiconductors (semi) with 21 %, the printed circuit boards (pcb) with 26 %, and the capacitors (cap) with 30 % of the appeared failures. Based on these data summarized in Figure 3.5a, the three mentioned components of power electronics and additionally the diode are taken into account for the reliability calculations later in this work. Figure 3.5b shows the cause distribution for the appeared failures. Hence, more than 77 % of the appeared failures are considered. Overheating, for instance due to overload, is the most likely effect to cause a failure of components, which takes 55 % of the overall failure causes. [156]

Furthermore, there are different consequences which follow for instance on semiconductor failures. These consecutive faults are

- short-circuit of a single inverter switch,
- short-circuit of two switches in one inverter leg,
- open-circuit of a single inverter switch, and
- open-circuit of one phase (internal or external),

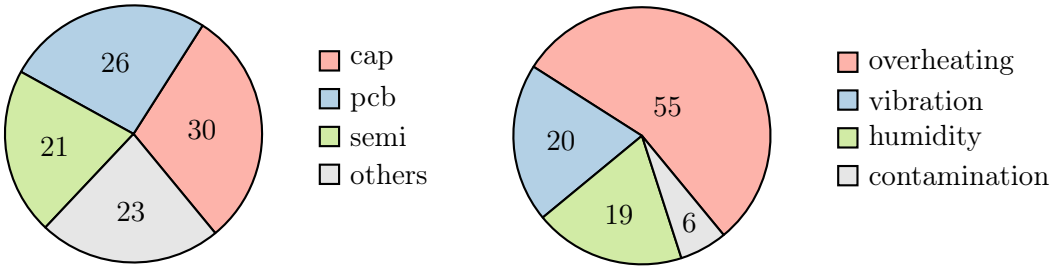

(a) (b)

Figure 3.5: Statistics on failures of power electronic components and their causes given in percent [156]. In (a) the semiconductors (semi), printed circuit boards (pcb), and the capacitors (cap) make the greatest part of the failing components. Overheating is assumed the most probable cause for failures, as depicted in (b).

Table 3.1: This table summarizes the number of the components – considering semiconductors, diodes, capacitors, and printed circuit boards – depending on the number of phases m for both the half- and full-bridge converter topologies.

	half-bridge	full-bridge
number of semiconductors	$2 \cdot m$	$4 \cdot m$
number of diodes	$2 \cdot m$	$4 \cdot m$
number of capacitors	1	m
number of printed circuit boards	1	m

which are explained and often considered for reliability or fault tolerance analysis [158]. In such failure cases, the inverter leg or inverter module needs to be shunted or switched off in order to avoid the influences of the faulty component on other components. In any case, this failure leads to a rapid increase in current and hence an overload operation or a power degradation, since the needed current for the nominal power cannot be carried. An overload and the respective increase in current lead to an overheating, as mentioned above, while decreasing the system's reliability and lifetime. In order to provide the ability to shunt inverter legs or module, fault detection needs to be implemented, as well as shunts replacing the failed components. The fault detection and the monitoring system, as well as its technical implementation of shunts, are worth a separate investigation, such as conducted for instance by [32]. However, these topics are not covered in this work, but assumed to be implemented.

Table 3.1 summarizes the number of components for the different inverter topologies. The number of semiconductors, diodes, capacitors, and printed circuit boards are opposed to each other for the conventional inverter topologies in Figure 3.4, depending on the number of phases m. It is visible that the number of semiconductors and diodes for the full-bridge topology is twice the number of components for the half-bridge topology. For the number of capacitors and printed circuit boards, the difference between the two topologies is defined by the multiplication of the components by the phase number m. The failure rates of the components and the resulting failure rates for the different topologies are presented later based on relevant literature references.

3.3 Solution Space: Electrical Drive Train

Since the solution space is already defined by the single components *electrical machine* and *power electronics*, the solution space for the overall drive train system needs to be completed. The interface between both components is the cabling and hence, the number of phases, which is considered as a degree of freedom within this work. Additionally, the overall failure cases need to be depicted, which basically include all previously mentioned component failures.

3.3.1 Number of Phases as Degree of Freedom

Conventional electrical machines or drive trains are mostly designed with three phases. Within this work, different phase numbers are analyzed and opposed to each other. Hence, the considered phase numbers are three phases as conventional phase number and above up to 11 phases. All systems, having a phase number above three, are called multiphase systems. Taking into account literature, for instance [6, 34, 83, 133, 152], multiphase arrangements have already been investigated and have also been used in practical applications, for instance ship propulsion, wind energy systems, and elevators. An extensive summary of multiphase drive applications can be found among others in [82].

Advantages and Challenges

Increasing the number of phases first of all increases the complexity of the system architecture. Since the number of components will be increased and the reliability of a system is calculated by the failure rate of each component, the reliability of the system is worsened. However, the change of the phase number comes along with several benefits, especially for safety-critical drive trains. By the increase of the number of phases, the system's fault tolerance is enhanced. Fault tolerance probably is the most crucial impact of increasing the phase number, since every single phase additionally being implemented above three phases, practically results in redundancy [45, 83]. This could already be shown in [71]; an open phase within a three-phase system can directly result in a system failure, whereas within a multiphase system, the system can still perform its functionality depending on the system's requirements.

Another benefit is that the stator losses decrease with increasing the number of phases, where a reduction between 5 % and 9 % is possible from five up to 12 phases [161]. This comes due to the fact that the current or power per phase can be reduced, in case of the same overall required power and a constant voltage. Besides, even though the number of semiconductors is increased proportionally with the number of phases, the size, weight, and cost of each semiconductor can be reduced, since less current has to be conducted [161]. In contrast, even though the single semiconductors are smaller and lighter, the overall size and weight of the inverter can still be higher – hence, worse – [60, 83] depending on the number of components which are necessary for the appropriate phase number and the inverter topology (see Table 3.1). Regarding the machine, a higher power density is possible by multiphase topologies compared to the conventional three-phase systems [60]. The torque ripple and torque fluctuations are decreased in healthy and failure case by increasing the number of phases, as shown in [P5, P11] and [82]. The harmonics, which are not producing torque, are also decreased, which leads to lower noise emissions and a higher efficiency [82].

In conclusion the advantages of multiphase drives are

- an increase of fault tolerance,
- a reduction of current and power per phase, and
- an increase of power density.

3.3.2 Failure Cases

The system generally contains all previously described faults of the electrical machine and the power electronics. Hence, for further assessment some assumptions need to be made in order to include the most important failures on a system point of view. In literature, the most analyzed type of failure is the open-phase fault [34], which means the loss of phase. As mentioned above, assuming shunted circuits and a fault detection possibility to be implemented, all other faults of power electronics and electrical machine can be represented by an open-phase fault. By shunting or switching off the phase in case of any fault concerning the phase, an open-phase fault is created covering the occurred faults. Besides, in case of a short-circuit of two phases, the fault is covered by a loss of these two phases. In general, the loss of phase is also the most critical fault for the system, since it directly leads to an overload condition or a degradation of performance. Figure 3.6 schematically shows the loss of phases for an m-phase system. The loss of i phases is the limit in order to sustain the requirements, which still leads to a fail-operational mode.

In conclusion, the solution space used within this work was defined, considering electrical machines, power electronics, and their interdependencies. This solution space forms the basis in order to apply the presented methodology to a safety-critical aircraft application.

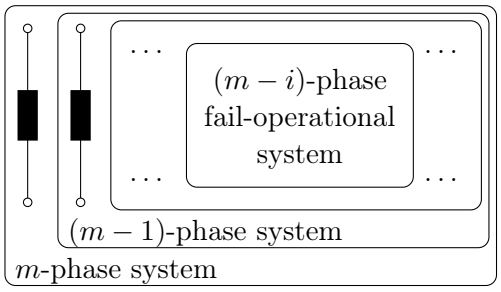

Figure 3.6: System consideration defined by the number and the loss of phases, based on [P11]. An m-phase system can lose i phases and still be fail-operational depending on the system requirements.

4 Application of the Potential Analysis to an Electrical Helicopter

The helicopter EC135 or H135, which is produced by Airbus Helicopters (formerly Eurocopter), is taken as platform for the drive train electrification and it is graphically presented in Figure 4.1. This kind of helicopter is used for both civil and military applications. Thus, it is a transportation vehicle for human beings and can therefore be considered as a safety-critical system as mentioned previously in section 2.1.

Only the electric traction drive of the helicopter's main rotor will be considered for the potential analysis, whereas the tail rotor is not included in this study. In case of interest, a possible machine design for the tail rotor could be taken from [25, 151], in which a six-phase PSM was implemented. For further consideration within this work the tail rotor is neglected, as mentioned previously.

Furthermore, the new electrical drive train is considered to be a direct drive, which means that no gearbox is installed, as mentioned in section 1.2.2. This leads to a high-torque and low-speed machine for this application resulting appropriately high requirements, as being scrutinized within this chapter.

For the reason of practicality or applicability, the installation space was limited to where the conventional drive train – including the turbines and the gearbox – is usually installed. Thus, the white area in Figure 4.1 symbolizes the available installation space for the electrical drive train. This assumption ensures the typical use cases of the helicopter considering the internal usable volume, which means the hold or the trunk in this case.

So first, it is necessary to define the starting point for the potential analysis of the electrical drive train for the helicopter and to explain which parameters are decisive for the electrification

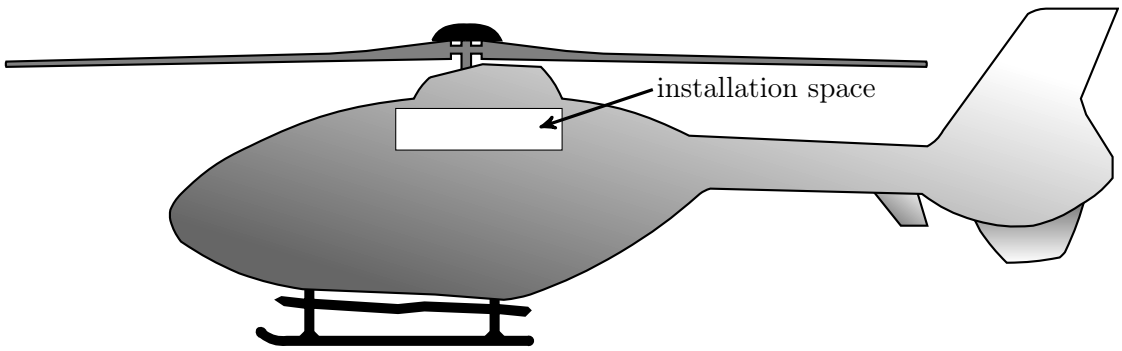

Figure 4.1: Provided installation space within the platform being the helicopter EC135, which is determined by replacing the conventional propulsion system in order to ensure the applicability of the system.

Table 4.1: Key parameter of the EC135, which are taken from the data sheet [41]. Additionally, the requirements are defined and listed which need to be achieved to ensure a system functionality of the helicopter application.

parameter	value	unit
nominal power	510	kW
maximum power	575	kW
nominal rotational speed	395	min^{-1}
tare weight	1,482	kg
maximum take-off weight (MTOW)	2,980	kg
installation space (length x width x height)	$2 \cdot 1.5 \cdot 0.5$	m^3
total system failure	$< 10^{-9}$	h^{-1}
minimum power level after one failure	85	%
minimum power level after two failures	65	%

of the traction drive. These application requirements define the targets for the potential assessment, whereas the targets can be directly linked to the subsequent step, which is the selection of components for the special drive train, followed by the reliability assessment for different topologies by means of Markov models. All considerations are based on environmental constraints, which mostly are – in case of the conversion design – already included to the platform geometry. In general, these steps can be explained by the four factors explained in section 2.1.

4.1 Key Parameters of the Electrical Helicopter

This section concludes the key parameters of the chosen platform, the EC135. This brings a certain level of requirements, as the existing system needs to operate under the desired conditions. Table 4.1 summarizes all needed requirements, which are necessary to ensure the applicability of the system based on the conventional helicopter application EC135. The power requirement considering the electrical machine is defined based on the system power of the conventional turbines [41]. From these data, the boundary conditions are defined. Hence, the nominal and the maximum power of the machine is set to 510 kW and 575 kW, respectively. The rotational speed is limited to $395\,\mathrm{min}^{-1}$ in order to avoid the rotor tips exceeding the supersonic speed limit.

Furthermore, designing systems for air transportation is especially challenged by weight and reliability restrictions. Based on these requirements and one corresponding flight scenario, the parameters, which need to be taken into account for the assessment, are identified and weighted.

4.1.1 Volume and Weight

On the one hand, the available volume for the drive train including inverter and electrical machine is defined by the installation space of the turbines and gearbox of the conventional helicopter (see white area in Figure 4.1). This space is estimated to be two meters long, one

and a half meters wide, and half a meter high. These values can be derived from [41]. On the other hand, the weight limitations of the application play a crucial role for the assessment. Hence, the tare weight of the conventional helicopter is 1,482 kg and the maximum take-off weight (MTOW) of the system based on the conventional geometry and technical aspects is 2,980 kg. The tare weight here includes the conventional turbine propulsion system, which has to be replaced by the electrical drive train.

4.1.2 Reliability and Fault Tolerance

Due to safety issues, all aircraft, as well as autonomous vehicles, are exposed to high reliability constraints. Hence, reliability and fault tolerance are crucial indicators for aircraft assessments. The total system failure rate needs to be below one failure in time (1 FIT), which is defined as one failure per 10^9 hours, as mentioned earlier. Additionally, fault tolerance is required, since after one failure a minimum available power of 85 % has to be provided and after two occurred failures 65 % of the nominal power. Therefore, redundancy needs to be provided, whereas structural redundancy – such as suggested by [158] – is not applicable in this case due to the hard requirements regarding weight and volume. Hence, functional redundancy is the only possibility for this application case. Functional redundancy can be ensured by increasing the number of phases, as mentioned earlier.

4.1.3 Flight Scenario

The EC135 is used for different flight scenarios within the civil area. Beside the simple transportation of persons for business or private reasons, the helicopter is typically used for emergency medical purposes, such as ambulance service or search and rescue missions. These flight scenarios can last several hours depending on the places of action. In general, the overall lifetime of the helicopter is defined to be 20 years, which leads to 60,000 operating hours by assuming an operating time of eight hours per day.

However, for the electrification a one-hour flight scenario is assumed in order to ensure the applicability of emergency medical services or simple transportation. Even though the range of operation is therefore limited, the energy needed is reduced and hence, the electrification is more likely to be realizable within the already given high restrictions. The rotational speed of the rotor is kept as constant as possible. The different flight modes – taking off, climbing, hovering, cruising, descending, and landing – are characterized by different pitch settings, leading to different power or torque requirements which are decisive for the design of the drive train. The nominal power is 510 kW output power at the shaft. [41]

Thus, the applicability is highly dependent on the system weight and volume, since exceeding the maximum take-off weight results in the helicopter's inability to operate. Safety, on the other hand, is indispensable for such an application. In the following sections, the different components or topologies – presented in the previous chapter 3 – are confronted with each other, evaluated, and finally combined to preliminary recommendations based on the application's requirements.

4.2 Selection of Components in Electrical Drive Trains

This section covers the potential analysis of the components mentioned in the previous chapter – the electrical machine types and the converter topologies. Both components are first separately analyzed and partly selected for the application. After that, the interdependency based on a different number of phases will be shown for an interim conclusion regarding the applicability of the components. These evaluations are conducted based on the parameters and requirements on the helicopter's drive train system, mentioned earlier within this chapter.

4.2.1 Potential Analysis of Electrical Machine Types

In case of the helicopter – a high-torque low-speed application – and the appropriate requirements, efficiency is also one of the key aspects regarding the traction drive, since it directly influences the operation range of the vehicle or the installation space needed for the traction drive. This dependency links directly to a high torque density, which means that the achievable weight or volume of the machine plays a crucial role. Furthermore, a safety-critical system, such as the helicopter, requires a high reliability or rather fault tolerance. Cost and complexity always are decisive for the introduction to the market. All these parameters are evaluated in this subsection, whereas first the weighting factors are explicitly defined in order to get a final quantitative evaluation of the two electrical machine types.

Weighting Factors for Helicopter Application

As depicted in section 2.4, weighting factors can emphasize the different importance of parameters within an assessment. The weighting factors K_{w} for the helicopter application can be derived from the previously evaluated priorities. The weighting factors are summarized in Table 4.2 by naming specific values. These values are defined by literature, expert knowledge and experience, as shown in [P4]. Hence, the values enable a more objective assessment without overrating certain parameters. Repairability as comparative parameter is exempted for this evaluation, since repair is not possible during the flight.

Power density, reliability, and fault tolerance are the most critical parameters considering an electrification of an helicopter. Therefore, all three parameters are weighted with 1.0. Efficiency and volume also play an important role, whereas they are not as important as the three previously mentioned parameters. Henceforth, they are valued with 0.9. Cost and complexity have been rated with 'low priority' in section 2.4. The weighting values are therefore defined as 0.2 and 0.3, respectively, since the cost at this current state of technology is still of lower priority than complexity.

Cost and Complexity

The difference in cost is highly influenced by the use of rare-earth material for the permanent magnets. Hence, the production cost is directly depending on supply and demand of the product and therefore on the countries providing these resources. The difference in cost can be even worse in the future. The relatively small air gap of induction machines increases the cost of machine, due to the exact positioning of the rotor and avoiding eccentricity. The other

Table 4.2: Quantitative weighing factors for the comparative analysis. The seven remaining key parameters are weighted by K_w according to their importance [P4].

parameter	K_w
cost	0.2
complexity	0.3
efficiency	0.9
volume	0.9
power density	1.0
reliability	1.0
fault tolerance	1.0

parts within the machine do not differ regarding the production cost. Especially due to the low speed of the machine, the small air gap of the induction machine is not decisive, nor are the centrifugal forces on the permanent magnets of the synchronous machine. This is also the reason for the difference in complexity, since in this case the small air gap for the complexity of construction for the induction machine outweighs the synchronous machine.

Efficiency

Regarding efficiency, Figure 4.2 illustrates the search result for existent electrical machines applying efficiency over power density, which was previously published in [P13]. The database does not distinguish between different applications, but different machine types independent of where they are used. It contains permanent magnet synchronous machines and induction machines and shows directly that the actual power density range is still quite limited. Based on the found data, machines up to 600 W/kg are standard machines. However, the new electrification trends, especially regarding aircraft applications, tend to higher requirements from 5 to 15 kW/kg. As mentioned by De Doncker et al. [29] in 2011, machines came up providing power densities of up to 3.5 kW/kg. Hence, the limitation of the database does not allow an estimation of an efficiency range, but still shows a tendency regarding the choice of machine type. By using permanent magnet synchronous machines, a higher efficiency is achievable compared to induction machines. This statement can be proved by Figure 4.2 for the depicted range and is generally mentioned in literature – for instance in [44] – especially for low-speed applications.

Volume and Weight

The regression models presented in section 2.5 are used in order to assess weight and volume, which are assumed to be directly proportional to each other. Hence, the regression mass can be taken as decisive parameter for the weight and volume assessment. Figure 4.3 results from these models by evaluating the characteristics for the given nominal operating point. Figure 4.3a shows the comparison of both machine types for the fixed nominal speed of $395\,\mathrm{min}^{-1}$ dependent on the nominal power and the comparison dependent on the nominal speed for the fixed nominal power of 510 kW is depicted in Figure 4.3b. In both cases, as expected for the high-torque low-speed applications, the permanent magnet synchronous

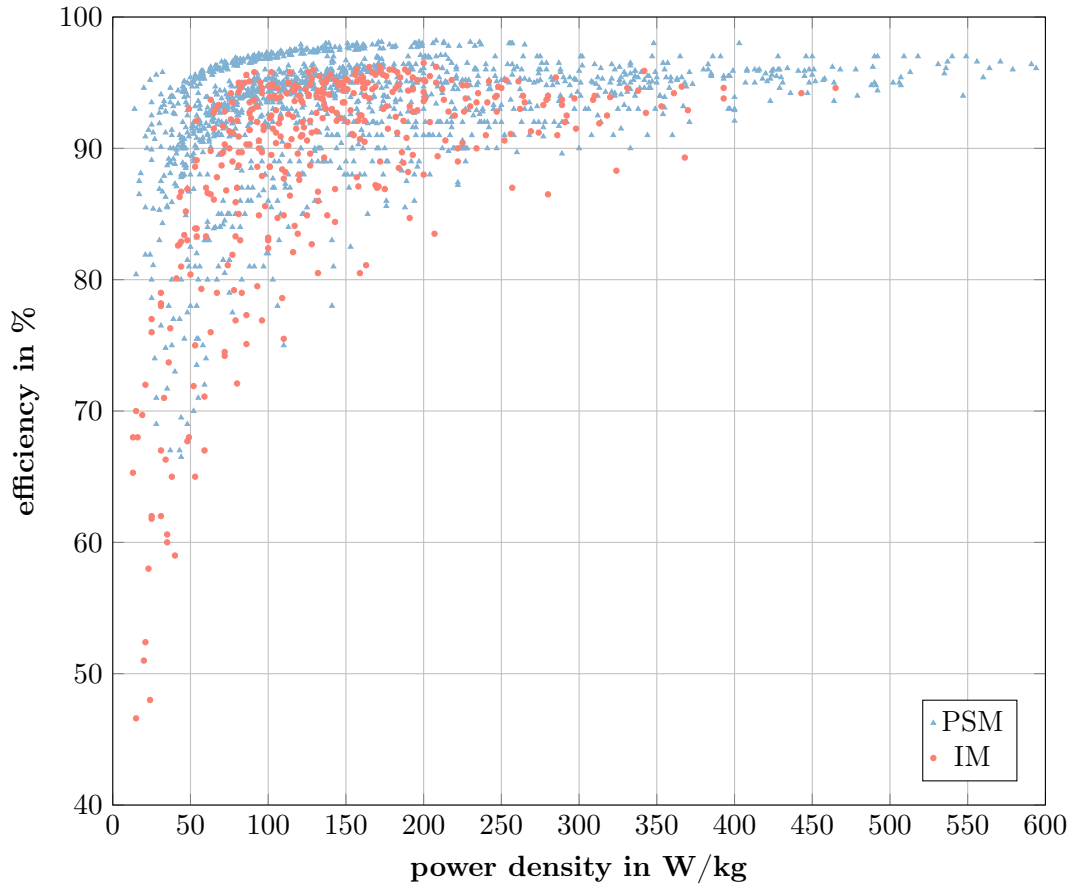

Figure 4.2: Comparison of electrical machines existing on the market regarding efficiency over power density and considering both the permanent magnet synchronous machines (PSM) and the induction machines (IM) [P13].

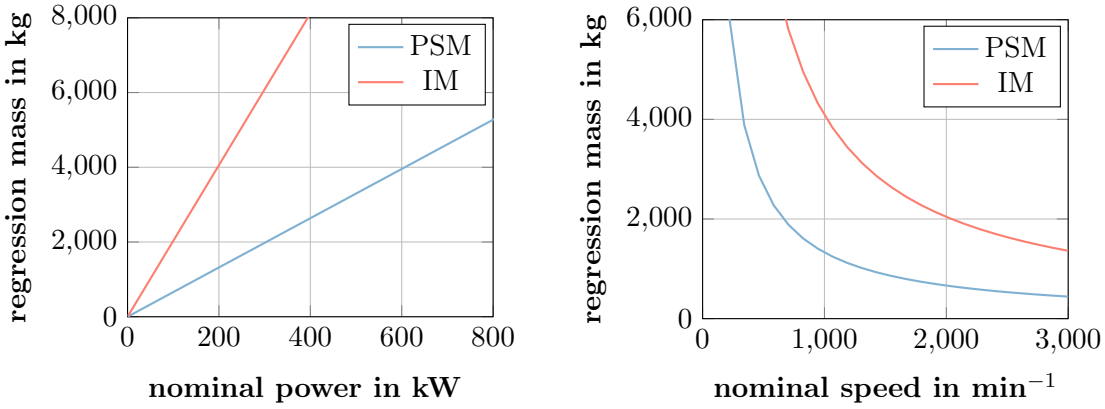

(a) (b)

Figure 4.3: Regression mass over power for a speed of 395 min^{-1} (a) and over rotational speed for a fixed power of 510 kW (b). The mass values obtained by regression are not to be taken as absolute values, whereas the general tendency between induction machine (IM) and permanent magnet synchronous machine (PSM) can be seen.

machine (PSM) is more auspicious than the induction machine (IM). As previously mentioned, the regression mass from this function cannot be considered as the identical realistic weight. Evaluating the data at low speeds and high torque also shows a cumulative number of permanent magnet synchronous machines in comparison with induction machine, which hardly appear under this boundary conditions. Hence, this comparative approach does not serve for quantitative but just qualitative statements. This leads to the evaluation of power density, where the permanent magnet synchronous machine is rated higher than the induction machine. This assumption is valid, especially since the installation space is highly restricted and of the same volume for both machine types.

In general, taking into account the maximum available installation space for the machine of approximately 1.5 m^3, the achievable weight can be calculated by the relationship between torque density and machine diameter set up by Dubois [33]. Dubois claims a possible torque density of approximately 28 Nm/kg for an outer machine diameter of 1.5 m considering the active parts. The ideal length for this study case was calculated to be approximately 0.12 m and the rotational speed was set to 1,500 min^{-1}. Since the required rotational speed for the electrical helicopter is 395 min^{-1}, the scaling factor for the length is calculated by the inverse ratio of both speeds. Taking into account the resulting value of approximately 3.8, the length for the helicopter application equals 0.46 m. The previously mentioned nominal power and speed results in the required torque as follows.

$$T_\mathrm{n} = \frac{P_\mathrm{n}}{2\pi \cdot n_\mathrm{n}} = \frac{510 \cdot 10^3\,\mathrm{W} \cdot 60\,\mathrm{s}}{2\pi \cdot 395} = 12{,}330\,\mathrm{Nm} \tag{4.1}$$

Consequently, this required torque leads to the weight of the active parts of the machine of approximately 440 kg, which corresponds to approximately 15 % of the MTOW. This serves as a rough estimation, since the auxiliary or passive parts are not included and at this design stage are hardly assessable.

Reliability and Fault Tolerance

The reliability of electrical machines can be assumed to be approximately equally distributed based on relevant literature. This becomes visible in [P10] or in [137, 140], where the statistical distribution of the failures in electrical machines is presented. Figure 4.4 indicates that the bearing (40 %) and winding failures (40 %) are more likely to fail in comparison with the rotor failure (10 %) – including the permanent magnets or the rotor bars – or others (10 %). Since the main difference of the two machine types is characterized by the rotor, the assumption to have approximately the same failure rate is accepted. In literature, for instance, the failure rate can be found to be approximately 2,200 FIT for induction machines and approximately 4,000 FIT for synchronous machines [117]. The comparison to other references, such as [5, 40, 98], shows that the values presented are in the range of 10^{-6} to 10^{-5} failure per hour for conventional three-phase machines. The statistical evaluation conducted in [P15] obtained a comparable value of 2,464 FIT for induction machines, which indicates that the reliability value did not change significantly during the last decades.

Since the presented data are valid for synchronous machines in general, the reliability should be better for the permanent magnet synchronous machines. First, the rotor does not contain any excitation winding. Second, the application requires relatively low rotational speeds, which

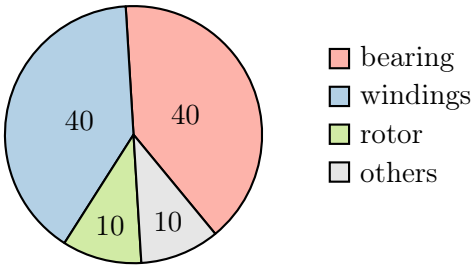

Figure 4.4: Statistical failure distribution for electrical machines given in percent, showing the accumulation of bearing and winding failures in comparison with rotor and other failures [P10].

Table 4.3: Comparison of electrical machine types for aircraft applications taking into account different parameters and appropriate weighting factors based on [P4].

machine type		IM	PSM
parameter	K_w		
cost	0.2	10	9
complexity	0.3	10	9
efficiency	0.9	8	10
volume	0.9	8	10
power density	1.0	7	10
reliability	1.0	10	10
fault tolerance	1.0	8	10
total value (without K_w)		61.0	68.0
relative value		0.90	1.00
total value (with K_w)		44.4	52.5
relative value		0.85	1.00

is an advantage regarding the reliability of the rotor. This qualitative statement cannot be verified by references. Hence, the worst case is assumed for the permanent magnet synchronous machine and both machines are rated equally.

The difference in fault tolerance is higher between the two machine types. The previously published papers [P10, P11] depicted the basic differences based on overload capability, partial load mode, and torque ripple in failure case. Based on these parameters and the application's boundary conditions, the permanent magnet synchronous machine turns out to be more fault tolerant than the induction machine.

In conclusion, the resulting evaluation is shown in Table 4.3 being graded from 1 to 10 based on the explanations of the previous paragraphs. The best-graded type is valued by 10 and the other machine type by the appropriate degraded value. The sum of all weighted parameters leads to the final decision that – for the application of the helicopter – the permanent magnet synchronous machine is advantageous in order to achieve the requirements. Therefore, only this machine type is considered for further assessment in combination with power electronics being investigated in the following subsection.

4.2.2 Potential Analysis of Converter Topologies

A conventional and mostly used three-phase machine can be supplied with an AC-voltage by the six-pulse- or the H-bridge converter topology. In both cases, the two bridge topologies mentioned in section 3.2.1 – half- and full-bridge – are taken into account.

As mentioned earlier, fault tolerance is a decisive factor for safety-critical drive trains and therefore the previously chosen permanent magnet synchronous machine and the power electronics have to be simulated in fault cases. Here, the drive train is set up as three-phase system and an existing machine – which was designed by Pyrhönen [119] – is used as basis for the inverter topology comparison. Although the machine parameters are not matching the application requirements mentioned within this work, the obtained results can relatively be adapted to the helicopter's power requirements; especially for an early stage assessment. The differences between the six-pulse- and the H-bridge topology can hence be determined after the occurrence of a fault. The respective fault is defined as an open-circuit failure of one phase, which is a valid assumption for all faults occurring, if the fault is instantaneously detected, located, and isolated, as for instance also described in [45, 152]. This directly leads to the advantage of the H-bridges, the possibility of separation of the phases, which simplifies the fault monitoring and consequently the isolation of the failing phase.

The simulation model contains a switch, which opens one phase of the three-phase system after a specific amount of time in order to simulate the open-circuit or loss of phase. The instant of failure is set to 0.4 s. The simulation results are depicted in Figure 4.5 where the two power converter topologies are relatively opposed to each other. After the transient response of the simulation model, the loss of phase and the difference between the six-pulse- and the H-bridge can be directly seen after 0.4 s. Figure 4.5a depicts the speed fluctuations for both converter topologies, where the speed ripples and the amplitude is higher using the six-pulse-bridge in comparison with the H-bridge topology. Furthermore, the simulation results for the power are illustrated in Figure 4.5b, where this difference can be shown in a worse extent. The power and hence torque ripple occur smoother for the H-bridge, where the ripple peaks even

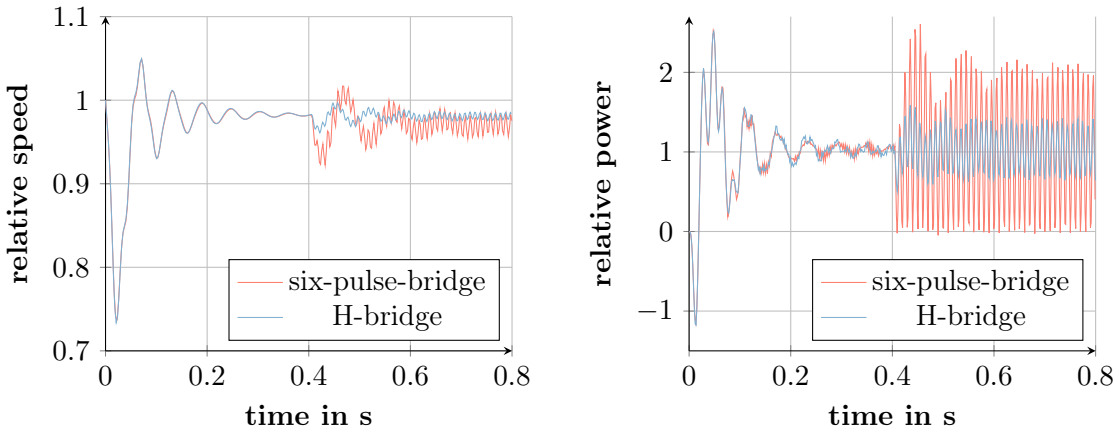

(a) (b)

Figure 4.5: Failure simulation for six-pulse-bridge and H-bridge converter topology. The results show a failure case (one phase open-circuit) after 0.4 s for both topologies and the relative response of speed over time (a) and power over time (b) [P8].

drop down to zero for the six-pulse-bridge. Additionally, the peak-to-peak values occur to be approximately ±100 % for the six-pulse-bridge, whereas the H-bridge topology results in peak-to-peak values of only approximately ±40 %. This means, that the H-bridge topology enables an operation after the occurring fault with a degraded power, whereas the system remains functional. In contrast, since the six-pulse-bridge is unable to drive two out the three phases, a phase failure leads to the complete system failure. Besides, the control was not adapted after the phase failure, which means that the voltage and is kept constant, whereas the current is changing if a constant torque is required. Furthermore, overload operation is not applicable in case of a phase loss, since the high requirements of the application result in an already highly saturated machine in nominal operation.

Therefore, the H-bridge topology is auspicious and indispensable regarding fault tolerance based on the one-phase-failure assessment within a three-phase system. Increasing the number of phases is a possible way to ensure higher fault tolerance. Especially in this case, modularity is an advantage of the H-bridge topology. The six-pulse-bridge can only be used if the phase number is a multiple of three. Thus, assuming the power to be equally distributed over the number of phases, leads to a lower power degradation in the case of a phase loss for the H-bridge, since in case of a phase loss of one six-pulse-bridge, the complete six-pulse-bridge fails. For instance, in case of a phase loss of a six-phase machine, the H-bridge topology provides 83 % of the nominal power and the six-pulse-bridge only 50 %, always under the assumption that the control of the drive train is able to handle the failure. In contrast, due to the higher number of components, the H-bridge topology turns out to hold 20 % more weight and a 60 % higher volume than its counterpart does after first analytical approximations [P8].

This means in summary, that the six-pulse-bridge is not recommendable for any phase number defined by a multiple of three, whereas the half-bridge and full-bridge topologies need to be further opposed to each other based on a reliability assessment for different numbers of phases higher than three.

4.2.3 Interdependency of Components

With the increase of the number of phases, the complexity increases as well, since a higher number of components is used. Therefore, the upper limit regarding the number of phases is set to eleven. According to the increase of the phase number, the reliability value decreases due to the higher possibility of failing components. Thus, it is crucial to assess the reliability reduction. A first approximation of the failure rate for the electrical machine with different phase numbers can be obtained by a given value of 800 FIT for the classical three-phase configuration and a given value for each phase of 150 FIT [40]. Based on these data, the approximated failure probability $P_{\mathrm{PSM}}(m,t)$ can be determined by

$$P_{\mathrm{PSM}}(m,t) = (8 + 1.5 \cdot (m-3)) \cdot t \cdot 10^{-7}\,\mathrm{h}^{-1}, \quad \text{for } m \geq 3, \tag{4.2}$$

where m is the phase number and t the lifetime or operating time of the machine. Accordingly, the reduction of reliability compared to a typical three-phase machine can be calculated in percent over the lifetime in hours.

$$\Delta P_{\mathrm{PSM}}^{m/3} = \frac{P_{\mathrm{PSM}}(m,t) - P_{\mathrm{PSM}}(3,t)}{P_{\mathrm{PSM}}(3,t)} \tag{4.3}$$

The reduction percentage obtained from equation (4.3) can be seen in Figure 4.6 for the different number of phases, where the zero line stands for the three-phase machine. The mentioned operating time of aircraft systems of approximately 60,000 hours leads to a small decrease of reliability of below 6 % for a nine-phase machine compared to a three-phase machine.

Hence, the advantage of an increased fault tolerance by increasing the number of phases can be proved by calculating the remaining system power in failure cases for the different number of phases. The power of the machine can be assumed to be equally distributed over the number of phases. Table 4.4 summarizes the results of the calculation of the remaining system power. The values which do not meet the required power are bracketed, which means values below 85 % for the first and below 65 % after the second phase failure. The 65 % limit is also assumed for the third and forth phase failure, since this amount of remaining system power is assumed to be necessary in order to ensure the applicability of the system. The em dash ('—') means that the system is not functional after a certain number of phase failures.

Consequently, in Table 4.4 it can be seen that the phase numbers five and six exceed the limits of power degradation. Systems with seven phases and above can meet the requirements, whereas seven phases result in compliance without safety margin. Nevertheless, the phase numbers to be assessed in the following are seven to eleven for the drive train system of the helicopter. The next section covers the calculation of total system failure probabilities for these phase numbers by means of Markov models.

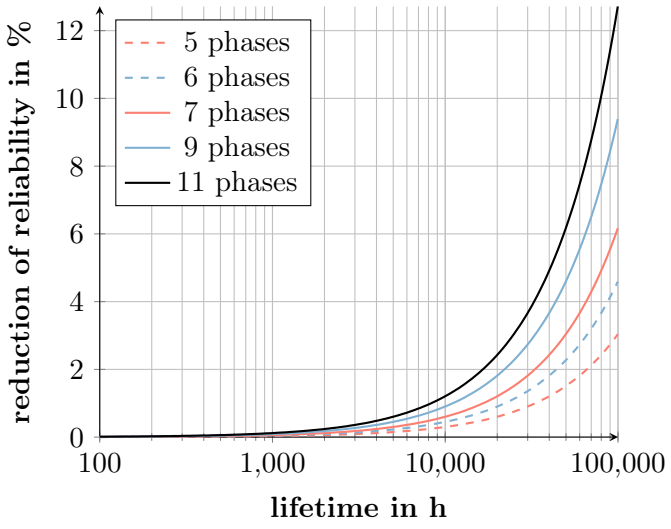

Figure 4.6: Reliability reduction due to an increase of the machine's number of phases. The zero line represents a three-phase machine and the characteristics for the higher phases depict the reduction of reliability in percent over lifetime [P14].

Table 4.4: General assessment of remaining power in kW for a different number of phases and different number of phase-failure cases having a nominal power of 510 kW based on [P14]. The italic values in brackets are the values, which do not meet the application requirements, whereas '—' means not functional.

phases / failures	5	6	7	9	11
1	(*408*)	(*425*)	437	453	464
2	(*306*)	340	364	397	417
3	—	(*255*)	(*291*)	340	371
4	—	—	(*219*)	(*283*)	(*325*)

4.3 System Evaluation by Means of Multi-State Reliability Markov Models

The Markov method, which was presented in section 2.7, is implemented as a multi-state reliability Markov model within this part. Multi-state here means that the system has the capability of a power degradation in case of critical faults before failing completely, which is also expected by the system requirements.

First, it is important to select the appropriate time steps for the calculation. In general, all possible time units can be used for the calculation of Markov models. However, the assessment for the electrical helicopter is executed in hours, since a lifetime of technical systems is typically given in hours and failure rates are provided per hour. Furthermore, no repair possibility is provided, hence no backwards transitions to previous states are allowed, which is also a reason to talk about flight or operating hours and no longer time units, such as days or years. Repair is exempted due to the flight scenario of one hour and due to the fact that during this flight no repair is possible, contrary to ships for instance.

Second, selecting the number of states for the assessment of the drive train is crucial in order to describe each part and the system appropriately. The number of states and the transition types in general depend on the topology of the components. On the one hand, the number or topology of components enables redundancy effects and hence influences the number of degradation states. On the other hand, possible faults depend on the topology as well, which defines if the states are passed through sequentially or for instance if states are skipped due to an occurring fault.

Third, the most crucial and most difficult point within Markov modeling is to determine the transition probabilities dependent on the assessed component or system topology. In this assessment, the Markov model consists of degradation states, which means that the system is not used in overload mode but considers a certain power degradation in a failure case. Since overload is not applied, overheating is avoided, the probabilities for a phase failure stay the same and hence, the transition probabilities stay the same for each state transition.

Thus, the different models are explained as follows for the electrical machine and the drive train system including the power electronics. The results of the model application for the electrical drive train of the helicopter are summarized and discussed step by step.

4.3.1 Markov Modeling for the Electrical Machine

Starting with the assessment of the electrical machine, the number of states for the machine results from Table 4.4. Based on this table, it becomes obvious that a system with seven phases withstands two phase failures, whereas a system with nine and eleven phases tolerates three phase failures. This leads to a Markov model with four and five states, respectively. Both Markov models are shown in Figure 4.7. The initial state on the left represents a failure-free operation. The last red colored state expresses the complete inability to operate or the condition in which the requirements in order to sustain the vehicle's function cannot be achieved. All other states in between correspond to different degradation levels characterized by reduced performance due to the loss of phases (open-circuit fault), which means a partial loss of functionality of the machine due to critical faults. Considering only the different phase number and the previously mentioned appropriate failure rates for phase failures found in [40], the values of 1,400 FIT, 1,700 FIT, and 2,000 FIT can be used for the phase numbers seven, nine, and eleven, respectively. Due to the assumption that in this case, no overload is accepted and based on a one-hour flight scenario, the FIT values can be directly used for all transition probabilities of the respective Markov model. This means, that λ_{12}, λ_{23}, λ_{34}, (and λ_{45}) are defined equally by the mentioned FIT values corresponding to the number of phases. In reality, the values would have to be recalculated, since the phase number is decreasing and consequently the failure rate as well. However, the failure probability is increasing after an occurring failure, because the system is not restarted and therefore the probability for the next failure would increase. Since the structure and the procedure of keeping the failure rates constant are the same for both models considering the different phase numbers, this procedure is accepted for the comparative assessment of the machine.

The results of the presented Markov models are graphically presented in Figure 4.8 for ten operating hours, whereas Table 4.5 concludes the specific values resulting from the calculation for only five operating hours. Both visualizations illustrate the development of the total failure probability over time based on the system requirements. In other words, the total failure probability is equal to the probability to end up in the last red state of the models. However, for the helicopter only the first value needs to be considered for comparison, which is the appropriate value for the one-hour flight scenario mentioned earlier.

Figure 4.8 provides the clear choice of the most promising number of phases. The nine-phase machine offers the lowest total failure probability. The expectation, that the failure probability of eleven phases is even lower than for nine phases, is not fulfilled. Due to the remaining power requirement, the number of states is different between seven phases and the two phase numbers mentioned above, that is the reason for the difference of approximately 10^4 in failure probability for the seven phases. Nine and eleven phases differ slightly due to the different FIT value. Hence, due to the same number of states and the different number of phases, the nine-phase machine has a higher reliability than the eleven-phase machine.

Therefore, the nine-phase version is selected for further assessment. Finally, the overall drive train system is modeled by means of Markov models within the next section, where more drive train components – besides the electrical machine – are considered in order to include them to the model calculation.

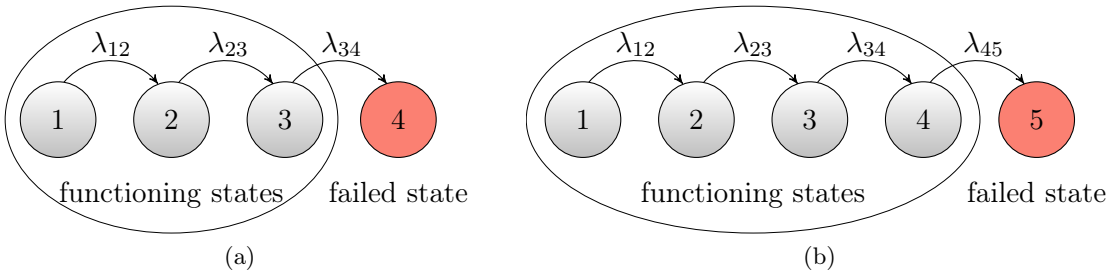

Figure 4.7: Markov models for machines with a different number of phases. A model for a seven-phase machine is shown in (a), whereas (b) includes the model for a nine- and eleven-phase machine.

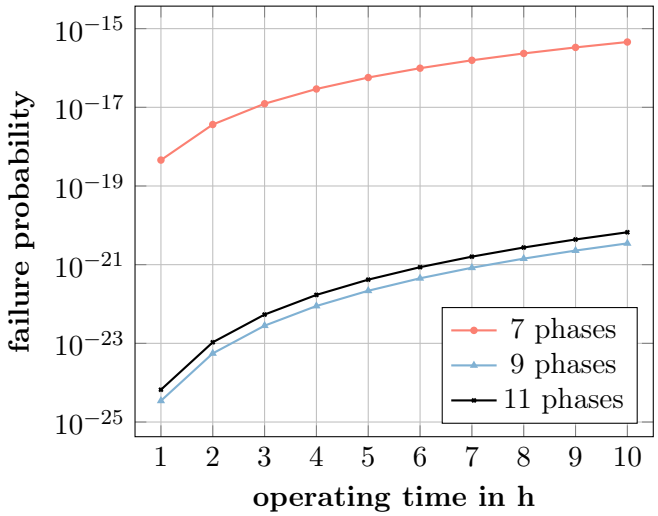

Figure 4.8: Development of the electrical machines' failure probabilities over time. The results for the three different numbers of phases are depicted over the range of ten operating hours, which leads to the conclusion that the nine-phase machine is the most promising considering its failure probability. The specific values can be found in Table 4.5.

Table 4.5: Failure probabilities of the electrical machine resulting from the Markov model calculation for one to five operating hours for seven, nine, and eleven phases. The graphical results for the different phase numbers are depicted in Figure 4.8.

operating hours / number of phases	1	2	3	4	5
7	$4.56 \cdot 10^{-19}$	$3.65 \cdot 10^{-18}$	$1.23 \cdot 10^{-17}$	$2.93 \cdot 10^{-17}$	$5.71 \cdot 10^{-17}$
9	$3.46 \cdot 10^{-25}$	$5.55 \cdot 10^{-24}$	$2.81 \cdot 10^{-23}$	$8.90 \cdot 10^{-23}$	$2.17 \cdot 10^{-22}$
11	$6.63 \cdot 10^{-25}$	$1.06 \cdot 10^{-23}$	$5.39 \cdot 10^{-23}$	$1.70 \cdot 10^{-22}$	$4.16 \cdot 10^{-22}$

4.3.2 Markov Modeling for the Drive Train System

Before starting the system evaluation, the power electronics are assessed for the preferable nine-phase configuration. Hence, three conventional topologies considering power electronics are taken into account. First, three six-pulse-bridges can be used to supply nine phases which results in three sub-machines, each consisting of three phases driven by one six-pulse-bridge. However, after a fault within one six-pulse-bridge, one complete three-phase sub-machine fails and hence, it only results in a two-state Markov model. This means, that the topology using three six-pulse-bridges can be neglected, since it does not meet the requirements of power degradation. Second and third, an 18-pulse-bridge – consisting of nine half-bridges – and an H-bridge topology with nine H-bridges, hence, one H-bridge per phase are possible topologies to be used for the nine phases. Both topologies are assessed by Markov models, which are explained as follows.

With regard to the construction of the Markov models, the topology configuration and the respective failure rates, depending on the number of components, must be identified. In order to avoid an immediate system failure in case of a control unit malfunction, the control unit is assumed to be implemented redundantly. Henceforth, the control unit, cables, and terminals are neglected in this case, since the influence on both topologies is comparably low. First, the machine's failure rate for an open-circuit (oc) phase fault is taken as for the previous calculation from [40] and results in 1,700 FIT for the nine-phase machine. This failure rate stays the same for both topologies. Second, the short-circuit (sc) rate can be found in [98] and equals 6,700 FIT for one phase; for the presented nine-phase case, the value is obtained by multiplying it by nine, resulting in 60,300 FIT for a short-circuit between two phases. Third, the different failure rates for the components of the power electronics are depicted in [104]. Hence, the value for one semiconductor (semi) is 250 FIT, for one diode (di) 100 FIT, for one capacitor (cap) 80 FIT, and for one printed circuit board (pcb) 200 FIT.

Now, it must be stated that the number of diodes and semiconductors for the 18-pulse-bridge and the H-bridge topology differs by the factor of two, whereas the number of capacitors and printed circuit boards is nine times higher for the H-bridge than for the 18-pulse-bridge topology. These considerations lead to the resulting failure rates being concluded in Table 4.6 for each component depending on the topology and consequently on the number of components.

Table 4.6: Reliability values for the system components given in FIT (10^{-9} per hour). The rates are distinguished by 18-pulse-bridge and H-bridges for a nine-phase drive train topology [40, 98, 104].

topology	18-pulse-bridge		H-bridge	
components	quantity	FIT	quantity	FIT
machine's open-circuited phase (oc)	—	1,700	—	1,700
machine's short-circuited phases (sc)	—	60,300	—	—
semiconductor (semi)	18	4,500	36	9,000
diode (di)	18	1,800	36	3,600
capacitor (cap)	1	80	9	720
printed circuit board (pcb)	1	200	9	1,800
total system FIT	—	68,580	—	16,820

Furthermore, it can be seen that the overall reliability value – in the last row of Table 4.6 – for the 18-pulse-bridge is already worse than for the H-bridge topology based on the components which are taken into account and especially due to the possibility of a short-circuit between the phases.

Transition Probabilities for the 18-Pulse-Bridge Topology

The Markov model for the 18-pulse-bridge can be seen in Figure 4.9a. For this topology, only one capacitor and one printed circuit board is assumed to be used. Additionally, the nine phases are connected in star, which leads to the possibility of short-circuits between the phases. Both characteristics enable long transitions provoking performance degradation or complete system failure. These long transition probabilities are calculated from the failure rates, which are defined by the sums of the respective components:

$$\lambda_{13} = \lambda_{24} = \lambda_{\mathrm{sc}} = 60{,}300\,\mathrm{FIT}\ ; \tag{4.4}$$

$$\lambda_{15} = \lambda_{25} = \lambda_{\mathrm{cap}} + \lambda_{\mathrm{pcb}} = (80 + 200)\,\mathrm{FIT} = 280\,\mathrm{FIT}\ ; \tag{4.5}$$

$$\Longrightarrow \quad \lambda_{35} = \lambda_{\mathrm{sc}} + \underbrace{\lambda_{\mathrm{cap}} + \lambda_{\mathrm{pcb}}}_{\widehat{=}\ \lambda_{15}} = (60{,}300 + 280)\,\mathrm{FIT} = 60{,}580\,\mathrm{FIT}\ . \tag{4.6}$$

The short sequential transitions from one state to the next are composed by the failure rates for an open-circuited phase, the semiconductors, and the diode. Only the last transition is additionally influenced by the failure rates of the short-circuited phases, the capacitor, and the printed circuit board.

$$\begin{aligned}\lambda_{12} = \lambda_{23} = \lambda_{34} &= \lambda_{\mathrm{oc}} + \lambda_{\mathrm{semi}} + \lambda_{\mathrm{di}} = \\ &= (1{,}700 + 4{,}500 + 1{,}800)\,\mathrm{FIT} = 8{,}000\,\mathrm{FIT}\ ; \end{aligned} \tag{4.7}$$

$$\lambda_{45} = 8{,}000\,\mathrm{FIT} + \underbrace{\lambda_{\mathrm{sc}} + \lambda_{\mathrm{cap}} + \lambda_{\mathrm{pcb}}}_{\widehat{=}\ \lambda_{35}} = 68{,}580\,\mathrm{FIT}\ . \tag{4.8}$$

The model does not include any aging effects or the parallel operation of phases, which can be seen by the constant probability for a phase failure after changing to another state in the model. Here, the obtained result is already sufficient to assess the 18-pulse-bridge topology, since the result for the system's total failure probability of $2.80 \cdot 10^{-7}$ per hour does not meet the required reliability value for the application. Furthermore, the sensitivity of the model is very low with regard to the failure of multiple phases at the same time. This means, that the failure probability of the overall system after one operating hour differs only 0.1 %, which is negligible. Hence, this sort of failure is not considered within the Markov model of the 18-pulse-bridge.

Transition Probabilities for the H-Bridge Topology

In contrast, in case of the H-bridge topology, the phases are galvanically insulated from each other, see also [5]. At first, this leads to the simplified model, where the sequential transition probabilities are calculated using all single failure rates, including capacitor and printed circuit boards, since they are separately realized for all nine phases. This also means that the occurrence of a loss of two phases due to a short-circuit between two phases is neglected.

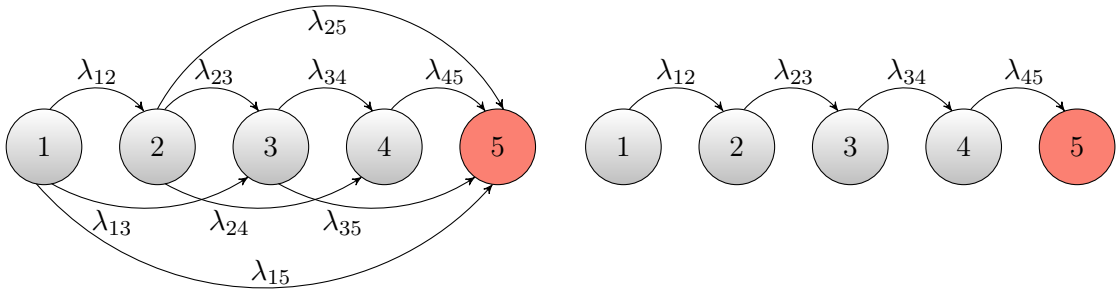

Figure 4.9: Markov model for the overall drive train system using the 18-pulse-bridge topology shown in model (a) and the H-bridge topology depicted in model (b). These models contain the electrical machine and the respective power electronics, including phase, semiconductor, diode, capacitor, and printed circuit board failures.

Thus, Figure 4.9b shows the mentioned Markov model for the drive train using the H-bridge topology, where the transition probabilities are calculated from all considered component FIT values.

$$\begin{aligned}\lambda &= \lambda_{12} = \lambda_{23} = \lambda_{34} = \lambda_{45} = \\ &= \lambda_{\mathrm{oc}} + \lambda_{\mathrm{semi}} + \lambda_{\mathrm{di}} + \lambda_{\mathrm{cap}} + \lambda_{\mathrm{pcb}} = \\ &= (1{,}700 + 9{,}000 + 3{,}600 + 720 + 1{,}800)\,\mathrm{FIT} = 16{,}820\,\mathrm{FIT}\end{aligned} \tag{4.9}$$

Defining this transition probability for all transitions is the best assumption result for the considered components, not taking into account the parallel operation of phases, the decrease of the number of components by the loss of phase, and the loss of multiple phases at the same time. In order to ensure a fair comparison, all possible and influencing failure events would need to be considered.

First, assuming that the failure of different phases at the same time is possible leads to the failure probability for multiple phases being the respective potential of the failure probability for one phase ($[P(t)]^2$, $[P(t)]^3$, and $[P(t)]^4$ for two, three, and four phases, respectively).

Second, one ninth of the original failure rate is used for the degradation of components due to a loss of phases and results in the appropriate new transition probability after occurring phase failures.

Third, the fact that the phases are operated simultaneously, physically leads to an increase of the failure probability. This can be examined by using the reliability function $R(t)$ and the appropriate failure probability function $P(t)$, where both can be expressed as exponential functions depending on the time t and the failure rate λ being equal to 16,820 FIT.

$$R(t) = \mathrm{e}^{-\lambda t} = \mathrm{e}^{-(1.68\cdot 10^{-5}\,\mathrm{h}^{-1})\cdot t} \tag{4.10}$$

$$P(t) = 1 - R(t) \tag{4.11}$$

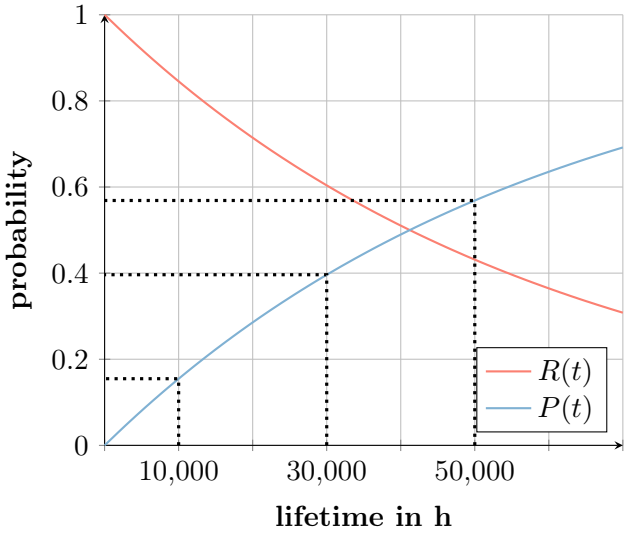

Figure 4.10: Reliability and failure probability functions. The reliability function $R(t) = \mathrm{e}^{-\lambda t}$ is shown in red, whereas the failure probability function $P(t) = 1 - \mathrm{e}^{-\lambda t}$ is shown in blue. The dotted lines represent the time, when the phase failures are assumed to take place and hence, define the new transition probabilities.

Figure 4.10 illustrates the two functions from equation (4.10) and (4.11) and shows, how the new transition probabilities are calculated for the Markov model. Since the $MTBF$ of the system is approximately 59,500 h, which complies with the required lifetime of the helicopter, the range in which the phase failures occur is limited from zero to 60,000 h. Assuming the time, to 10,000 h, 30,000 h, and 50,000 h, when the phase failures occur, leads to the new transition probability distribution and therefore to the new failure rates:

$$\begin{aligned} \lambda_{12} &= 1.68 \cdot 10^{-5}\,\mathrm{h}^{-1}\ ; \\ \lambda_{23} &= 1.55 \cdot 10^{-1}\,\mathrm{h}^{-1}\ ; \\ \lambda_{34} &= 3.96 \cdot 10^{-1}\,\mathrm{h}^{-1}\ ; \\ \lambda_{45} &= 5.69 \cdot 10^{-1}\,\mathrm{h}^{-1}\ . \end{aligned} \tag{4.12}$$

Finally, considering these transition probabilities of approximately 10^{-1} indicates, that also in this case – as for the 18-pulse-bridge –, the probability for multiple phase failures, as well as the degradation of components, can be neglected. Even though, both failure types lead to long transitions, which would impair the reliability behavior, neglecting these failure types is valid, since the result hardly differs in comparison with the sequential Markov model.

Result for the Electrical Drive Train

Figure 4.11 illustrates both resulting Markov models for the 18-pulse-bridge and the H-bridge topology over ten operating hours. Table 4.7 concludes the precise values for five operating hours in order to show the calculation results. Neither the figure nor the table aims to compare these two topologies, as after occurring failure, the failure probability for the next states is not adapted for the Markov model of the 18-pulse-bridge. Hence, a direct comparison would

not be fair. However, it is clearly visible that both topologies are not matching the reliability value of 10^{-9} per hour, which is displayed at the bottom being equal to the time-axis.

As a result, the preferred phase number is selected to be nine, as described previously. However, the bottleneck within the considered drive train system is defined by the power electronics considering fault tolerance. Therefore, the next chapter targets a possible solution for this problem. Further literature is available [13, 49], also depicting the problem of fault tolerance within electric drive trains for aircraft and resulting in redundancy or different subsystems in order to increase the fault tolerance. Additionally, chapter 5 presents an alternative drive train based on hydrogen in order to overcome the volume and weight problem with batteries, as briefly mentioned later.

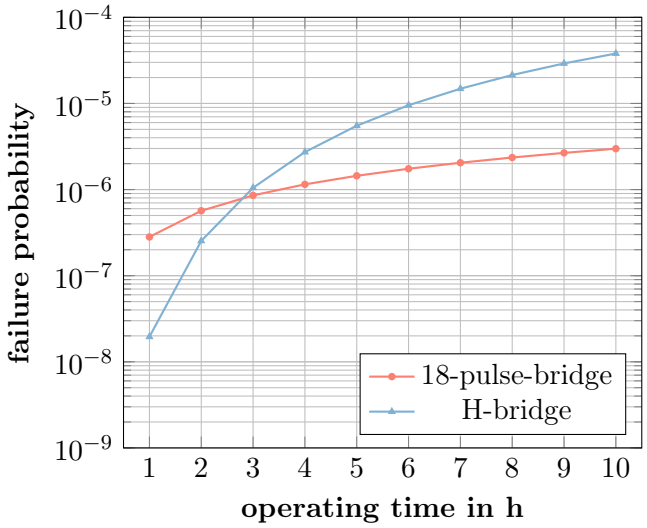

Figure 4.11: Results from the overall drive train Markov model evaluation. The 18-pulse-bridge and the H-bridge topologies, respectively displayed in red and blue, do not comply with the requirements as of 10^{-9} per hour. The specific values for the two topologies can be found in Table 4.7.

Table 4.7: Failure probabilities of the overall drive train resulting from the Markov model calculation from one to five operating hours, using the 18-pulse-bridge and the H-bridge topology. The resulting graphical characteristics for both topologies are depicted in Figure 4.11.

operating hours topology	1	2	3	4	5
18-pulse-bridge	$2.82 \cdot 10^{-7}$	$5.67 \cdot 10^{-7}$	$8.56 \cdot 10^{-7}$	$1.15 \cdot 10^{-6}$	$1.45 \cdot 10^{-6}$
H-bridge	$1.95 \cdot 10^{-8}$	$2.54 \cdot 10^{-7}$	$1.05 \cdot 10^{-6}$	$2.73 \cdot 10^{-6}$	$5.51 \cdot 10^{-6}$

5 Alternative Drive Train Concepts

The practical implementation of the drive train, mentioned in chapter 4, is not feasible using a battery storage, which delivers energy to the fully electrified helicopter. First, the current technology results in a too heavy battery [P7] due to the high energy requirements; hence, the helicopter would not be capable to take-off, due to an exceedance of the MTOW. Second, the fault tolerance of the drive train system does not meet the requirements, since a fault – for instance in the battery, the connection between battery and power electronics, or in the bridges – results in a total failure of the system or in a high power degradation. Therefore, this chapter provides two different drive train concepts to solve the previously mentioned problems. On the one hand, different ways of connecting power electronics and electrical machine by means of multilevel inverter are presented in order to increase the fault tolerance of the system and to provide flexibility of system integration. On the other hand, an assessment based on energy and power densities is conducted for an alternative drive train concept based on hydrogen.

5.1 Increasing Fault Tolerance by Different Topologies

Alternative topologies regarding the power electronics and different ways of connecting power electronics and electrical machine are auspicious regarding fault tolerance, weight, and volume of the system. However, the focus is set on fault tolerance based on Markov models and neither weight nor volume is considered within this section. More detailed information on multilevel topologies regarding weight and volume can be found in [P8]. As explained in the previous chapter, the nine-phase machine topology is considered to be optimal regarding fault tolerance and is therefore here taken into account as basis for comparison. Hence, the next step is to find an optimal way of connecting electrical machine and power electronics in order to increase the fault tolerance of the system. In literature, the multilevel technology has been increasingly presented as promising during the last decades, among others in [47]. Therefore, multilevel inverters are examined within this section while focusing on different topologies and the appropriate calculations considering reliability and fault tolerance in accordance with section 4.3.

5.1.1 Multilevel Inverter

The general idea of using multilevel inverters is the supply with a nearly ideal sinusoidal voltage by means of in series connected submodules and hence to split the voltage providing system into several subsystems. This means that the voltage is distributed over several modules in order to reduce the voltage load on the single semiconductors. This effect results in lower weight, volume, and price of each semiconductor. Especially, high system voltages can hence be realized by a higher number of voltage levels resulting in a higher number of submodules [81, 144]. However, the higher number of semiconductors – increasing the system's fault

tolerance – can lead to a higher weight or volume depending on the chosen number of levels. The signal quality becomes comparable to the ideal sinusoidal waveform of the voltage, due to a higher number of steps being proportional to the number of levels. The higher quality of the waveforms of the voltage results in lower torque ripple of the machine. Moreover, due to the possibility to use low-voltage semiconductors, efficiency is improved by multilevel inverters [P8], which has also a crucial impact on drive trains for mobile applications considering their operation range. [28, 47, 126]

Furthermore, the serial connection of the modules leads to another advantage regarding the energy source. Connecting each module to one energy source, which supplies the module with a DC-voltage (for instance a battery), leads to a higher flexibility considering the positioning of the energy sources. Additionally, the fault tolerance of the energy providing system is also increased, since in case of failure only one single part of the overall energy source fails and therefore only a degradation of power is expected.

One type of multilevel inverter is the cascaded H-bridge (CHB) which is based on the H-bridge topology, whereas *cascaded* means that H-bridge modules are connected in series in order to provide the overall phase voltage. It was initially published in a patent by Baker and Bannister in 1975 [3]. Beside the CHB, more multilevel topologies have been presented in literature, where further information about the function of multilevel inverters, waveforms, and differences between the topologies can be found [28, 47, 92, 126]. The derivation resulting in the choice of multilevel topology is not covered in this work, whereas it could be shown that the CHB topology is the optimal topology resulting in a lower number of components compared to other multilevel inverters [P8] and due to its high modularity [47]. Besides, the choice of the number of levels is also out of scope. Briefly explained, the number of levels is defined by the ratio of the minimal voltage of the machine phase and the minimal battery voltage, which means that the voltage needs to be divided into portions to be handled by the battery modules. The detailed consideration can be seen in [P8], where the voltages are assumed for the helicopter application.

Henceforth, the number of levels is regarded to be 17 levels per phase. Figure 5.1 shows a 17-level CHB inverter, which consists of eight H-bridge modules in order to provide 17 levels per phase. The high modularity especially is an advantage for the alignment of the inverter to the electrical machine dependent on the installation space.

5.1.2 Different Topologies with Multilevel Cascaded H-Bridge Inverter

The inverter structure of a cascaded H-bridge – illustrated in Figure 5.1 – and the different connections of the inverter outputs A and B lead to different topologies for the nine-phase drive train. Within the following assessment, only two topologies – which can be seen in Figure 5.2 – are being examined, where both include nine machine phases and 17 levels per phase, as previously mentioned. Thus, the assessed topologies are nine phase systems with

(a) star-connection and

(b) designing nine phases completely isolated from each other.

Figure 5.2a shows the first topology which is characterized by the star-connection of all nine phases. This can be obtained by connecting each of the nine phases on the one side to the inverter output A and on the other side to a star point. All nine inverter outputs B are

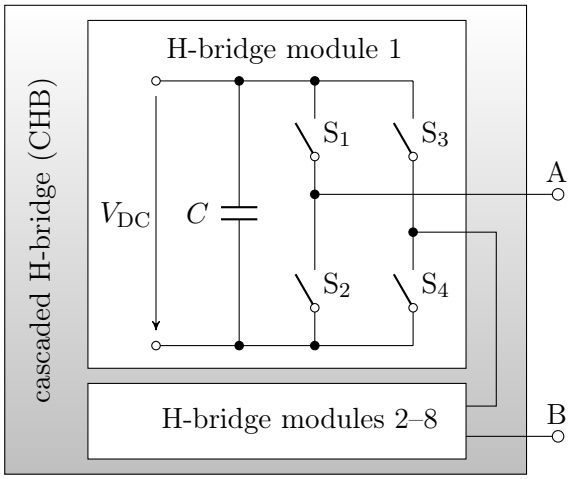

Figure 5.1: 17-level CHB inverter structure for one phase. Eight H-bridge modules are used to provide 17 levels per phase, whereas this structure can be used to supply different connection topologies of the machine by appropriately connecting the inverter outputs A and B to the phases of the machine.

internally connected to each other. The second topology is illustrated in Figure 5.2b, where all 17-level inverters are isolated from each other and each phase connects the output A to the output B of every single CHB inverter.

Each H-bridge is connected to one battery module, which generally increases the fault tolerance of the storage, since the total number of 72 battery modules is included. For this assessment of fault tolerance, the storage system is neglected, but the provided advantage needs to be mentioned here. The redundancy of the control unit is required and assumed for this assessment and hence, not considered within the calculation.

Furthermore, the structure is designed such that the outputs of a failing module are short-circuited, for instance by an installed shunt circuit, in order to enable the usage of all other remaining modules within the phase. Without shunt circuit, the complete phase would fail, which debilitates the advantage of the multilevel approach. However, compared to the conventional converter types – presented in the previous chapter – the failure of semiconductors, diodes, capacitors, or printed circuit boards does not directly lead to a phase failure. Hence, this redundancy enables a higher fault tolerance for the drive train, which is quantitatively defined in the next subsection.

5.1.3 Assessment of Reliability and Fault Tolerance

The procedure to assess the fault tolerance of the drive train using a CHB inverter is comparable to the previous Markov illustrations. The following paragraphs explain how to obtain the failure probabilities, which need to be taken into account for the appropriate transitions.

First and before evaluating the whole drive train, the probability for a total failure of a module needs to be calculated in order to obtain the failure probability per phase for the inverter. The worst-case scenario is the occurrence of all failed modules within one phase. Only if all failed modules are from the same phase, the loss of one complete phase becomes probable.

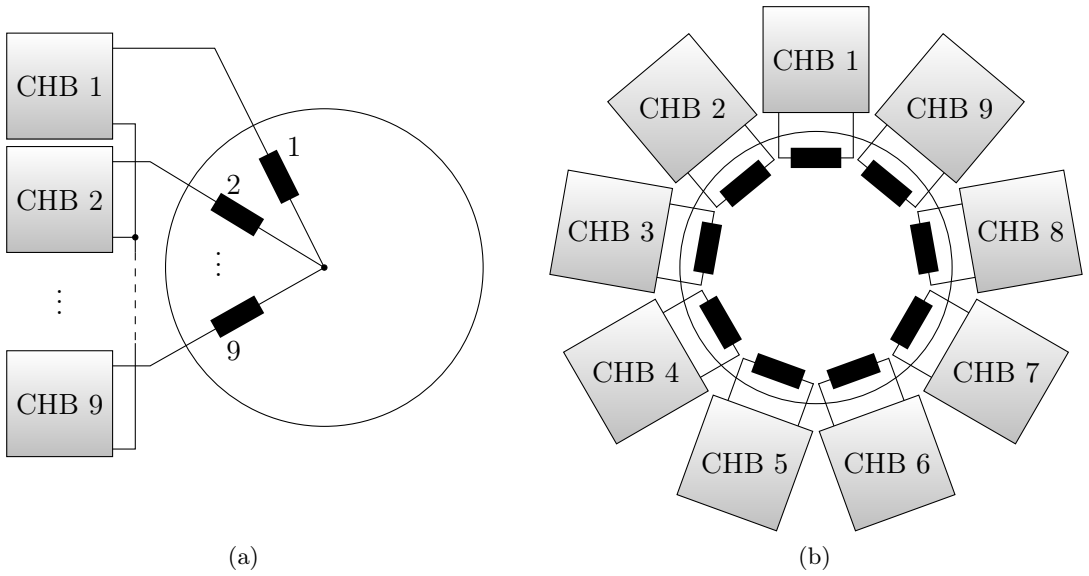

Figure 5.2: Different connection topologies using CHB inverters. The two topologies – nine phases with a star-connection (a) and nine separated phases (b) – are considered for the assessment of reliability and fault tolerance.

The probability that all modules are failing in the same phase – resulting in one ninth to the power n, if n is the number of failing modules – is not taken into account. Hence, the failure rate is calculated from all considered components, here eight capacitors, eight printed circuit boards, 32 semiconductors, and 32 diodes. These quantities result in the failure rate of 13,440 FIT for one phase of the inverter, see Table 5.1. Every loss of module is linked to a power degradation of 12.5 % of the CHB voltage, resulting from the distribution over eight modules. In order to maintain the required voltage, the current within the CHB is increased by 12.5 %, which needs to be conducted by the remaining semiconductors. Taking the overload capability of semiconductors, the current produces an overload situation, which decreases the operating time of the semiconductor [P3] [19]. The number of states is derived from the safety related turn-off of the phase, where the lower limit is set to one remaining minute of operating time within this work. The turn-off of the phase is acceptable, since the loss of one phase only leads to a decreasing system performance, but not to a drive train failure. Hence, based on these two assumptions, five states are used in order to represent the Markov model for the one-phase cascaded H-bridge. The transition probabilities – as previously shown – increase exponentially, whereas in this case 10,000 h, 20,000 h, and 30,000 h are the chosen time spots for the new transition values. It needs to be mentioned, that this is a worst-case scenario, since no maintenance or repair strategies are included, which finally would increase the system's reliability. All the resulting values for current increase, the appropriate remaining operating time, and the transition probabilities are depicted in Figure 5.3. This information is needed to build the Markov model for the cascaded H-bridge inverter. The result obtained by the Markov model calculation for the phase failure probability caused by the CHB inverter is $4.793 \cdot 10^{-9}$ for one hour and can be henceforth used for the overall system calculation.

Additionally, the failure rate for the loss of one phase due to faults occurring in the electrical machine is known from the previous calculation and equals 1,700 FIT, as well as the failure

Table 5.1: Number of components and FIT rates for the CHB topology. The number of components and the FIT rates are equal for both CHB inverter topologies (a) and (b). The values are shown for one phase and for the total inverter.

component	FIT/component	one phase quantity	one phase FIT	total inverter quantity	total inverter FIT
semiconductors	250	32	8,000	288	72,000
diodes	100	32	3,200	288	28,800
capacitors	80	8	640	72	5,760
printed circuit board	200	8	1,600	72	14,400
total FIT	—	—	13,440	—	120,960

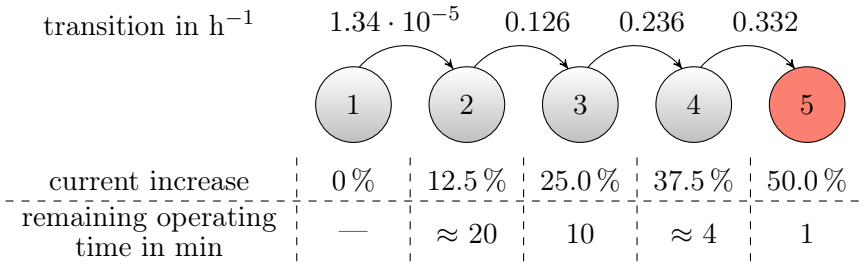

Figure 5.3: Markov model for one phase of the CHB inverter topologies. The number of states is derived from the remaining operating time due to overload conditions [19], which are defined by the increase of current.

rate for a short-circuit between two phases being equal to 60,300 FIT. Thus, the failure rate for the loss of phase is the sum of machine's failure rate and the CHB failure rate multiplied by nine due to the number of phases. The resulting value for the first short transition in both cases therefor is 1,743 FIT. Now, the modeling of both topologies (a) and (b) is explained and the remaining transition probabilities are defined depending on the topology.

Topology (a)

The nine-phase topology with star-connection, which is especially characterized by the long transitions resulting from the possibility of short-circuits, can be defined by the Markov model in Figure 5.4a. The number of states is again related to the power requirements distributed over the number of phases. Assuming the time when the phase failures occur to be 10,000 h, 20,000 h, and 30,000 h, and taking into account the short-circuit between two phases, leads to the transition probability distribution and hence, the new failure rates:

$$\begin{aligned}
\lambda_{12} &= 1.74 \cdot 10^{-6}\,\mathrm{h}^{-1}\ ; \qquad \lambda_{13} = 6.03 \cdot 10^{-5}\,\mathrm{h}^{-1}\ ; \\
\lambda_{23} &= 1.73 \cdot 10^{-2}\,\mathrm{h}^{-1}\ ; \qquad \lambda_{24} = 4.53 \cdot 10^{-1}\,\mathrm{h}^{-1}\ ; \\
\lambda_{34} &= 3.43 \cdot 10^{-2}\,\mathrm{h}^{-1}\ ; \qquad \lambda_{35} = 7.01 \cdot 10^{-1}\,\mathrm{h}^{-1}\ ; \\
\lambda_{45} &= (0.51 + 8.36) \cdot 10^{-1}\,\mathrm{h}^{-1} = 8.87 \cdot 10^{-1}\,\mathrm{h}^{-1}\ .
\end{aligned} \tag{5.1}$$

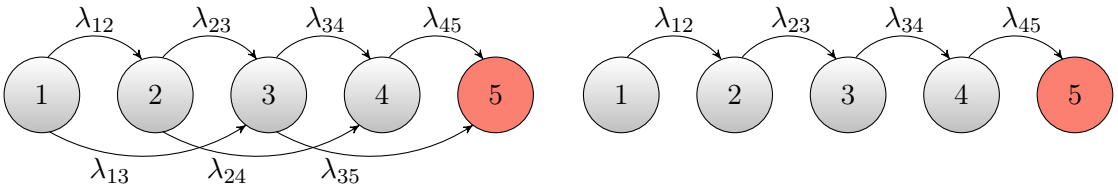

Figure 5.4: Markov models for drive train with CHB inverter for two topologies. The two topologies differ in the possibility of faults. For the nine phases with one star-connection (a), phase short-circuits are considered, whereas for nine separated phases (b), this fault type ($\lambda_{13}, \lambda_{24}, \lambda_{35}$) is neglected.

Topology (b)

Figure 5.4b illustrates the Markov model for the nine totally separated phases. The difference to topology (a) is that short-circuits between phases are not possible and hence can be neglected. The number of states stays constant. Therefore, the failure rate distribution is given as follows:

$$\begin{aligned} \lambda_{12} &= 1.74 \cdot 10^{-6}\,\mathrm{h}^{-1}\ ; \\ \lambda_{23} &= 1.73 \cdot 10^{-2}\,\mathrm{h}^{-1}\ ; \\ \lambda_{34} &= 3.43 \cdot 10^{-2}\,\mathrm{h}^{-1}\ ; \\ \lambda_{45} &= 5.09 \cdot 10^{-2}\,\mathrm{h}^{-1}\ . \end{aligned} \tag{5.2}$$

Results for the Electrical Drive Train Using CHB Inverter Topologies

The results of the Markov model calculations are concluded in Figure 5.5 and Table 5.2. Taking into account the one-hour flight scenario shows that the drive train topology with a nine-phase machine using the cascaded H-bridge inverter complies with the application requirements. The short-circuit between two phases is the significant fault case which decides if the topology is able to comply with the required reliability value of 10^{-9} per hour. Furthermore, the multilevel topology provides the significant advantage that the components (semiconductor, diode, capacitor, and printed circuit board) exist in every module. Therefore, the failure of these components does not directly provoke a phase failure, such as compared to the H-bridge Markov model in section 4.3. These aspects finally lead to the reliability values of 10^{-5} per hour for topology (a) including the star-connection, and 10^{-12} per hour for topology (b) implemented with nine galvanically separated phases.

In conclusion, topology (b) with the nine separated phases is the preferred option for the helicopter application. For a final system conclusion, the consideration of battery modules, control unit, or other components is recommended; although not further discussed within this work, whereas it needs to be highlighted that the mentioned reliability value is a worst-case assessment for the included components. This provides a certain, not quantifiable, safety factor, which enables the expansion of the number of considered components.

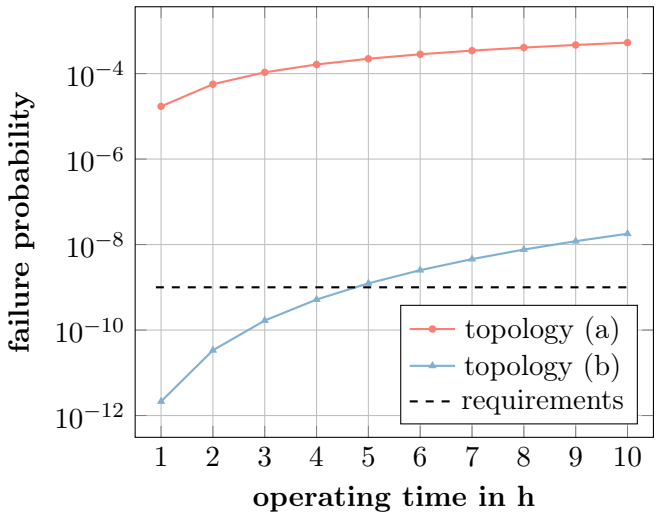

Figure 5.5: Results from the overall drive train Markov model evaluation using CHB inverters. Topology (a), displayed in red, does not comply with the requirements. In contrast based on a one-hour flight, topology (a) is illustrated in blue, which complies with the requirements as of 10^{-9} per hour. The specific values are shown in Table 5.2.

Table 5.2: Failure probabilities of the drive train resulting from the Markov model calculation using multilevel inverter comparing the two topologies (a) and (b). The characteristics for the two topologies are depicted in Figure 5.5.

operating hours / topology	1	2	3	4	5
(a)	$1.71 \cdot 10^{-5}$	$5.64 \cdot 10^{-5}$	$1.07 \cdot 10^{-4}$	$1.63 \cdot 10^{-4}$	$2.22 \cdot 10^{-4}$
(b)	$2.14 \cdot 10^{-12}$	$3.36 \cdot 10^{-11}$	$1.67 \cdot 10^{-10}$	$5.17 \cdot 10^{-10}$	$1.24 \cdot 10^{-9}$

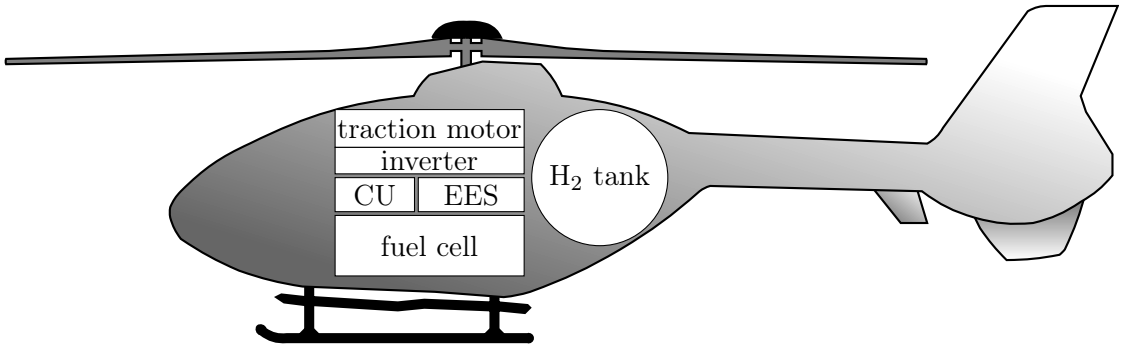

Figure 5.6: Conceptual illustration of the components of a fuel-cell-based drive train within a helicopter (CU: control unit; EES: electric energy storage).

5.2 Hydrogen-Based Drive Train System

Another possibility to overcome the weight problem is an alternative drive train system based on hydrogen. This section includes a conceptual study based on volumetric and gravimetric power densities for a drive train system consisting of a hydrogen (H_2) tank, a fuel cell, a high temperature superconducting (HTS) electrical machine, a DC-DC-converter, an inverter, a control unit, and a smaller electric energy storage compared to the drive train system with a conventional battery storage. These components are conceptually illustrated in Figure 5.6, whereas the dimensions and the placement are not realistic. The following sections will explain the state of the art considering the characterizing values for the power or energy density of the fuel cell, the inverter, the superconducting machines, and the H_2 tank. The focus is set on the values needed for the study, whereas technical information about the working principle of the components for this purpose will not be explained in detail and can be read in [46, 75, 77, 95, 129]. Furthermore, the parts, such as control unit, additional battery, and also the cooling system [120] are not included into the present preliminary investigation.

One of the main differences between a conventional and an electrical drive train system of a helicopter is the power supply and hence the different power constraints regarding the machine design. Within a conventional system, the overall needed power is provided by turbines using kerosene. However, it is a fuel cell using hydrogen, which must be designed in order to deliver the overall system power, whereas the electrical machine only generates the kinetic energy for the main rotor being the main system load. Finally, this feasibility study aims to provide a preliminary statement regarding the applicability of a fuel cell system to an electrical helicopter, taking into account components which have already been implemented or mentioned in publications. This will be discussed in the following sections.

5.2.1 Fuel Cell

The energy and power supply of the system is realized by a fuel cell. Fuel cells convert the chemically stored energy of hydrogen while reacting with oxygen to electrical energy and therefore create electrical power. In order to meet the requirement of electric vehicles, fuel cells need to have a preferably low weight and volume, hence a high energy conversion efficiency in order to ensure a low hydrogen consumption. Only few years ago, fuel cells could not compete

Table 5.3: Gravimetric and volumetric power densities for two fuel cell types being used in the "Toyota Mirai" and projected within the "AutoStack CORE" [74, 164].

fuel cell type	power density in kW/kg	power density in kW/l
Toyota Mirai	2.0	3.1
AutoStack	2.8	3.4

with battery electric storage systems within the field of electric vehicles in regard to price, volume, and weight [35].

Within a project called "AutoStack CORE" [74] a power density of 2.8 kW/kg and 3.4 kW/l was claimed, which shows that the state of the art of fuel cells is progressing. Nevertheless, for further assessment the more modest data of the implemented fuel cell installed on the "Toyota Mirai" [164] were taken into account. These projects show that fuel cells nowadays start to compete regarding the main characteristics (for example size and volume) of energy storage devices. All data of the mentioned fuel cells can be seen in Table 5.3.

The efficiency of fuel cells is a highly discussed topic in literature, since it is often unclear if the auxiliary devices, such as hydrogen pump or compressor, which are necessary to operate the fuel cell, are already included to the efficiency value or not. Hence, for this assessment an energy conversion efficiency of 45 % to 65 % is assumed for further calculations. Oversizing, which is usually necessary to balance aging effects, for better efficiency, or faster power changing [79], as well as the detailed design of the fuel cell are not important at an early stage and while assessing the feasibility of the system.

5.2.2 Converter

As previously discussed, within a fuel cell system, the electrical energy is directly provided to the system in contrary to the conventional helicopter system, where the electrical energy is supplied throughout kinetic energy. The energy coming from the fuel cell still needs to be converted, so that the energy can be used to drive the machine in the most optimal operating point. This conversion is conducted by a DC-DC-converter and a DC-AC-converter, whereas a correctly working control is assumed. Therefore, the evaluation of control methods is not taken into account here for the assessment.

As previously mentioned, multilevel converter is a promising topology considering dimensions and weight compared to the conventional converter types. The data of an experimental electric converter sample of the Fraunhofer Institute (Germany) [96] are used for design analysis of the DC-DC- and DC-AC-converter. Those designs provide a high power density and were especially designed for the operation with fuel cell systems. The DC-DC-converter's power densities are 62 kW/kg and 143 kW/l, whereas the DC-AC-converter's values are lower with 30 kW/kg and 69 kW/l [96]. The mentioned power density values are again depicted in Table 5.4. Finally, each of the converter efficiencies can be assumed to be 99 %.

Table 5.4: Gravimetric and volumetric power densities for the power electronics divided into DC-DC- and DC-AC-converter [96].

power electronics	power density in kW/kg	power density in kW/l
DC-DC-converter	62.0	143.0
DC-AC-converter	30.0	69.0

5.2.3 Superconducting Electrical Machine

Until today, a lot of investigations have been carried out in the field of superconducting machines, especially on high temperature superconducting (HTS) machines. Many of them have focused on aircraft applications, for which more information and examples can be found in [73, 89, 90, 93]. During the last decade, the topic of superconducting machines became more popular due to new application fields with high power density constraints and due to new technologies, such as fuel cells with significantly improved efficiency, volume, and weight [35, 112, 142]. Although the investigation results of Madavan et al. [90] are very promising providing a power density of 13 kW/kg for superconducting machines, for further evaluation the more modest values of already realized machines are studied here. A gravimetric power density of 7.5 kW/kg and a volumetric power density of 51.9 kW/l can be retrieved from [94] at a nominal speed of 3,000 min^{-1}. These values only include the active parts of the machine, whereas the inactive or auxiliary parts are neglected, such as the cooling system, which in case could be assumed to have approximately 60 % of the machine's weight [23].

The inappropriate speed of 3,000 min^{-1} instead of approximately 400 min^{-1} is also the reason for changing the starting criteria of a direct drive. In literature, it was impossible to find a corresponding machine with a matching rotational speed. Therefore, a gearbox needs to be included to the assessment in order to ensure a fair and logical statement. Calculating the gear transmission ratio of the rotational speed at the transmission output n_1 over the input speed n_2 leads to

$$i_\mathrm{g} = \frac{n_1}{n_2} = \frac{3{,}000\,\mathrm{min}^{-1}}{400\,\mathrm{min}^{-1}} = 7.5\ , \tag{5.3}$$

whereas the needed power is just influenced by the gearbox efficiency. Efficiencies for superconducting machines of more than 97 % can be found in literature, for instance in [91]. One of the advantages of this drive train topology is that the cryogenic cooling, which is required for the HTS machine, can be performed by the hydrogen stored at 20 K, hence no additional cooling is needed on board. The hydrogen can also be used for the cooling of the other components, such as power electronics and fuel cell. Furthermore, the cooling of the superconductors during operation can be maintained by providing approximately 20 W [95], whereas this is effectively only possible after a pre-cooling of the active parts of the rotor. Due to the superconducting behavior of the conductors in the rotor, the thermal limits are barely reached and high currents can be handled. HTS machines are advantageous considering volume, weight, and losses, such that all values can be assumed 50 % lower than for conventional electrical machines. [46, 129]

In conclusion, Niemann and Winter [108] mentioned possible efficiencies of more than 98 % regarding the planetary gearbox. This finally leads to an efficiency of approximately 95 % for both machine and gearbox. Considering the volumetric and gravimetric power densities

Table 5.5: Gravimetric and volumetric power densities for the HTS machine [94] and the gearbox [108], whereas the machine values only contain the active parts.

component	power density in kW/kg	power density in kW/l
HTS machine	7.5	51.9
planetary gearbox	5.0	6.7

of plenary gearboxes provided by [108] leads to values of maximum 5.0 kW/kg and 6.7 kW/l, respectively. All power densities taken into account for further calculations are summarized in Table 5.5.

5.2.4 Hydrogen Tank

The needed energy for such a drive train is provided by the hydrogen stored in special tanks. Two of the most suitable tank configurations, a spherical and a cylindrical, were selected for the assessment. The geometrical suitability of the conversion design platform was not considered.

Spherical tanks have a lower surface area than cylindrical tanks for the same volume and therefore, less material and hence less weight for spherical tanks. The following transformation of equations proves this fact, although the possible pressure or the material density is neglected for this consideration.

The starting point in order to get the final ratio between the two surfaces is formed by the commonly known equations for the volume (V) and the surface (A) of a spherical (sph) and a cylinder (cyl), where r is the radius of the corresponding body. For both cases the dependency between surface and volume is of special interest in order to obtain the surfaces' ratio.

$$\left.\begin{aligned} V_{\mathrm{sph}} &= \tfrac{4}{3}\pi \cdot r_{\mathrm{sph}}^3 \\ A_{\mathrm{sph}} &= 4\pi \cdot r_{\mathrm{sph}}^2 \end{aligned}\right\} \Rightarrow\ V_{\mathrm{sph}} = A_{\mathrm{sph}} \cdot \frac{r_{\mathrm{sph}}}{3} \tag{5.4}$$

The cylinder is additionally defined by its height h_{cyl}, which can be expressed as the radius times a factor κ.

$$\left.\begin{aligned} V_{\mathrm{cyl}} &= \pi \cdot r_{\mathrm{cyl}}^2 \cdot h_{\mathrm{cyl}} &&= \pi \cdot r_{\mathrm{cyl}}^3 \cdot \kappa \\ A_{\mathrm{cyl}} &= 2\pi \cdot r_{\mathrm{cyl}} \cdot (r_{\mathrm{cyl}} + h_{\mathrm{cyl}}) &&= 2\pi \cdot r_{\mathrm{cyl}}^2 \cdot (1+\kappa) \end{aligned}\right\} \Rightarrow\ V_{\mathrm{cyl}} = A_{\mathrm{cyl}} \cdot \frac{r_{\mathrm{cyl}}}{2} \cdot \frac{\kappa}{1+\kappa} \tag{5.5}$$

Both volumes need to be equal for the consideration regarding the given installation space within the helicopter. Due to this assumption, κ can be defined dependent on the radii of both the spherical and the cylinder based on the basic volume equations (5.4) and (5.5).

$$\begin{aligned} V_{\mathrm{sph}} &= V_{\mathrm{cyl}} \\ \frac{4}{3}\pi \cdot r_{\mathrm{sph}}^3 &= \pi \cdot r_{\mathrm{cyl}}^3 \cdot \kappa \\ \Longrightarrow \quad \kappa &= \frac{4}{3} \cdot \left(\frac{r_{\mathrm{sph}}}{r_{\mathrm{cyl}}}\right)^3 \end{aligned} \tag{5.6}$$

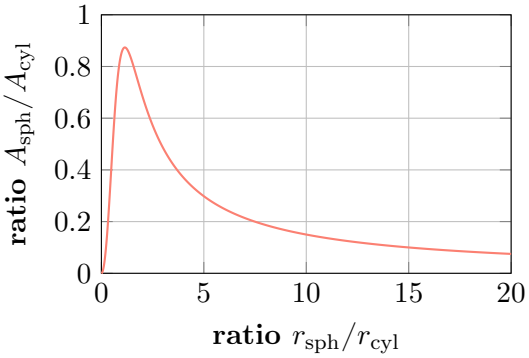

Figure 5.7: The ratio between the spherical and cylindrical surface depending on the ratio between the spherical and cylindrical radius. This behavior indicates that the cylindrical surface is always higher than the spherical surface, independent of the ratio between the two radii.

Taking into account the final equations (5.4) and (5.5) and apply κ from equation (5.6) to the equated volumes of both bodies, finally leads to the ratio between the two surfaces in equation (5.7) and the behavior shown in Figure 5.7.

$$\begin{aligned} V_{sph} &= V_{cyl} \\ A_{sph} \cdot \frac{r_{sph}}{3} &= A_{cyl} \cdot \frac{r_{cyl}}{2} \cdot \frac{\kappa}{1+\kappa} \\ \Longrightarrow \quad \frac{A_{sph}}{A_{cyl}} &= \frac{2 \cdot \left(\frac{r_{sph}}{r_{cyl}}\right)^2}{1 + \frac{4}{3} \cdot \left(\frac{r_{sph}}{r_{cyl}}\right)^3} \end{aligned} \tag{5.7}$$

Figure 5.7 shows that the spherical surface is always smaller than the cylindrical one. This fact is always independent from the ratio of the two radii.

For further calculations, realized projects deliver values summarized in Table 5.6. The values for the cylindrical tank are taken from the hydrogen driven electric car from "BMW AG", where hydrogen gas is stored at 350 bar and below 77 K [78]. Respectively, the values for the spherical tank are used from [139], where liquid hydrogen is stored at approximately 20 K. These values also prove the difference of the weight between the cylindrical and spherical tanks. However, both types are considered for the assessment, since the geometrical implementation within the helicopter could be easier with cylindrical tanks, which have higher degree of freedom regarding the installation space. Additionally, the comparison between two different ways of storage is not really valid, since the different pressure conditions play an important role in the design of the tanks. Furthermore, the scaling for the required energy of the system is an approximation, which needs to be proved for a more detailed assessment. For further calculations, these details are omitted.

The gravimetric and volumetric data collection enables the feasibility assessment for the fuel cell system, which is shown in the following section. This investigation is based on the evaluation of the available installation space and the available weight after the removal of certain components, which are not necessary for the alternative drive train concept.

Table 5.6: Gravimetric and volumetric energy densities for both the cylindrical and the spherical storage tank geometries considered within the assessment [78, 139].

storage tank	energy density in kWh/kg	energy density in kWh/l
cylindrical	2.5	1.0
spherical	5.8	1.6

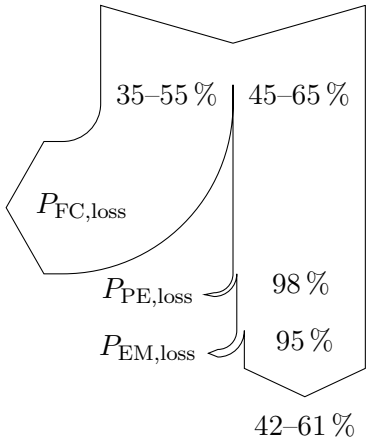

Figure 5.8: Sankey diagram of the alternative drive train system with a fuel cell and a superconducting machine. The diagram illustrates clearly that the system efficiency depends on the realized fuel cell efficiency.

5.2.5 Feasibility Assessment for a Fuel Cell Drive Train

Figure 5.8 shows a Sankey diagram for the energy conversion efficiencies for the components fuel cell (FC), power electronics (PE), and HTS machine (EM), which were explained in the previous sections. The power electronics here contain both the DC-DC-converter and the inverter, whereas the machine efficiency also takes the gearbox into account, as mentioned in section 5.2.3. For an accurate calculation of the energy conversion efficiency, the power characteristics including the duration and the efficiency at each operating point is required, but these data are mostly not available. Therefore, constant power is assumed in order to simplify the calculation and hence the efficiencies of the components are taken as energy conversion efficiencies by approximation. In conclusion, Figure 5.8 illustrates the significant impact of the fuel cell efficiency on the overall conversion efficiency. Thus, the fuel cell mainly influences the attractiveness and feasibility of the electrification. Within this assessment, all dependencies are neglected referring to any not explicitly mentioned component of the helicopter. However, the power demand of the tail rotor is considered for the overall system power demand, since the tail rotor is required to ensure a realistic applicability.

Based on the power and energy densities of each component mentioned above, a preliminary assessment can be conducted. The evaluation leads to a first response to the question if a drive train predicated on a fuel cell system can be considered as a possible solution for the presented aircraft application. First, the available installation space is calculated by the replacement of the conventional drive train components, followed by a feasibility assessment for one flight scenario and brief recommendation for further investigations.

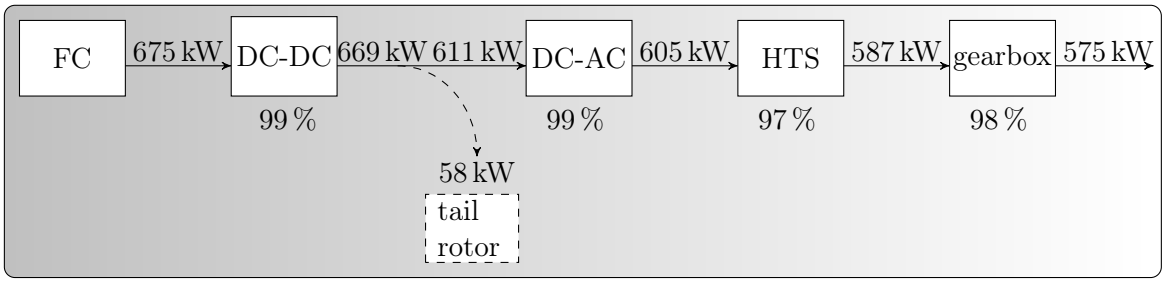

Figure 5.9: Power chain for the fuel-cell-based drive train. The chain includes the efficiencies of each component resulting in the input power starting from the mechanical output power for the helicopter's main rotor.

Available Installation Space

Taking into account the gas turbine system including the fuel tank and the gearbox of the conventional EC135, a total weight and volume benefit can be deduced by removing these components. Two turbines have a weight of 228 kg (approximately 330 l) and the filled fuel tank of approximately 650 kg (737 l); [42], [P1]. Since no exact values were found in literature, the weight and volume of the typically used gearbox with two stages will be presumed to have a weight of approximately 143.5 kg, taken from a EC135 training manual, and a volume is assumed of approximately 350 l. This leads to a benefit of 1,021.5 kg and 1,417 l.

In contrast, the volume of the hold (approximately 3,200 l) will not be considered, since it is necessary to keep this space in order to ensure the applicability of the helicopter. Furthermore, the space for auxiliary parts, such as pumps and mounting parts, is assumed to be equally distributed for both concepts. Thus, the installation space gained by the removal of the gearbox, turbines, and the fuel tank will be used for further considerations. The statistics from the German automobile club (ADAC) claim the average operating time of a SAR helicopter to be 8–10 hours per day [P1]. For the assessment a one-hour flight scenario is taken into account, which was mentioned within the key parameter description in section 4.1. It can be assumed as reasonably suitable to meet the requirements of one single classical SAR-mission, since fueling is possible between each mission.

A One-Hour Flight

A literature research [10, 151] results in an assumption for the power which is needed to supply the tail rotor. As mentioned before, the tail rotor is not considered for the assessment regarding weight or volume improvement, even though in order to fairly assess the fuel cell system, it has to provide the needed power for the tail rotor. Ultimately, this power can be conservatively assumed to be 10 % of the main rotor's power during hovering [10]. Therefore, this supplement needs to be taken into account for the DC-DC-converter, the fuel cell, and the hydrogen tank.

Table 5.7 contains all weights and volumes of the considered system components and summarizes the total values for both the spherical and cylindrical tank topology on the basis of the "Toyota Mirai" fuel cell with assuming a fuel cell efficiency of 65 %. This means, that the more modest power densities are taken into account in contrast to a very high fuel cell efficiency.

Table 5.7: Resulting weight and volume for a one-hour flight scenario. Assuming the output power to be 575 kW and a fuel cell efficiency of 65 % for the "Toyota Mirai" cell type.

component	weight in kg	volume in l
gearbox	115.0	85.8
machine	78.2	11.3
DC-AC-converter	20.2	8.8
DC-DC-converter	10.8	4.7
fuel cell	337.6	217.8
H_2-tank (spherical)	179.1	649.3
H_2-tank (cylindrical)	415.5	1,083.8
TOTAL (spherical)	740.9	977.7
TOTAL (cylindrical)	977.3	1,367.2

Moreover, some further assumptions are necessary for a final assessment. Each component value is calculated from the aforementioned power densities and the required output power of the respective component. The appropriate power demand is illustrated in Figure 5.9 taking into account the component efficiencies. Since the maximum output power is the maximum power of the system, no overload conditions are acceptable within this drive train assessment.

Additionally, the H_2-tank is requested to provide enough energy for the assumed one-hour flight, this means 1,038.8 kWh are needed if the aforementioned fuel cell efficiency is 65 % and the maximum power is taken by the traction drive during the complete flight time. Hence, this value characterizes a worst-case consideration regarding the required energy, since usually the maximum power is only requested while hovering, taking off, and landing. However, the fuel cell efficiency of 65 % is assumed at the upper limit. This finally leads to the assumption values for volume and weight regarding the spherical and the cylindrical tank type, which offer a certain amount of reserve for the final statement or more detailed calculations.

Since 65 % is a very high value for the fuel cell efficiency, a parameter study is presented in Figure 5.10 for the total system mass and in Figure 5.11 for the total system volume. The fuel cell efficiency varies between 0.45 and 0.65; both tank topologies are considered, as well as both fuel cell types. The green area symbolizes the available weight and installation space. Hence, all results from system configurations, which are running out of the green area, are barely implementable due to the requirements of the helicopter.

Furthermore, the red lines represent the resulting values with a cylindrical tank and the black lines stand for the system with spherical tank. The values for the fuel cell types from the "Toyota Mirai" and the "AutoStack" form the upper and the lower limit for both tank types, respectively. This behavior for both mass and volume is directly proportionally to the change of the power densities. Hence, the black patterned area illustrates which weight or volume reduction is achievable with today's state of technology.

Specifically, the result of Figure 5.10 and Figure 5.11 shows that the implementation of a fuel-cell-based system with spherical tank is possible and very promising independent of the fuel cell efficiency. Although the realization with a cylindrical tank within the restrictions

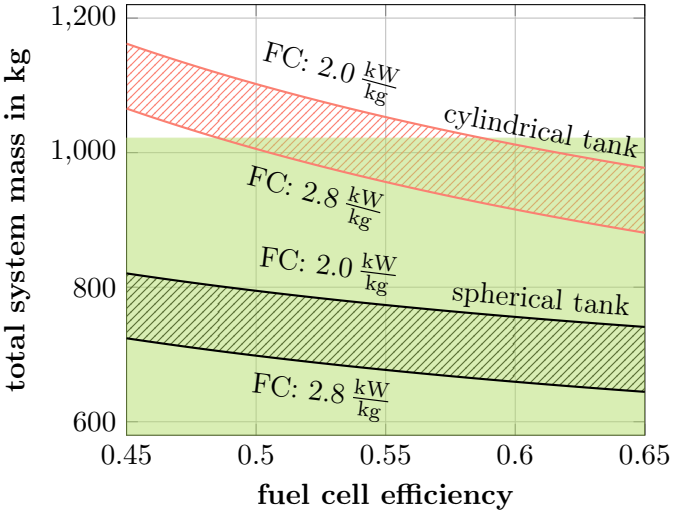

Figure 5.10: Total system mass for a range of the fuel cell efficiency from 0.45 to 0.65. The green area represents the available weight, which indicates that the fuel cell (FC) topology with a spherical tank (see black-patterned area) can be implemented within the restricted weight range, whereas the application of a cylindrical tank (see red patterned area) is constrained.

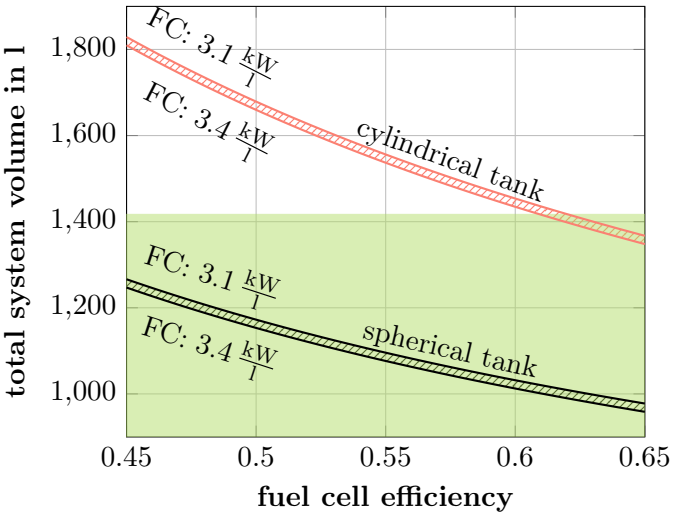

Figure 5.11: Total system volume for a range of the fuel cell efficiency from 0.45 to 0.65. The green area indicates the available installation space and demonstrates that the fuel cell (FC) topology with a spherical tank (see black-patterned area) can be implemented within the limited installation space, whereas the cylindrical tank (see red patterned area) is barely implementable.

still seems feasible considering the mass constraints, the volumetric boundaries are pushing at achievable limits. The fuel cell efficiency needs to accomplish at least 61 %; a fact which is still problematic.

Therefore, the next paragraphs provide possible solutions to achieve such requirements. Additional components are mentioned which are not taken into account within this assessment, but are worth the effort to include in further investigations.

Alternative Positioning or Design

The previous sections have shown that a drive train system based on hydrogen technology is implementable, whereas this conclusion is based on the preliminary assessment and today's state of technology. For a final statement data about the complete helicopter, which means all other technical systems within the EC135, need to be collected in order to assess the symbiotic effects by replacing the combustion system with an electrical one. The tail rotor, which was mentioned earlier, is one example for the numerous systems that could be adapted to the concept of electrification and hence optimized regarding weight and volume. Furthermore, the volume of the hold (3,200 l) could be used to show the possibility of the technical implementation while neglecting the applicability of the helicopter for any kind of transportation.

Other than that, the positioning of the components is a critical factor for the practicability of this approach. Compared to the military use, where weapon systems are placed outside of the helicopter's main body, tanks or even fuel cells can be placed outside or partially outside of the main cabin, since the outer space is not used for any other devices or functional matters in civil or cargo applications. Another idea, which is worth to be investigated, is not only the external placement of the system components, but also a subdivision of a component in order to reduce the volume. Hence, the number of component can be determined by the requirements of a system. For instance, the optimal number of subdivided hydrogen tanks can be defined based on the required range of an operation.

Finally, the presented approach is based on conversion design, taking into account the existent platform of the EC135. With a new purpose design strategy, which also includes the outer geometrical design changes and not only the replacement of components within the helicopter, the values for weight, range, or reliability could be further improved. A hybrid solution should also be considered for further investigations. In conclusion, considering the different possibilities mentioned to increase the installation space within the helicopter and the preliminary oversized design of the tank – which provides an energy reserve and therefore also a volume reserve – allows the implementation of additional components in order to ensure an overall feasibility.

Additional Components

Not all components needed for the implementation were included in the assessment. For instance, one problem that needs to be solved is the fuel cell's response time. Figure 5.12 shows the different behavior regarding the time constant of three energy supplies, here being the fuel cell, the battery, and the ultracapacitor [143, 168]. It can be seen that using only the fuel cell leads to a problem with the dynamics of the energy source, since the full amount of power cannot be provided immediately. One way to overcome this problem would be an

oversizing of the fuel cell in order to provide the needed power instantaneously. However, this is not a feasible solution, since the weight restrictions would be violated.

A hybrid energy supply seems auspicious, such as possible combinations of different supply devices which for example was shown in the publication of Thounthough et al. [143]. Although up to now this aspect was not covered within this work, the use of ultracapacitors is a possible solution for the low dynamic characteristic of the fuel cell. Combining both types leads to the synergistic effect of balancing power and energy density. In order to complete the system assessment and to strengthen the proof of feasibility, the values for each ultracapacitor are added to the weight and volume consideration for the one-hour flight based on the respective values of the spherical tank type and the fuel cell of "Toyota Mirai" with the more moderate power density (2.0 kW/kg and 3.1 kW/l). The visualization for the other tank or fuel cell type can be found analogically. In order to ensure the required power supply to the system it is necessary to focus on Figure 5.9 and Figure 5.12. On the basis of those two illustrations, the amount of power results in 669 kW for the drive train including the tail rotor and it needs to be provided for a time duration of 60 s until the fuel cell starts to operate in the nominal point. In this way, the worse dynamic characteristic of the fuel cell can be neglected since the ultracapacitor undertakes the power supply at the beginning.

In the following, the calculations of weight and volume of the ultracapacitor can be conducted based on the values found in a data sheet [136] and discussed with Karl S. Young from an American company "Precision Technology, Inc." from Olympia, WA, USA. Based on these data, the ratio between gravimetric and volumetric energy density can be calculated. The current technology regarding commercially available ultracapacitors discloses the values 6.0 Wh/kg for the gravimetric and 8.5 Wh/l for the volumetric energy density, respectively [136]. These values define the ratio between the two quantities as to approximately 1.4 kg/l. After Karl S. Young, various research labs already realized an ultracapacitor with 50 Wh/kg on the basis of graphene, which is said to provide 100 Wh/kg at the current state of the art. However, this value is obtained by only considering the material, whereas the capacitor providing such a value has not yet been developed. For the future, a possible value of even 250 Wh/kg is

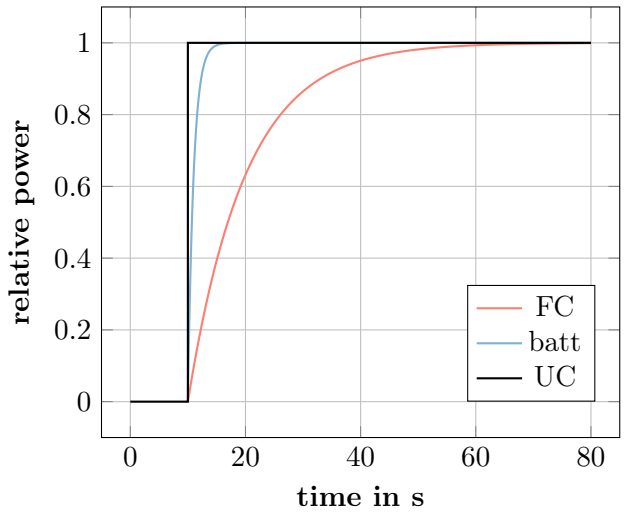

Figure 5.12: Power response of the different energy supply devices, such as fuel cells (FC), batteries (batt), and ultracapacitors (UC) based on [143].

Table 5.8: Additional weight and volume for different ultracapacitor types providing 669 kW for 60 s to ensure the power requirements during operation based on [136].

type	gravimetric energy density	weight	volume
1	6 Wh/kg	1,858 kg	1,327 l
2	50 Wh/kg	223 kg	159 l
3	100 Wh/kg	112 kg	80 l

mentioned. Furthermore, a linear dependency between with a factor of 1.4 kg/l can be assumed in order to derive the volume for the higher energy densities. This assumption is valid until approximately 150 Wh/kg, Young said, and is hence taken as acceptable for the fundamental evaluation.

Thus, three types of ultracapacitors are taken into account, whereas the gravimetric energy densities and resulting values of weight and volume are summarized in Table 5.8. The graphical conclusion for the integration of fuel cell and ultracapacitors and the resulting system weight and volume is presented in Figure 5.13a and Figure 5.13b for a one-hour flight as a function of the fuel cell efficiency. Additionally, the first two values of Table 5.8 represent the limits of the current technology regarding the energy density of ultracapacitors. The state of the art – based on commercial production and research – is illustrated by the red patterned area showing the minimum and the maximum of the reached weight and volume. The black dashed lines in the figures describe the third value, which stands for the auspicious future value of 100 Wh/kg for the gravimetric energy density and the assumed value of 140 Wh/l for the volumetric energy density.

The dependency on the fuel cell efficiency remains the most crucial factor, since the quantity of the needed hydrogen defines the tank size. As mentioned earlier, the green area indicates the available installation space considering weight and volume in the appropriate sub-figure of Figure 5.13.

Comparing both sub-figures shows that the most critical quantity is the weight, since the evaluation indicates that the red patterned area only just overlaps the feasible area marked in green. Considering commercially available capacitors, this concept is not yet realizable. Although, taking into account the values from research, the concept is getting closer to a possible realization based on the current technological progress regarding the volume of the ultracapacitors. Furthermore, considering the overall weight, the upper power density limit of 50 Wh/kg needs to be reached in order to comply with the weight restrictions.

Therefore, it becomes clear that at the current state the concept including the ultracapacitor is not feasible, if the capacitor needs to replace the full amount of energy typically provided by the fuel cell during operation. This assumption was made in order to comply with the worst-case requirements. In reality, the start up condition for the helicopter's rotor will not need the full power, which means that a future work needs to cover the real energy demand. Consequently, the ultracapcitor can be designed smaller and lighter and thus, the concept becomes feasible.

Ultimately, for the final implementation of such an alternative system, the overall possible mass reduction has to be executed for the complete helicopter, since the assessment was only based on the power needed for the propulsion system and no other consumers were included to

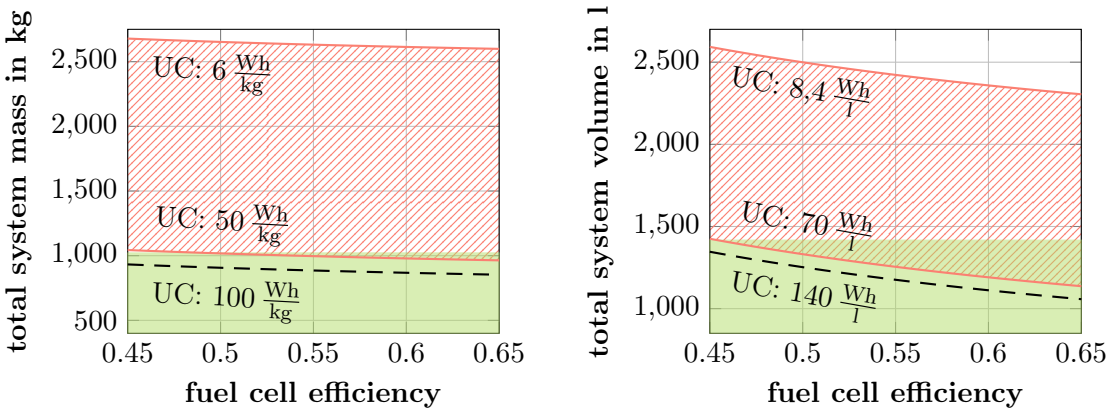

(a) (b)

Figure 5.13: Total system mass and volume for a range of the fuel cell efficiency from 0.45 to 0.65. The green area stands for the available weight or volume, which indicates that the alternative concept including an ultracapacitor (UC) can barely be realized within the restricted range and the current technology (see red patterned area). However, future trends are auspicious (see black dashed line).

the power balance. This also means that existing subsystems and components are likely to be replaced by new electrical components and hence, the overall system could be redesigned. That step comes along with new challenges but also new perspectives regarding the implementation. Even at this point, it is possible to draw an interim conclusion regarding the hydrogen-based system. The current state of technology already allows an application to such a system in a helicopter based on the presented assessment considering the power and energy densities for the needed components. Hence, the electrification of the helicopter's drive train is feasible while using the mentioned components.

6 Conclusion

The final chapter concludes the presented thesis, which was dedicated to introducing a methodology in order to analyze the potential of electrical drive trains according to the appropriate application requirements. The first section summarizes the methodological key aspects of this work, as well as the technical conclusion taking into account the feasibility study considering the electrification of a helicopter as application example. The second section focuses on aspects, which are worth to work on in the future, aspects that could not be achieved within this work, and critical aspects considering the conducted research work.

6.1 Achieved Targets

The methodology proposed within this work was composed by different methods, which have been used previously throughout different disciplines. These methods were explained and introduced to the assessment of drive trains for electric vehicles. By means of the hierarchical system approach, regression analysis, Markov models, and power or energy balancing, this work analyzed possible components and topologies for the electrification of a safety-critical mobile application, whereby the helicopter EC135 served as application example. The mentioned methodology simplifies the analysis and especially the choice of components for an electrical drive train at an early stage of a project. All considered methods were applied to different system topologies and they can easily be adapted to any other technical system based on changed data for the respective components or the overall system.

Technically speaking, the models were successfully adapted and applied to evaluate the electrical machine and the power electronics. Multiphase electrical machines in combination with multilevel inverters are auspicious for safety-critical traction systems and comply with the requirements regarding reliability and fault tolerance. It was shown that a nine-phase permanent magnet synchronous machine connected to a 17-level cascaded H-bridge inverter is a promising topology to be applied to the helicopter. This topology complies with the requirements regarding the allowed failure probability of the system. Alternatively, a drive train concept based on a fuel cell and a superconducting machine was presented. Based on the evaluation considering energy and power densities, it could be shown that this kind of topology is realizable considering weight and volume of the system. In general, the most critical aspect is the trust in the published data, which are used for the assessment, whereas at an early stage of a project and for the preliminary selection of components or topologies, the data is necessary for the models.

Methodologically, the regression analysis is a statistical model, which is highly dependent on the collected data. Hence, in case of new electrification approaches and the appropriate challenging requirements, the results can be used qualitatively but not quantitatively. The four factors simplify the consideration of complex systems and enable a fair comparison

or potential analysis. Furthermore, Markov models are a powerful method to evaluate the system's reliability and fault tolerance, whereas it could be clearly shown that the results of the Markov models are highly sensitive on the appropriate choice of number of states and the faults being considered for the assessment. Disregarding the quality of the reliability values, this means that the difference in failure probabilities extremely influences the result depending on the number of states and transition types. Hence, the quality of the reliability values is partly decisive since the structure of the models – depending on the topology or architecture – is the key indicator. These aspects directly lead to the critical reflection of the work's results.

6.2 Reflection of Critical Aspects and Outlook

This section depicts possible future topics based on the results and experiences gained within this work. The reality check of failure probabilities and the resulting weight and volumes for the overall system are aspects that need to be clarified. Additionally, the fuel-cell-based technology is worth to be investigated further. Especially, the prototyping of a multiphase drive train and its evaluation on a test bench need to be conducted in the future. All these topics are shortly explained, trying to work out some of the disregarded side effects, which can be covered by future research works. Additionally, taking the V-model into account, the following step after the selection of the components and the topologies is the design of the components. It constitutes the detailed design of the components including some aspects mentioned here.

Reality Check of Failure Probabilities

First, in order to ensure the quality of the results, the failure probabilities and fault statistics need to be verified. The study conducted in [P15] needs to be expanded to different machine types and especially to the traction applications. Collected data could be evaluated and used by the presented methodology in order to find comparative results and for instance new applicable topologies. This is a challenging approach, since drive train or vehicle manufacturer do not publish these confidential data. However, the values in [P15] indicated that the values did not change significantly over the last decades, but as mentioned by Lienig and Bruemmer [85] the accuracy of failure rates has a crucial impact on the assessment. Using specific values for the failure rates pretends high accuracy, whereas often the scenarios – including test circumstances, such as time range and application – are not clearly explained or published. Furthermore, the electrification of vehicles within the field of aircraft is a newly arising topic and therefore there is practically no experience on failure probabilities under such conditions. That is also the reason why many references use different failure rates. Hence, in order to obtain more accurate values for the failure rates, the application of components will need to be accurately assessed based on the different load scenarios including environmental conditions.

Additionally, overload capability was not covered in this work. However, overload needs to be applied in future studies in order to avoid a further power degradation and therefore include thermal characteristic of the system. This brings the choice of cooling systems into play and a possible adaption of control in the drive train system, since currents may be increased.

Reality Check of Weight and Volume

The weight and volume evaluation needs to be conducted in more detail for the multiphase system including the multilevel inverter. The detailed analysis on weight and volume of the system requires a detailed design of the considered drive train components. Additionally, components – such as the control units – need to be implemented redundantly in order to provide fault tolerance. All these auxiliary components need to be included to the volume or weight assessment. Another component, which is highly influencing volume and weight, is the cooling system. Different cooling systems need to be opposed to each other. However, the even more important aspect at this point is to oppose the obtained benefits by cooling the drive train system – linked to an increase of current densities and overload capability – to the overall system weight and volume.

Even though the battery was also exempted from the assessment, the energy storage is of course one of the most decisive factors considering the weight of the aircraft system. Future battery technologies and other storage types, such as the presented hydrogen-based system, can motivate an expanded evaluation of the complete system, including the energy storage. The consideration of fault tolerance regarding the battery is structurally covered in this work by choosing the cascaded H-bridge inverter structure. Each H-bridge is connected to a battery and therefore, the overall battery is distributed over as many batteries as cascaded H-bridges, in order to provide the required redundancy and consequently the required fault tolerance. However, the system weight is a crucial aspect for aircraft, which needs to be further investigated for the energy storage modules.

Conversion Design vs. Purpose Design

In this work, conversion design was applied to electrify the helicopter EC135. This existing platform consists of different subsystems and components, such as mechanical hydraulic devices, which were disregarded during the reliability assessment. Due to the certification processes that need to be fulfilled before being applied in reality, this is a valid approach. However, some components could be replaced by electrical actuators or devices in order to change the overall system. This step increases the complexity of the assessment and was not considered for the results of this work. However, some design procedures for subsystems can be found in literature, for instance in [25, 151] for the tail rotor. Future works can summarize all replaceable components and consequently include them to the system assessment within the conversion design.

In contrast, purpose design could lead on the one hand to different possibilities especially regarding installation space. On the other hand, purpose design could bring up some new topologies or architectures of VTOL vehicles, such as the concepts illustrated in the introduction of this work. Based on new architectures, the overall system design can change due to adapted system requirements. Hence, the number of phases, as well as the chosen topology, and the number of levels of the multilevel inverter are likely to be changed.

Evaluation of a Fuel-Cell-Based Topology

Apart from the aforementioned multiphase drive train system, the hydrogen-based topology is worth to be investigated further in detail since the presented assessment is only based on an energy balance. Here, the detailed design of each component based on the future state of the art is indispensable for further assessments. This implies works and topical investigations that need to be done on different fields – such as fuel cell, ultracapacitor, and superconducting machine –, since today's state of technology shows that the current power or energy densities yet limit the applicability. The overall system design is a crucial factor especially the coupling of the components to use the symbiotic characteristic of the hydrogen as energy carrier and cooling medium. Furthermore, the necessary safety constructions need to be clarified in order to store the hydrogen safely, as well as the hydrogen production can be investigated for an overall system design.

Beside the fuel-cell-based topology, another topology can be assessed, which was not considered within this work. The application of a hybrid drive train system, such as known from electric cars or ships, can be evaluated. This could be another possibility to solve the weight problem especially regarding the battery.

Prototyping the Multiphase Drive Train and Its Evaluation on a Test Bench

An important topic to follow is the practical implementation of a multiphase topology in order to examine the statements made within this work in reality. These statements are based on theoretical and also statistical investigations. Therefore, it is indispensable to assess the performance on a real-time test bench. The nine-phase machine, in combination with a multilevel converter, needs to be designed in detail to be able to construct and scrutinize it. Referring to the V-model mentioned in section 1.2.1, this means to finish the top-down path until the components are designed in detail and finally to continue on the bottom-up path to verify the results by testing the components and the system. In reality, a prototype of the permanent magnet synchronous machine with nine phases has to be built, where different machine types can be included, in order to practically prove the conclusion of this work. Furthermore, a multilevel inverter has to be designed and constructed. A comparable concept was built on a test bench and its feasibility is shown in [19] for a grid application.

Having completed the hardware side of the test bench, the control of healthy and faulty operating modes – for instance by simulating open-phase faults – can be implemented and tested depending on differently located failures or different failure modes. Additionally, the machine's behavior on different fault locations can be evaluated. The thermal characteristic of the machine's components are especially worth to be assessed in order to avoid thermal problems. Hence, by means of this test bench the reality check can be conducted while aiming at the evaluation of the results obtained from this work.

Bibliography

Reference List

[1] Airbus. *Seamless urban mobility? Soon no longer a flight of fancy.* Online; accessed May 12, 2017. URL: http://www.airbusgroup.com/int/en/news-media/corporate-magazine/Forum-90/PopUp.html.

[2] Audi AG. *Der Technikträger Audi A3 e-tron – Allrounder für den urbanen Alltag.* Online; accessed November 11, 2015. URL: https://www.audi-mediacenter.com/de/pressemitteilungen/der-techniktraeger-audi-a3-e-tron-allrounder-fuer-den-urbanen-alltag-983.

[3] R. H. Baker and L. H. Bannister. "Electric power converter". US3867643A. Online; accessed July 27, 2017. Feb. 1975. URL: https://patents.google.com/patent/US3867643A/en.

[4] V. S. Barbu and N. Limnios. *Semi-Markov Chains and Hidden Semi-Markov Models toward Applications: Their Use in Reliability and DNA Analysis.* Vol. 191. New York, NY: Springer New York, 2008. ISBN: 978-0-387-73171-1. DOI: 10.1007/978-0-387-73173-5.

[5] J. W. Bennett, B. C. Mecrow, D. J. Atkinson, and G. J. Atkinson. "Safety-critical design of electromechanical actuation systems in commercial aircraft". In: *IET Electric Power Applications* Vol. 5. No. 1 (Jan. 2011), pp. 37–47. ISSN: 1751-8660. DOI: 10.1049/iet-epa.2009.0304.

[6] N. Bianchi, S. Bolognani, and M. Dai Pre. "Design and Tests of a Fault-Tolerant Five-phase Permanent Magnet Motor". In: *37th IEEE Power Electronics Specialists Conference.* Jeju, South Korea, June 2006, pp. 1–8. ISBN: 0-7803-9716-9. DOI: 10.1109/pesc.2006.1712153.

[7] R. Billinton and R. N. Allan. *Reliability Evaluation of Power Systems.* Second Edition. Boston, MA, USA: Springer US, 1996. ISBN: 978-1-4899-1862-8. DOI: 10.1007/978-1-4899-1860-4.

[8] A. Binder. *Elektrische Maschinen und Antriebe [Electrical Machines and Drives].* Berlin, Heidelberg, Germany: Springer Berlin Heidelberg, 2012. ISBN: 978-3-540-71849-9. DOI: 10.1007/978-3-540-71850-5.

[9] A. Birolini. *Reliability Engineering: Theory and Practice.* 8th ed. Berlin, Heidelberg: Springer Berlin Heidelberg, 2017. ISBN: 978-3-662-54208-8. DOI: 10.1007/978-3-662-54209-5.

[10] W. Bittner. *Flugmechanik der Hubschrauber: Technologie, das flugdynamische System Hubschrauber, Flugstabilitäten, Steuerbarkeit.* 4th ed. Berlin, Heidelberg: Springer Berlin Heidelberg, 2014. ISBN: 978-3-642-54285-5. DOI: 10.1007/978-3-642-54286-2.

[11] bmwarchive.org. *The New BMW i3*. Online; accessed January 24, 2018. URL: http://www.bmwarchive.org/article/2013-07-10-the-new-bmw-i3.html.

[12] B. W. Boehm. "Guidelines for Verifying and Validating Software Requirements and Design Specifications". In: *Euro IFIP 79*. Ed. by P. A. Samet. North Holland, 1979, pp. 711–719.

[13] A. Boglietti, A. Cavagnino, A. Tenconi, and S. Vaschetto. "The safety critical electric machines and drives in the more electric aircraft: A survey". In: *35th Annual Conference of IEEE Industrial Electronics*. Porto, Portugal, Nov. 2009, pp. 2587–2594. DOI: 10.1109/IECON.2009.5415238.

[14] G. Bolch, S. Greiner, H. d. Meer, and K. S. Trivedi. *Queueing networks and Markov chains: Modeling and performance evaluation with computer science applications*. 2nd ed. Hoboken, NJ, USA: John Wiley & Sons, Inc., 2006. ISBN: 978-0-471-56525-3.

[15] I. Bolvashenkov and H.-G. Herzog. "Approach to predictive evaluation of the reliability of electric drive train based on a stochastic model". In: *International Conference on Clean Electrical Power (ICCEP)*. Taormina, Italy, June 2015, pp. 486–492. ISBN: 978-1-4799-8704-7. DOI: 10.1109/ICCEP.2015.7177561.

[16] I. Bolvashenkov and H.-G. Herzog. "Degree of Fault Tolerance as a Comprehensive Parameter for Reliability Evaluation of Fault Tolerant Electric Traction Drives". In: *Transactions on Environment and Electrical Engineering* Vol. 1. No. 3 (Sept. 2016), pp. 50–61. ISSN: 2450-5730. DOI: 10.22149/teee.v1i3.39.

[17] I. Bolvashenkov and H.-G. Herzog. "Degree of fault tolerance of the multi-phase traction electric motors: Methodology and application". In: *IEEE 16th International Conference on Environment and Electrical Engineering (EEEIC)*. Florence, Italy, June 2016, pp. 1–6. DOI: 10.1109/EEEIC.2016.7555635.

[18] I. Bolvashenkov, H.-G. Herzog, A. Rubinraut, and V. Romanovskiy. "Possible Ways to Improve the Efficiency and Competitiveness of Modern Ships with Electric Propulsion Systems". In: *IEEE Vehicle Power and Propulsion Conference (VPPC)*. Coimbra, Portugal, Oct. 2014, pp. 1–9. DOI: 10.1109/VPPC.2014.7007120.

[19] I. Bolvashenkov, T. Lahlou, and H.-G. Herzog. "Experimental verification of the normative thermal stability of a MOSFET full bridge power inverter". In: *Thirteenth International Conference on Ecological Vehicles and Renewable Energies (EVER)*. Monte-Carlo, Monaco, Apr. 2018, pp. 1–6. ISBN: 978-1-5386-5966-3. DOI: 10.1109/EVER.2018.8362370.

[20] Bombardier Transportation. *Battery-Driven Bombarbier Electrostar*. Online; accessed May 22, 2018. 2015. URL: https://www.bombardier.com/content/dam/Websites/bombardiercom/Projects/supporting-documents/BT_Battery-Driven-Bombardier-Electrostar_LowRes.pdf.

[21] I. Bouchareb, A. Bentounsi, and A. Lebaroud. "Classification method for faults diagnosis in reluctance motors using Hidden Markov Models". In: *IEEE 23rd International Symposium on Industrial Electronics (ISIE)*. Istanbul, Turkey, June 2014, pp. 984–991. DOI: 10.1109/ISIE.2014.6864746.

[22] P. Brémaud. *Markov Chains*. New York, NY, USA: Springer New York, 1999. ISBN: 978-1-4419-3131-3. DOI: 10.1007/978-1-4757-3124-8.

[23] G. Brown. "Weights and Efficiencies of Electric Components of a Turboelectric Aircraft Propulsion System". In: *49th AIAA Aerospace Sciences Meeting including the New Horizons Forum and Aerospace Exposition*. Orlando, Florida, USA, Jan. 2011. DOI: 10.2514/6.2011-225.

[24] D. Bücherl, R. Nuscheler, W. Meyer, and H.-G. Herzog. "Comparison of electrical machine types in hybrid drive trains: Induction machine vs. permanent magnet synchronous machine". In: *International Conference on Electrical Machines (ICEM)*. Vilamoura, Portugal, Sept. 2008, pp. 1–6. DOI: 10.1109/ICELMACH.2008.4800155.

[25] L. Castellini, M. D'Andrea, and M. Villani. "Electric powertrain for helicopter tail rotor". In: *6th International Electric Drives Production Conference (EDPC)*. Nuremberg, Germany: IEEE, Nov. 2016, pp. 268–273. DOI: 10.1109/EDPC.2016.7851349.

[26] W.-K. Ching and M. K. Ng. *Markov Chains: Models, Algorithms and Applications*. Vol. 83. New York, NY, USA: Springer Science+Business Media, Inc, 2006. ISBN: 978-0-387-29335-6.

[27] P. Dalgaard. *Introductory Statistics with R*. Statistics and Computing. New York, NY, USA: Springer New York, 2008, pp. 275–288. ISBN: 978-0-387-79053-4. DOI: 10.1007/978-0-387-79054-1.

[28] B. L. Dokić and B. Blanuša. *Power Electronics: Converters and Regulators*. 3rd ed. Cham, Germany: Springer International Publishing, 2015. ISBN: 978-3-319-09401-4. DOI: 10.1007/978-3-319-09402-1.

[29] R. d. Doncker, D. W. J. Pulle, and A. Veltman. *Advanced Electrical Drives*. Dordrecht: Springer Netherlands, 2011. ISBN: 978-94-007-0179-3. DOI: 10.1007/978-94-007-0181-6.

[30] M.-S. Donea. *Multiphysikalische Betrachtungen des elektrischen Antriebsstranges für das Flugzeug Do 128-6*. Vol. 27. Forschungsberichte Elektrische Antriebstechnik und Aktorik. Aachen: Shaker Verlag, July 2017. ISBN: 978-3-8440-5377-7.

[31] G. T. Doran. "There's a S.M.A.R.T. Way to Write Management's Goals and Objectives". In: *Management Review* No. 70 (Nov. 1981), pp. 35–36. URL: http://community.mis.temple.edu/mis0855002fall2015/files/2015/10/S.M.A.R.T-Way-Management-Review.pdf.

[32] T. J. Dos Santos Moraes, M. Trabelsi, N. K. Nguyen, E. Semail, F. Meinguet, and M. Guerin. "Inverter open circuit faults diagnosis in series-connected six-phases permanent magnet drive". In: *IEEE 11th International Symposium on Diagnostics for Electrical Machines, Power Electronics and Drives (SDEMPED)*. Tinos, Greece: IEEE, Aug. 2017, pp. 188–194. ISBN: 978-1-5090-0409-6. DOI: 10.1109/DEMPED.2017.8062354.

[33] M. R. J. Dubois. "Optimized Permanent Magnet Generator Topologies for Direct-Drive Wind Turbines". PhD thesis. Delft, Netherlands: Delft University of Technology, Jan. 2004. ISBN: 0-9734585-0-X.

[34] M. J. Duran and F. Barrero. "Recent Advances in the Design, Modeling, and Control of Multiphase Machines—Part II". In: *IEEE Transactions on Industrial Electronics* Vol. 63. No. 1 (Jan. 2016), pp. 459–468. ISSN: 0278-0046. DOI: 10.1109/TIE.2015.2448211.

[35] S. Eaves and J. Eaves. "A cost comparison of fuel-cell and battery electric vehicles". In: *Journal of Power Sources* Vol. 130. No. 1-2 (2004), pp. 208–212. ISSN: 03787753. DOI: 10.1016/j.jpowsour.2003.12.016.

[36] K. Echtle. *Fehlertoleranzverfahren*. Berlin, Heidelberg: Springer Berlin Heidelberg, 1990. ISBN: 978-3-540-52680-3. DOI: 10.1007/978-3-642-75765-5.

[37] M. Ehsani, Y. Gao, and A. Emadi. *Modern electric, hybrid electric, and fuel cell vehicles: Fundamentals, theory, and design*. 2nd ed. Power electronics and applications series. Boca Raton, USA: CRC Press, 2010. ISBN: 978-1-4200-5398-2.

[38] M. Ehsani, K. M. Rahmann, and H. A. Toliyat. "Propulsion system design of electric vehicles". In: *Proceedings of the 1996 IEEE IECON. 22nd International Conference on Industrial Electronics, Control, and Instrumentation*. Taipei, Taiwan, Aug. 1996, pp. 7–13. ISBN: 0-7803-2775-6. DOI: 10.1109/IECON.1996.570893.

[39] A. Eilenberger, M. Schrödl, and F. Demmelmayr. "Elektrofahrzeuge mit Permanentmagnet-Synchronmaschinen". In: *e & i Elektrotechnik und Informationstechnik* Vol. 128. No. 1-2 (2011), pp. 40–46. DOI: 10.1007/s00502-011-0804-z.

[40] N. P. Ermolin and I. P. Žerichin. *Zuverlässigkeit elektrischer Maschinen*. 1st ed. Berlin: VEB Verlag Technik, 1981.

[41] Eurocopter. *EC 135 Technical Data*. Online; accessed June 11, 2018. URL: http://www.hdf.fr/public/PDF/EC_135_PDF.pdf.

[42] European Aviation Safety Agency (EASA), ed. *Type Certificate Data Sheet No. E.029 for Arrius 2 series engines*. 5th ed. Online; accessed Feb. 24, 2017. Safran Helicopter Engines. Bordes, France, Aug. 2016. URL: http://www.easa.europa.eu/system/files/dfu/EASA%20TCDS%20E.029_%20issue%2005_20160108_1.0.pdf/.

[43] D. Filusch, M. Breiteneder, and H.-G. Herzog. "Design of a Hyperconducting Synchronous Machine for High-Torque Applications". In: *23rd International Conference on Electrical Machines (ICEM)*. Alexandroupoli, Greece, Sept. 2018, pp. 2092–2098. ISBN: 978-1-5386-2477-7. DOI: 10.1109/ICELMACH.2018.8506697.

[44] T. Finken, M. Felden, and K. Hameyer. "Comparison and design of different electrical machine types regarding their applicability in hybrid electrical vehicles". In: *International Conference on Electrical Machines (ICEM)*. Vilamoura, Portugal, Sept. 2008, pp. 1–5. DOI: 10.1109/ICELMACH.2008.4800044.

[45] D. Fodorean, M. Ruba, L. Szabo, and A. Miraoui. "Comparison of the main types of fault-tolerant electrical drives used in vehicle applications". In: *International Symposium on Power Electronics, Electrical Drives, Automation and Motion (SPEEDAM)*. Ischia, Italy, June 2008, pp. 895–900. DOI: 10.1109/SPEEDHAM.2008.4581328.

[46] M. Frank, P. v. Habelt, P. Kummeth, P. Massek, W. Nick, H. Rothfischer, H. Schmidt, B. Wacker, H.-W. Neumuller, G. Nerowski, J. Frauenhofer, R. Hartig, and W. Rzadki. "High-Temperature Superconducting Rotating Machines for Ship Applications". In: *IEEE Transactions on Applied Superconductivity* Vol. 16. No. 2 (June 2006), pp. 1465–1468. ISSN: 1051-8223. DOI: 10.1109/TASC.2005.864263.

[47] L. Franquelo, J. Rodriguez, J. Leon, S. Kouro, R. Portillo, and M. Prats. "The age of multilevel converters arrives". In: *IEEE Industrial Electronics Magazine* Vol. 2. No. 2 (June 2008), pp. 28–39. ISSN: 1932-4529. DOI: 10.1109/MIE.2008.923519.

[48] E. D. Ganev. "High-Performance Electric Drives for Aerospace More Electric Architectures Part I – Electric Machines". In: *IEEE Power Engineering Society General Meeting*. Tampa, FL, USA, June 2007, pp. 1–8. ISBN: 1-4244-1296-X. DOI: 10.1109/PES.2007.385463.

[49] A. Garcia, J. Cusido, J. A. Rosero, J. A. Ortega, and L. Romeral. "Reliable electro-mechanical actuators in aircraft". In: *IEEE Aerospace and Electronic Systems Magazine* Vol. 23. No. 8 (Aug. 2008), pp. 19–25. ISSN: 0885-8985. DOI: 10.1109/MAES.2008.4607895.

[50] J. Gausemeier and S. Möhringer. "New Guideline VDI 2206 – A flexible procedure model for the design of Mechatronic systems." In: *International Conference on Engineering Design (ICED)*. Ed. by A. Folkeson, K. Gralen, M. Norell, and U. Sellgren. Stockholm, Sweden, Aug. 2003.

[51] V. Gollnick. "Untersuchungen zur Bewertung der Transporteffizienz verschiedener Verkehrsmittel [A methodology to assess the transport efficiency of various transport vehicles]". original language: German. PhD thesis. Munich, Germany: Technische Universität München, Mar. 2003. URL: http://nbn-resolving.de/urn/resolver.pl?urn:nbn:de:bvb:91-diss2004031618499.

[52] S. Graebener, M. Tarnowski, and D. Goehlich. "Commercial vehicle drive train technology and topology pre-selection". In: *Tenth International Conference on Ecological Vehicles and Renewable Energies (EVER)*. Monte Carlo, Monaco, Mar. 2015, pp. 1–5. ISBN: 978-1-4673-6785-1. DOI: 10.1109/EVER.2015.7113011.

[53] C. Graham and D. Talay. *Stochastic Simulation and Monte Carlo Methods: Mathematical Foundations of Stochastic Simulation*. Vol. 68. Berlin, Heidelberg, Germany: Springer Berlin Heidelberg, 2013. ISBN: 978-3-642-39362-4. DOI: 10.1007/978-3-642-39363-1.

[54] N. Hashemnia and B. Asaei. "Comparative study of using different electric motors in the electric vehicles". In: *International Conference on Electrical Machines (ICEM)*. Vilamoura, Portugal, Sept. 2008, pp. 1–5. DOI: 10.1109/ICELMACH.2008.4800157.

[55] E. Hatzipantelis and J. Penman. "The use of hidden Markov models for condition monitoring electrical machines". In: *Sixth International Conference on Electrical Machines and Drives (Conf. Publ. No. 376)*. Oxford, UK, Sept. 1993, pp. 91–96. ISBN: 0-85296-596-6.

[56] D. P. Heap. *Report on the International exhibition of electricity held at Paris: August to November, 1881*. Online; accessed Dec. 27, 2016. Washington, USA: U.S. Government Printing Office, 1884. URL: https://books.google.de/books?id=empAAAAAIAAJ.

[57] Q. Hecker, J. A. Butron Ccoa, W. Meyer, and H.-G. Herzog. "Automated design of squirrel-cage induction machines by predefined torque-speed-characteristic". In: *International Electric Machines & Drives Conference (IEMDC)*. Chicago, IL, USA, May 2013, pp. 1160–1165. ISBN: 978-1-4673-4974-1. DOI: 10.1109/IEMDC.2013.6556306.

[58] R. Höhn, S. Höppner, A. Rausch, M. Broy, K. Bergner, and W. Hesse. *Das V-Modell XT: Anwendungen, Werkzeuge, Standards [The V-model XT: Applications, Tools, Standards]*. Springer-Lehrbuch. Berlin and Heidelberg, Germany: Springer, 2008. ISBN: 978-3-540-30249-0.

[59] R. A. Howard. *Dynamic Programming and Markov Processes*. Second printing. The Technology Press of The Massachusetts Institute of Technology and John Wiley & Sons, Inc., New York, London, 1962.

[60] J. Huang, M. Kang, J.-q. Yang, H.-b. Jiang, and D. Liu. "Multiphase machine theory and its applications". In: *The 11th International Conference on Electrical Machines and Systems (ICEMS)*. Wuhan, China, Oct. 2008, pp. 1–7. ISBN: 978-7-5062-9221-4.

[61] Hybrid-Autos.info. *Citro"en C-ZERO 2011*. Online; accessed January 24, 2018. URL: http://www.hybrid-autos.info/Elektro-Fahrzeuge/Citro%C3%ABn/citroen-c-zero-2011.html.

[62] Hybrid-Autos.info. *Peugeot iOn*. Online; accessed January 24, 2018. URL: http://www.hybrid-autos.info/Elektro-Fahrzeuge/Peugeot/peugeot-ion.html.

[63] Hybrid-Autos.info. *Smart fortwo electric drive 2009*. Online; accessed January 24, 2018. URL: http://www.hybrid-autos.info/Elektro-Fahrzeuge/Smart/smart-fortwo-electric-drive-2009.html.

[64] Hyundai Motor Deutschland GmbH. *ix35 Fuell Cell*. Online; accessed January 24, 2018. URL: http://www.hyundai.de/Modelle/Alle-Modelle/ix35-Fuel-Cell.html.

[65] IEEE Computer Society. *1220-2005 – ISO/IEC Standard for Systems Engineering – Application and Management of the Systems Engineering Process*. Piscataway, NJ, USA, July 2007. DOI: 10.1109/IEEESTD.2007.386502.

[66] IEEE Computer Society. *15288-2008 – ISO/IEC/IEEE International Standard – Systems and software engineering System life cycle processes*. Piscataway, NJ, USA, Jan. 2008. DOI: 10.1109/IEEESTD.2008.6093923.

[67] IEEE Reliability Society. *1332-1998 – IEEE Standard Reliability Program for the Development and Production of Electronic Systems and Equipment*. Piscataway, NJ, USA, Mar. 2013. DOI: 10.1109/IEEESTD.2013.6477227.

[68] IEEE Reliability Society. *1413-2010 – IEEE Standard Framework for Reliability Prediction of Hardware – Redline*. New York, NY, USA, Apr. 2010. DOI: 10.1109/IEEESTD.2010.5953402.

[69] E. Illiano. "Die stromerregte Synchronmaschine als hocheffizienter Traktionsmotor in Elektrofahrzeugen". In: *ATZelektronik* No. 4 (Apr. 2013), pp. 304–309.

[70] R. Isermann. "Mechatronic systems—Innovative products with embedded control". In: *Control Engineering Practice* Vol. 16. No. 1 (2008), pp. 14–29. ISSN: 09670661. DOI: 10.1016/j.conengprac.2007.03.010.

[71] T. M. Jahns. "Improved Reliability in Solid-State AC Drives by Means of Multiple Independent Phase Drive Units". In: *IEEE Transactions on Industry Applications* Vol. IA-16. No. 3 (May 1980), pp. 321–331. ISSN: 00939994. DOI: 10.1109/TIA.1980.4503793.

[72] O. Johann and J. Müller. "Die fremderregte Synchronmaschine Potenziale in der Elektromotoren-Entwicklung". In: *ATZelektronik* No. 4 (Apr. 2013), pp. 286–289.

[73] C. E. Jones, P. J. Norman, S. J. Galloway, M. J. Armstrong, and A. M. Bollman. "Comparison of Candidate Architectures for Future Distributed Propulsion Aircraft". In: *IEEE Transactions on Applied Superconductivity* Vol. 26. No. 6 (Feb. 2016), pp. 1–9. ISSN: 1051-8223. DOI: 10.1109/TASC.2016.2530696.

[74] L. Jörissen. *AutoStack CORE: Development and test of a 95-kW fuel cell stack*. Online; accessed Mar. 14, 2017. URL: https://www.zsw-bw.de/en/projects/h2-und-brennstoffzellen/autostack-core-development-and-test-of-a-95-kw-fuel-cell-stack.html.

[75] G. Klaus, M. Wilke, J. Frauenhofer, W. Nick, and H.-W. Neumuller. "Design Challenges and Benefits of HTS Synchronous Machines". In: *IEEE Power Engineering Society General Meeting*. Tampa, FL, USA, June 2007, pp. 1–8. DOI: 10.1109/PES.2007.385756.

[76] Kongsberg Maritime. *Autonomous ship, key facts about the YARA Birkeland project*. Online; accessed May 12, 2017. URL: https://www.km.kongsberg.com/ks/web/nokbg0240.nsf/AllWeb/4B8113B707A50A4FC125811D00407045?OpenDocument.

[77] K.-D. Kreuer. *Fuel Cells: Selected Entries from the Encyclopedia of Sustainability Science and Technology*. New York, NY, USA: Springer New York, 2013. ISBN: 978-1-4614-5784-8. DOI: 10.1007/978-1-4614-5785-5.

[78] K. Kunze and O. Kircher. "Cryo-Compressed Hydrogen Storage". In: *Cryogenic Cluster Day*. Online; accessed Apr. 19, 2017. Oxford, UK, Sept. 2012, pp. 1–33. URL: https://www.stfc.ac.uk/stfc/cache/file/F45B669C-73BF-495B-B843DCDF50E8B5A5.pdf.

[79] P. Kurzweil. *Brennstoffzellentechnik: Grundlagen, Materialien, Anwendungen, Gaserzeugung*. 3rd ed. Wiesbaden, Germany: Springer Fachmedien Wiesbaden, 2016. ISBN: 978-3-658-14934-5. DOI: 10.1007/978-3-658-14935-2.

[80] H.-C. Lahne. *Erforschung von Designaspekten bei "High-Speed"-Asynchronmaschinen hinsichtlich der Verwendung in der Luftfahrt*. 1. Auflage. Vol. 21. Forschungsberichte Elektrische Antriebstechnik und Aktorik. Herzogenrath: Shaker, Sept. 2016. ISBN: 978-3-8440-4663-2.

[81] J.-S. Lai and F. Z. Peng. "Multilevel converters—a new breed of power converters". In: *IEEE Transactions on Industry Applications* Vol. 32. No. 3 (June 1996), pp. 509–517. ISSN: 00939994. DOI: 10.1109/28.502161.

[82] E. Levi. "Multiphase Electric Machines for Variable-Speed Applications". In: *IEEE Transactions on Industrial Electronics* Vol. 55. No. 5 (Apr. 2008), pp. 1893–1909. ISSN: 0278-0046. DOI: 10.1109/TIE.2008.918488.

[83] E. Levi, R. Bojoi, F. Profumo, H. A. Toliyat, and S. Williamson. "Multiphase induction motor drives – a technology status review". In: *IET Electric Power Applications* Vol. 1. No. 4 (July 2007), p. 489. ISSN: 17518660. DOI: 10.1049/iet-epa:20060342.

[84] G. Levitin. *The Universal Generating Function in Reliability Analysis and Optimization*. Springer Series in Reliability Engineering. New York, NY, USA: Springer-Verlag London Limited, 2005. ISBN: 978-1-85233-927-2.

[85] J. Lienig and H. Bruemmer. *Fundamentals of Electronic Systems Design*. Cham: Springer International Publishing, 2017, pp. 45–73. ISBN: 978-3-319-55839-4. DOI: 10.1007/978-3-319-55840-0.

[86] T. M. Liggett. *Continuous Time Markov Processes: An Introduction*. Vol. 113. Graduate studies in mathematics. Providence, R.I., USA: American Mathematical Society, 2010. ISBN: 978-0-8218-4949-1.

[87] Lilium GmbH. *Lilium celebrates successful flight tests and introduces 5-seater VTOL jet*. Online; accessed May 12, 2017. URL: https://lilium.com/news/.

[88] A. Lisnianski, I. Frenkel, and Y. Ding. *Multi-state System Reliability Analysis and Optimization for Engineers and Industrial Managers*. London: Springer-Verlag, 2010, pp. 1–113. ISBN: 978-1-84996-319-0. DOI: 10.1007/978-1-84996-320-6.

[89] C. A. Luongo, P. J. Masson, T. Nam, D. Mavris, H. D. Kim, G. V. Brown, M. Waters, and D. Hall. "Next Generation More-Electric Aircraft: A Potential Application for HTS Superconductors". In: *IEEE Transactions on Applied Superconductivity* Vol. 19. No. 3 (June 2009), pp. 1055–1068. ISSN: 1051-8223. DOI: 10.1109/TASC.2009.2019021.

[90] N. Madavan, J. Heidmann, C. Bowman, P. Kascak, E. Jankovsky, and R. Jansen. "A NASA Perspective on Electric Propulsion Technologies for Commercial Aviation". In: *Workshop on Technology Roadmap for Large Electric Machines*. Online; accessed Mar. 13, 2017. University of Illinois, Urbana-Champaign, Illinois, USA, Apr. 2016, pp. 1–32. URL: https://machineroadmap.ece.illinois.edu/files/2016/04/Madavan.pdf.

[91] N. Maki, T. Takao, S. Fuchino, H. Hiwasa, M. Hirakawa, K. Okumura, M. Asada, and R. Takahashi. "Study of Practical Applications of HTS Synchronous Machines". In: *IEEE Transactions on Appiled Superconductivity* Vol. 15. No. 2 (June 2005), pp. 2166–2169. ISSN: 1051-8223. DOI: 10.1109/TASC.2005.849603.

[92] M. Malinowski, K. Gopakumar, J. Rodriguez, and M. A. Pérez. "A Survey on Cascaded Multilevel Inverters". In: *IEEE Transactions on Industrial Electronics* Vol. 57. No. 7 (July 2010), pp. 2197–2206. ISSN: 0278-0046. DOI: 10.1109/TIE.2009.2030767.

[93] P. Malkin and M. Pagonis. "Superconducting electric power systems for hybrid electric aircraft". In: *Aircraft Engineering and Aerospace Technology* Vol. 86. No. 6 (2014), pp. 515–518. ISSN: 0002-2667. DOI: 10.1108/AEAT-05-2014-0065.

[94] P. J. Masson, G. V. Brown, D. S. Soban, and C. A. Luongo. "HTS machines as enabling technology for all-electric airborne vehicles". In: *Superconductor Science and Technology, IOP Publishing* Vol. 20. No. 8 (June 2007), pp. 748–756. DOI: 10.1088/0953-2048/20/8/005.

[95] P. J. Masson, D. S. Soban, E. Upton, J. E. Pienkos, and C. A. Luongo. "HTS Motors in Aircraft Propulsion: Design Considerations". In: *IEEE Transactions on Appiled Superconductivity* Vol. 15. No. 2 (June 2005), pp. 2218–2221. ISSN: 1051-8223. DOI: 10.1109/TASC.2005.849616.

[96] S. Matlok. *Bidirectional full SiC 200 kW DC-DC Converter for Electric, Hybrid and Fuel Cell Vehicles*. Online; accessed Mar. 15, 2017. Fraunhofer Institute for Integrated Systems and Device Technology IISB. Erlangen, Germany, 2015. URL: http://www.mikroelektronik.fraunhofer.de/content/dam/mikroelektronik/Datenbltter/IISB_200kW-Rekordwandler_DB.pdf.

[97] McKinsey. *Politically desired number of electric cars in selected countries worldwide in 2020*. Originally published in WirtschaftsWoche, Feb. 2011, page 9. Online; accessed Mar. 24, 2016. Retrieved from Statista; URL: http://www.statista.com/statistics/271818/politically-desired-number-of-electric-cars-in-selected-countries/.

[98] B. C. Mecrow, A. G. Jack, D. J. Atkinson, and J. A. Haylock. "Fault Tolerant Drives for Safety Critical Applications". In: *IEEE Colloquium on New Topologies for Permanent Magnet Machines*. London, UK, June 1997, pp. 1–5. DOI: 10.1049/ic:19970522.

[99] Mercedes-AMG GmbH. *SLS AMG Coupé Electric Drive*. Online; accessed January 24, 2018. URL: http://www.mercedes-amg.com/webspecial/sls_e-drive/deu.php.

[100] W. Meyer. "Automatisierter Entwurf elektromechanischer Wandler". original language: German. Herbert Hieronymus, Druck und Verlag. PhD thesis. Munich, Germany: Technische Universität München, Mar. 2009. ISBN: 978-3-89791-406-3.

[101] A. Mitra and A. Emadi. "On the suitability of large switched reluctance machines for propulsion applications". In: *Transportation Electrification Conference and Expo (ITEC)*. Dearborn, MI, USA, June 2012, pp. 1–5. DOI: 10.1109/ITEC.2012.6243423.

[102] G. E. Mobus and M. C. Kalton. *Principles of Systems Science*. New York, NY, USA: Springer New York, 2015. ISBN: 978-1-4939-1919-2. DOI: 10.1007/978-1-4939-1920-8.

[103] A. Moiszi, M. Schugt, and M. Tybel. "Gap in the V-model of E-drives: Closed by Parameter Identification". In: *ATZ elektronik* No. 8 (May 2013), pp. 36–39.

[104] M. Molaei, H. Oraee, and M. Fotuhi-Firuzabad. "Markov Model of Drive-Motor Systems for Reliability Calculation". In: *IEEE International Symposium on Industrial Electronics*. Montréal, QC, Canada, July 2006, pp. 2286–2291. DOI: 10.1109/ISIE.2006.295929.

[105] G. Müller and B. Ponick. *Grundlagen elektrischer Maschinen*. 10., wesentlich überarb. u. erw. Auflage. Vol. 1. Elektrische Maschinen. Weinheim: Wiley-VCH, 2014. ISBN: 978-3527412051.

[106] G. Müller and B. Ponick. *Theorie elektrischer Maschinen*. 6., völlig neu bearb. Aufl. Vol. 3. Elektrische Maschinen. Weinheim: Wiley-VCH, 2009. ISBN: 978-3527405268.

[107] G. Müller, K. Vogt, and B. Ponick. *Berechnung elektrischer Maschinen*. 6., völlig neu bearb. Aufl., 1. Nachdr. Vol. 2. Elektrische Maschinen. Weinheim: Wiley-VCH, 2011. ISBN: 3-527-40525-9.

[108] G. Niemann and H. Winter. *Maschinenelemente: Band 2: Getriebe allgemein, Zahnradgetriebe – Grundlagen, Stirnradgetriebe*. 2nd ed. Vol. 2. Berlin, Heidelberg: Springer Berlin Heidelberg, 2003. ISBN: 978-3-662-11874-0. DOI: 10.1007/978-3-662-11873-3.

[109] Nikola Motor Company. *Nikola One*. Online; accessed May 16, 2017. URL: https://nikolamotor.com/one.

[110] NIO. *U.S. Electric Car in 2020*. Online; accessed May 16, 2017. URL: http://www.nio.io/news/nio-us-electric-car-2020.

[111] J. R. Norris. *Markov chains*. 1st pbk. ed. Cambridge series on statistical and probabilistic mathematics. Cambridge, UK and New York, NY, USA: Cambridge University Press, 1998. ISBN: 978-0-521-63396-3.

[112] G. J. Offer, D. Howey, M. Contestabile, R. Clague, and N. P. Brandon. "Comparative analysis of battery electric, hydrogen fuel cell and hybrid vehicles in a future sustainable road transport system". In: *Energy Policy* Vol. 38. No. 1 (2010), pp. 24–29. ISSN: 0301-4215. DOI: 10.1016/j.enpol.2009.08.040.

[113] G. Patzak. *Systemtechnik – Planung komplexer innovativer Systeme*. Berlin, Heidelberg: Springer Berlin Heidelberg, 1982. ISBN: 978-3-540-11783-4. DOI: 10.1007/978-3-642-81893-6.

[114] B. Pauli. "Interactions between Reliability, Safety and Security". In: *ATZ worldwide* Vol. 119. No. 12 (Dec. 2017), pp. 44–47. ISSN: 2192-9076. DOI: 10.1007/s38311-017-0152-7.

[115] B. Pichlmaier, W. Breu, and A. Szajek. "Elektrifizierung bei Traktoren [Electrification of Tractors]". In: *ATZ offhighway* (Apr. 2014), pp. 78–88.

[116] V. I. Polonskiy. *Grebnie elektricheskie ustanovki [Ships electric propulsion systems]*. original language: Russian. Leningrad, Russia: Maritime Transport, 1958.

[117] R. Poore and T. Lettenmaier. *Alternative Design Study Report: WindPACT Advanced Wind Turbine Drive Train Designs Study: Heller-De Julio Generator Comparison (Appendix L)*. pp. 503–540. Kirkland, Washington, USA, Aug. 2003.

[118] U. Probst. *Leistungselektronik für Bachelors: Grundlagen und praktische Anwendungen*. 2., aktualisierte und erw. Aufl. Munich, Germany: Hanser, 2011. ISBN: 978-3-446-42876-8.

[119] J. Pyrhönen, T. Jokinen, and V. Hrabovcová. *Design of rotating electrical machines*. Second edition. Chichester, West Sussex, UK: Wiley, 2014. ISBN: 978-1-118-58157-5.

[120] R. Radebaugh. "Cryocoolers for aircraft superconducting generators and motors". In: *ADVANCES IN CRYOGENIC ENGINEERING: Transactions of the Cryogenic Engineering Conference (CEC)*. Vol. 57. AIP Conference Proceedings. Spokane, Washington, USA: AIP, 2012, pp. 171–182. DOI: 10.1063/1.4706918.

[121] A. Rambetius. *Lagegeberlose Regelung der elektrisch erregten Synchronmaschine für den Einsatz in Elektrofahrzeugen*. Elektrotechnik. München: Verlag Dr. Hut, 2016. ISBN: 978-3-8439-2484-9.

[122] K. Reichert, R. E. Neubauer, H. Reiche, and F. W. Berg. *Elektrische Antriebe energieoptimal auslegen und betreiben*. Impulsprogramm RAVEL. Bern, Switzerland: Eidg. Drucksachen- und Materialzentrale, Bern, 1993. ISBN: 3-905233-07-X.

[123] Ph. Reupold. "Lösungsraumanalyse für Hauptantriebsstränge in batterieelektrischen Straßenfahrzeugen [Solution space analysis of main propulsion systems within battery-electric road vehicles]". original language: German. PhD thesis. Munich, Germany: Technische Universität München, Dec. 2014. URL: http://nbn-resolving.de/urn/resolver.pl?urn:nbn:de:bvb:91-diss-20141203-1120693-0-3.

[124] W. Rippel. *Induction Versus DC Brushless Motors*. Online; accessed January 24, 2018. Jan. 2007. URL: http://www.teslamotors.com/blog/induction-versus-dc-brushless-motors.

[125] G. Rittmann. *Der Umgang mit Komplexität: Soziologische, politische, ökonomische und ingenieurwissenschaftliche Vorgehensweisen in vergleichender systemtheoretischer Analyse*. 1. Aufl. Baden-Baden, Germany: Nomos, 2014. ISBN: 978-3-8487-0990-8. DOI: 10.5771/9783845251271.

[126] J. Rodriguez, J.-S. Lai, and F. Z. Peng. "Multilevel Inverters: A Survey of Topologies, Controls, and Applications". In: *IEEE Transactions on Industrial Electronics* Vol. 49. No. 4 (Aug. 2002), pp. 724–738. ISSN: 0278-0046. DOI: 10.1109/TIE.2002.801052.

[127] R. R. Rossberg. *Deutsche Eisenbahnfahrzeuge von 1838 Bis Heute*. Berlin, Heidelberg: Springer Berlin Heidelberg, 1988. ISBN: 978-3-642-95771-0. DOI: 10.1007/978-3-642-95770-3.

[128] K. Sato, M. Yoshizawa, and T. Fukushima. "Traction systems using power electronics for Shinkansen High-speed Electric Multiple Units". In: *The 2010 International Power Electronics Conference (IPEC)*. Sapporo, Japan: IEEE, June 2010, pp. 2859–2866. ISBN: 978-1-4244-5394-8. DOI: 10.1109/IPEC.2010.5542320.

[129] R. Schiferl, A. Flory, W. C. Livoti, and S. D. Umans. "High-Temperature Superconducting Synchronous Motors: Economic Issues for Industrial Applications". In: *IEEE Transactions on Industry Applications* Vol. 44. No. 5 (Sept. 2008), pp. 1376–1384. ISSN: 00939994. DOI: 10.1109/TIA.2008.2002219.

[130] M. Schneider-Landolf, J. Spielmann, and W. Zitterbarth, eds. *Handbook of Theme-Centered Interaction (TCI)*. Göttingen: Vandenhoeck & Ruprecht, 2017. ISBN: 978-3-525-45190-8.

[131] *Scientific American Supplement, Vol. XIV, No. 362, December 9, 1882*. Online; accessed Dec. 27, 2016. New York, NY, USA: MUNN & CO. URL: http://www.gutenberg.org/dirs/8/6/8/8687/8687-h/8687-h.htm.

[132] E. Semail. *ENTRAINEMENTS ELECTRIQUES POLYPHASES : VERS UNE APPROCHE SYSTEME [Multiphase drives: towards a system approach]*. original language: French. Online; accessed Aug. 28, 2018. Energie électrique. Université des Sciences et Technologie de Lille – Lille I. Lille, France, 2009. URL: https://tel.archives-ouvertes.fr/tel-00420019/document.

[133] E. Semail, X. Kestelyn, and F. Locment. "Fault tolerant multiphase electrical drives: The impact of design". In: *The European Physical Journal Applied Physics* Vol. 43. No. 2 (Feb. 2008), pp. 159–163. ISSN: 1286-0042. DOI: 10.1051/epjap:2008057.

[134] Siemens AG. *Electric Mobility: Drive System for the World's Largest Dump Truck*. Online; accessed May 16, 2017. URL: https://www.siemens.com/innovation/en/home/pictures-of-the-future/mobility-and-motors/electric-mobility-world-s-largest-dump-truck.html.

[135] Siemens AG. *Electromobility: Setting a Course for Carbon-Free Shipping*. Online; accessed May 12, 2017. URL: https://www.siemens.com/innovation/en/home/pictures-of-the-future/mobility-and-motors/electromobility-electric-ferries.html.

[136] Skeleton Technologies GmbH. *SkelCap Industrial Cells: Data Sheet*. Online; accessed January 19, 2018. URL: https://www.skeletontech.com/industrial-cells.

[137] D. V. Spyropoulos and E. D. Mitronikas. "A Review on the Faults of Electric Machines Used in Electric Ships". In: *Advances in Power Electronics* Vol. 2013. No. 5 (Feb. 2013), pp. 1–8. ISSN: 2090-181X. DOI: 10.1155/2013/216870.

[138] D. W. Stroock. *An Introduction to Markov Processes*. Second edition. Vol. 230. Berlin, Heidelberg, Germany: Springer Berlin Heidelberg, 2014. ISBN: 978-3-642-40522-8. DOI: 10.1007/978-3-642-40523-5.

[139] R. M. Sullivan, J. L. Palko, R. T. Tornabene, B. A. Bednarcyk, L. M. Powers, S. K. Mital, L. M. Smith, X.-Y. J. Wang, and J. E. Hunter. *Engineering Analysis Studies for Preliminary Design of Lightweight Cryogenic Hydrogen Tanks in UAV Applications*. NASA–2006-214094. Online; accessed Mar. 9, 2017. National Aeronautics and Space Administration (NASA). Cleveland, Ohio, USA, May 2006. URL: https://ntrs.nasa.gov/archive/nasa/casi.ntrs.nasa.gov/20060021606.pdf.

[140] P. J. Tavner. "Review of condition monitoring of rotating electrical machines". In: *IET Electric Power Applications* Vol. 2. No. 4 (June 2008), p. 215. ISSN: 17518660. DOI: 10.1049/iet-epa:20070280.

[141] A. B. Thanheiser. "Energetische Modellierung und Echtzeitsimulation von elektrischen Fahrzeugantrieben [Energetic Modeling and Real Time Simulation of Electric Vehicle Drives]". PhD thesis. Munich, Germany: Technische Universität München, Nov. 2015. URL: http://nbn-resolving.de/urn/resolver.pl?urn:nbn:de:bvb:91-diss-20151116-1129482-1-8.

[142] C. E. Thomas. "Fuel cell and battery electric vehicles compared". In: *International Journal of Hydrogen Energy* Vol. 34. No. 15 (2009), pp. 6005–6020. ISSN: 0360-3199. DOI: 10.1016/j.ijhydene.2009.06.003.

[143] P. Thounthong, S. Raël, and B. Davat. "Energy management of fuel cell / battery / supercapacitor hybrid power source for vehicle applications". In: *Journal of Power Sources* Vol. 193. No. 1 (Aug. 2009), pp. 376–385. ISSN: 0378-7753. DOI: 10.1016/j.jpowsour.2008.12.120.

[144] L. M. Tolbert, F. Z. Peng, and T. G. Habetler. "Multilevel converters for large electric drives". In: *IEEE Transactions on Industry Applications* Vol. 35. No. 1 (Feb. 1999), pp. 36–44. ISSN: 00939994. DOI: 10.1109/28.740843.

[145] H. Tschöke. *Die Elektrifizierung des Antriebsstrangs: Basiswissen [The electrification of drive trains: Basic knowledge]*. Springer Fachmedien Wiesbaden, 2015. ISBN: 978-3-658-04643-9. DOI: 10.1007/978-3-658-04644-6.

[146] Volkswagen UK. *Electric Motor – The electric motor in the e-up!* Online; accessed January 24, 2018. URL: http://www.volkswagen.co.uk/technology/electric-technology/electric-motor.

[147] G. Vallée, K. Charoenpornwattana, C. Engelmann, A. Tikotekar, C. Leangsuksun, T. Naughton, and S. L. Scott. "A Framework for Proactive Fault Tolerance". In: *Third International Conference on Availability, Reliability and Security*. Barcelona, Spain, Mar. 2008, pp. 659–664. DOI: 10.1109/ARES.2008.171.

[148] Verein Deutscher Ingenieure. *VDI 2206 - Entwicklungsmethodik für mechatronische Systeme [Design methodology for mechatronic systems]*. Berlin, June 2004.

[149] F. Vester. *Die Kunst vernetzt zu Denken: Ideen und Werkzeuge für einen neuen Umgang mit Komplexität [The Art of Interconnected Thinking. Ideas and Tools for a New Approach to Tackling Complexity]*. 9th ed. Munich, Germany: Deutscher Taschenbuchverlag GmbH & Co. KG, 2012. ISBN: 978-3-423-33077-0.

[150] C.-H. Vigouroux. "Actualisation des connaissances sur les moteurs électriques". In: *Bulletin de l'Union des Physiciens* No. 96 (July 2002). Online; accessed Aug. 10, 2018, pp. 1241–1253. URL: https://ecitydoc.com/download/actualisation-des-connaissances-sur-les-moteurs-electriques_pdf.

[151] M. Villani, F. Parasiliti, M. Tursini, G. Fabri, and L. Castellini. "PM brushless motors comparison for a Fenestron®type helicopter tail rotor". In: *23rd International Symposium on power electronics, electrical drives, automation and motion (speedam)*. Anacapri, Italy, June 2016, pp. 22–27. DOI: 10.1109/SPEEDAM.2016.7525942.

[152] M. Villani, M. Tursini, G. Fabri, and L. Castellini. "Multi-phase permanent magnet motor drives for fault-tolerant applications". In: *IEEE International Electric Machines & Drives Conference (IEMDC)*. Niagara Falls, ON, Canada, May 2011, pp. 1351–1356. ISBN: 978-1-4577-0060-6. DOI: 10.1109/IEMDC.2011.5994802.

[153] E. H. Wakefield. *History of the electric automobile: battery-only powered cars*. Warrendale, PA, USA: Society of Automotive Engineers, Inc., 1994. ISBN: 1-56091-299-5.

[154] K.-H. Waldmann and U. M. Stocker. *Stochastische Modelle: Eine anwendungsorientierte Einführung*. Berlin, Heidelberg, Germany: Springer Berlin Heidelberg, 2004. ISBN: 978-3-540-03241-0. DOI: 10.1007/978-3-642-17058-4.

[155] H. Wang, F. Blaabjerg, K. Ma, and R. Wu. "Design for reliability in power electronics in renewable energy systems – status and future". In: *4th International Conference on Power Engineering, Energy and Electrical Drives (POWERENG)*. Istanbul, Turkey, May 2013, pp. 1846–1851. DOI: 10.1109/PowerEng.2013.6889108.

[156] H. Wang, K. Ma, and F. Blaabjerg. "Design for reliability of power electronic systems". In: *38th Annual Conference of IEEE Industrial Electronics (IECON)*. Montréal, QC, Canada, Oct. 2012, pp. 33–44. DOI: 10.1109/IECON.2012.6388833.

[157] W. Wang and B. Fahimi. "Comparative study of electric drives for EV/HEV propulsion system". In: *International Conference on Electrical Systems for Aircraft, Railway and Ship Propulsion (ESARS)*. Bologna, Italy, Oct. 2012, pp. 1–6. DOI: 10.1109/ESARS.2012.6387497.

[158] B. A. Welchko, T. A. Lipo, T. M. Jahns, and S. E. Schulz. "Fault Tolerant Three-Phase AC Motor Drive Topologies: A Comparison of Features, Cost, and Limitations". In: *IEEE Transactions on Power Electronics* Vol. 19. No. 4 (July 2004), pp. 1108–1116. ISSN: 0885-8993. DOI: 10.1109/TPEL.2004.830074.

[159] P. Wikstrom, L. A. Terens, and H. Kobi. "Reliability, availability, and maintainability of high-power variable-speed drive systems". In: *IEEE Transactions on Industry Applications* Vol. 36. No. 1 (2000), pp. 231–241. ISSN: 00939994. DOI: 10.1109/28.821821.

[160] S. Willerich and H.-G. Herzog. "Prediction of the magnetic field in the air-gap of synchronous machines on a preliminary design level — Machine modelling and field calculation". In: *IEEE International Electric Machines & Drives Conference (IEMDC)*. Coeur d'Alene, ID, USA, May 2015, pp. 1292–1298. ISBN: 978-1-4799-7941-7. DOI: 10.1109/IEMDC.2015.7409228.

[161] S. Williamson and S. Smith. "Pulsating torque and losses in multiphase induction machines". In: *IEEE Transactions on Industry Applications* Vol. 39. No. 4 (July 2003), pp. 986–993. ISSN: 00939994. DOI: 10.1109/TIA.2003.813722.

[162] Y. Wu, J. Kang, Y. Zhang, S. Jing, and D. Hu. "Study of reliability and accelerated life test of electric drive system". In: *6th International Power Electronics and Motion Control Conference (IPEMC)*. Wuhan, China, May 2009, pp. 1060–1064. DOI: 10.1109/IPEMC.2009.5157542.

[163] G. G. Yin and Q. Zhang. *Continuous-Time Markov Chains and Applications*. Second edition. Vol. 37. New York, NY, USA: Springer New York, 2013. ISBN: 978-1-4614-4345-2. DOI: 10.1007/978-1-4614-4346-9.

[164] T. Yoshida and K. Kojima. "Toyota MIRAI Fuel Cell Vehicle and Progress Toward a Future Hydrogen Society". In: *The Electrochemical Society Interface, Summer 2015* Vol. 24. No. 2 (2015), pp. 45–49. ISSN: 1064-8208. DOI: 10.1149/2.F03152if.

[165] S. S. H. Zaidi, W. G. Zanardelli, S. Aviyente, and E. G. Strangas. "Prognosis of electrical faults in permanent magnet AC machines using the hidden Markov model". In: *36th Annual Conference of IEEE Industrial Electronics (IECON)*. Glendale, AZ, USA, Nov. 2010, pp. 2634–2640. DOI: 10.1109/IECON.2010.5675138.

[166] Zentrum für Sonnenenergie- und Wasserstoff-Forschung Baden-Württemberg (ZSW). *Zahl der Elektroautos weltweit auf 1,3 Millionen gestiegen*. Online; accessed Mar. 24, 2016. URL: http://www.zsw-bw.de/infoportal/presseinformationen/presse-detail/zahl-der-elektroautos-weltweit-auf-13-millionen-gestiegen.html.

[167] M. Zeraoulia, M. E. H. Benbouzid, and D. Diallo. "Electric Motor Drive Selection Issues for HEV Propulsion Systems: A Comparative Study". In: *IEEE Transactions on Vehicular Technology* Vol. 55. No. 6 (Nov. 2006), pp. 1756–1764. ISSN: 0018-9545. DOI: 10.1109/TVT.2006.878719.

[168] H. Zhao and A. F. Burke. "Fuel Cell Powered Vehicles Using Supercapacitors-Device Characteristics, Control Strategies, and Simulation Results". In: *Fuel Cells* Vol. 10. No. 5 (May 2010), pp. 879–896. ISSN: 16156846. DOI: 10.1002/fuce.200900214.

Own Publications

[P1] I. Bolvashenkov, J. Kammermann, Q. Buchner, and H.-G. Herzog. "A Traction Drive of an Electrical Helicopter Based on Fuel Cells and Superconducting Electrical Machines: Preliminary Assessment of Feasibility". In: *The 7th International Energy Conference & Workshop – REMOO*. Venice, Italy, May 2017, pp. 01.055.1–01.055.11. ISBN: 978-3-9818275-5-2.

[P2] I. Bolvashenkov, J. Kammermann, Q. Buchner, and H.-G. Herzog. "A Traction Drive of an Electrical Helicopter based on Fuel Cells and Superconducting Electrical Machines: Preliminary Assessment of Feasibility". In: *International Journal of Contemporary ENERGY* Vol. 3. No. 2 (2017), pp. 80–87. DOI: 10.14621/ce.20170209. URL: http://contemporary-energy.net/Articles/v03n02a09-Igor-Bolvashenkov.pdf.

[P3] I. Bolvashenkov, J. Kammermann, and H.-G. Herzog. "Methodology for Determining the Transition Probabilities for Multi-State System Markov Models of Fault Tolerant Electric Vehicles". In: *Asian Conference on Energy, Power and Transportation Electrification (ACEPT)*. Singapore, Republic of Singapore, Oct. 2016, pp. 1–6. DOI: 10.1109/ACEPT.2016.7811537.

[P4] I. Bolvashenkov, J. Kammermann, and H.-G. Herzog. "Methodology for Selecting Electric Traction Motors and its Application to Vehicle Propulsion Systems". In: *23rd International Symposium on power electronics, electrical drives, automation and motion (speedam)*. Anacapri, Italy, June 2016, pp. 1214–1219. DOI: 10.1109/SPEEDAM.2016.7525853.

[P5] I. Bolvashenkov, J. Kammermann, and H.-G. Herzog. "Reliability assessment of a fault tolerant propulsion system for an electrical helicopter". In: *Twelfth International Conference on Ecological Vehicles and Renewable Energies (EVER)*. Monte Carlo, Monaco, Apr. 2017, pp. 1–6. DOI: 10.1109/EVER.2017.7935864.

[P6] I. Bolvashenkov, J. Kammermann, and H.-G. Herzog. "Research on Reliability and Fault Tolerance of Traction Multi-Phase Permanent Magnet Synchronous Motors Based on Markov Models for Multi-State Systems". In: *23rd International Symposium on power electronics, electrical drives, automation and motion (speedam)*. Anacapri, Italy, June 2016, pp. 1166–1171. DOI: 10.1109/SPEEDAM.2016.7525928.

[P7] I. Bolvashenkov, J. Kammermann, H.-G. Herzog, and I. Frenkel. "Comparison of the battery energy storage and fuel cell energy source for the safety-critical drives considering reliability and fault tolerance". In: *International Conference on Information and Digital Technologies (IDT)*. Zilina, Slovakia, July 2017, pp. 66–73. DOI: 10.1109/DT.2017.8024274.

[P8] I. Bolvashenkov, J. Kammermann, T. Lahlou, and H.-G. Herzog. "Comparison and Choice of a Fault Tolerant Inverter Topology for the Traction Drive of an Electrical Helicopter". In: *4th International Conference on Electrical Systems for Aircraft, Railway, Ship Propulsion, and Road Vehicles & International Transportation Electrification Conference (ESARS-ITEC)*. Toulouse, France, Nov. 2016, pp. 1–6. DOI: 10.1109/ESARS-ITEC.2016.7841328.

[P9] I. Bolvashenkov, J. Kammermann, T. Lahlou, and H.-G. Herzog. "Fault Tolerant Inverter Topology for the Sustainable Drive of an Electrical Helicopter". In: *Advances in Science, Technology and Engineering Systems Journal (ASTES)* Vol. 2. No. 3 (2017), pp. 401–411. DOI: 10.25046/aj020352. URL: http://astesj.com/v02/i03/p52/.

[P10] I. Bolvashenkov, J. Kammermann, S. Willerich, and H.-G. Herzog. "Comparative Study for the Optimal Choice of Electric Traction Motors for a Helicopter Drive Train". In: *10th Conference on Sustainable Development of Energy, Water and Environment Systems (SDEWES)*. Dubrovnik, Croatia, Sept. 2015.

[P11] I. Bolvashenkov, J. Kammermann, S. Willerich, and H.-G. Herzog. "Comparative Study of Reliability and Fault Tolerance of Multi-Phase Permanent Magnet Synchronous Motors for Safety-Critical Drive Trains". In: *International Conference on Renewable Energies and Power Quality (ICREPQ)*. Madrid, Spain, May 2016, p. 248. ISBN: 978-84-608-5473-9.

[P12] J. Kammermann, C. Bertram, S. Flügel, Q. Hecker, W. Meyer, and H.-G. Herzog. "Software Based Interaction of Multiple Domains for the Design of Electrical Machines". In: *17th International Conference on Electrical Machines and Systems (ICEMS)*. Hangzhou, China, Oct. 2014, pp. 624–629. DOI: 10.1109/ICEMS.2014.7013562.

[P13] J. Kammermann, I. Bolvashenkov, and H.-G. Herzog. "Approach for Comparative Analysis of Electric Traction Machines". In: *3rd International Conference on Electrical Systems for Aircraft, Railway, Ship Propulsion, and Road Vehicles (ESARS)*. Aachen, Germany, Mar. 2015, pp. 1–5. DOI: 10.1109/ESARS.2015.7101459.

[P14] J. Kammermann, I. Bolvashenkov, and H.-G. Herzog. "Improvement of Reliability and Fault Tolerance of Traction Drives by Means of Multiphase Actuators". In: *Drive Systems 2017; 7th VDE/VDI Symposium*. Karlsruhe, Germany, Nov. 2017, pp. 83–88. ISBN: 978-3-8007-4467-1.

[P15] J. Kammermann, I. Bolvashenkov, S. Schwimmbeck, and H.-G. Herzog. "Reliability of induction machines: Statistics, tendencies, and perspectives". In: *26th International Symposium on Industrial Electronics (ISIE)*. Edinburgh, United Kingdom, June 2017, pp. 1843–1847. DOI: 10.1109/ISIE.2017.8001529.

[P16] J. Kammermann, I. Bolvashenkov, S. Schwimmbeck, and H.-G. Herzog. "Techniques for Comparative Analysis and its Application to Electric Traction Machines". In: *The 19th International Conference on Electrical Machines and Systems (ICEMS)*. Chiba, Japan, Nov. 2016, pp. 1–5. ISBN: 978-4-88686-098-9.

[P17] J. Kammermann, R. Freiberger, D. Mahat, and H.-G. Herzog. "Assumptions for an Early Stage Comparative Analysis of Induction Machines and Permanent Magnet Synchronous Machines". In: *11th IEEE Vehicular Power and Propulsion Conference (VPPC)*. Montréal, QC, Canada, Oct. 2015, pp. 1–5. DOI: 10.1109/VPPC.2015.7352901.

Supervised Student Projects

[S1] M. Ambroselli. “Interdependence between the Power Electronic Driver and the Induction Machine Design for Optimized Volume and Efficiency”. Master’s Thesis. Technical University of Munich, University of Salerno, Mar. 2015.

[S2] Ph. August. “Simulation und Bewertung von Wechselrichtertopologien im Antriebsstrang hinsichtlich eines möglichen Fehlerfalles [Simulation and Review of Inverter Topologies in a Drive Train Regarding a Possible Failure]”. original language: German. Bachelor’s Thesis. Technical University of Munich, Mar. 2015.

[S3] M. Breiteneder. “Analyse des Wirkgefüges in elektrischen Antriebssträngen anhand des Vester’schen Sensitivitätsmodells [Analysis of interdependecies in electrical drive trains by means of Vester’s Sensitivity Model]”. original language: German. Seminar Report. Technical University of Munich, Sept. 2016.

[S4] M. Breiteneder. “Bewertung mehrphasiger Zwei-Level-Umrichter unterschiedlicher Topologien [Comparison of multiple phase two-level-inverter considering different topologies]”. original language: German. Bachelor’s Thesis. Technical University of Munich, Aug. 2015.

[S5] Q. Buchner. “Konzeptstudie eines elektrischen Antriebs mit Brennstoffzelle und supraleitender Maschine für einen Helikopter [Concept study of a propulsion system with a fuel cell and a superconducting machine for a helicopter]”. original language: German. Bachelor’s Thesis. Technical University of Munich, Aug. 2016.

[S6] C. Damhuis. “Antriebsstranganalyse eines elektrischen Helikopters hinsichtlich der Anzahl der Phasen [Drive train analysis of an electrical helicopter regarding the number of phases]”. original language: German. Bachelor’s Thesis. Technical University of Munich, Nov. 2016.

[S7] F. Fembacher. “Systembetrachtungen und deren Auswirkung auf die Auslegung eines elektrischen Antriebsstrangs [System Considerations and their Impact on the Design of Electrical Drive Trains]”. original language: German. Seminar Report. Technical University of Munich, Sept. 2016.

[S8] D. Filusch. “Überlastberechnung einer permanenterregten Synchronmaschine für den Einsatz in einem elektrischen Helikopter [Calculation of the overload capability of a permanently excited synrchonous machine to be applied in an electrical helicopter]”. original language: German. Master’s Thesis. Technical University of Munich, Oct. 2015.

[S9] D. Filusch. “Weichmagnetische Materialien in rotierenden Maschinen [Soft magnetic materials in rotating machines]”. original language: German. Seminar Report. Technical University of Munich, June 2014.

[S10] R. Freiberger. “Auslegung der elektrischen Antriebsmaschine eines "Battery Electric Vehicle" nach definierten Anforderungen [Design of an Electric Traction Machine of a Battery Electric Vehicle According to Defined Requirments]”. original language: German. Seminar Report. Technical University of Munich, Apr. 2017.

[S11] R. Freiberger. “Herleitung und Evaluierung des Drehmoment-Stromstärke-Verhaltens einer Asynchronmaschine auf Basis des Grundwellendrehmoments [Derivation and evaluation of torque-current-behavior of the induction machine based on the fundamental wave of torque]”. original language: German. Bachelor’s Thesis. Technical University of Munich, Apr. 2015.

[S12] J. Gerold. “Berechnungen zur analytischen Auslegung einer Transversalfluss Synchronmaschine [Analytical Design of Permanent Magnet Synchronous Machines with Transverse Flux Arrangement]”. original language: German. Bachelor’s Thesis. Technical University of Munich, July 2014.

[S13] K. V. Guðmundsson, L. Wang, and M. Dong. “Comparison of Electrical Machines”. Seminar Report. Technical University of Munich, Jan. 2014.

[S14] V. Kohli. “Superconducting Electrical Machines”. Seminar Report. Technical University of Munich, June 2014.

[S15] J. Lekuona. “Multiphase Machines and their Control in Healthy and Faulty Mode”. Seminar Report. Technical University of Munich, Aug. 2018.

[S16] D. Mahat. “Herleitung und Evaluierung des Drehmoment-Stromstärke-Verhaltens der Synchronmaschinen auf Basis des Grundwellendrehmoments [Derivation and evaluation of torque-current-behavior of the synchronous machines based on the fundamental wave of torque]”. original language: German. Bachelor’s Thesis. Technical University of Munich, Apr. 2015.

[S17] D. Rodríguez Arias. “Design of an Asynchronous Machine and Direct Torque Control Models using Simulink and xPC Target Tools”. Master’s Thesis. Technical University of Munich, Apr. 2013.

[S18] S. Roth. “Simulation elektrischer Maschinen zur Antriebsstrangbewertung hinsichtlich eines möglichen Fehlerfalles [Simulation of Electrical Machines for Drive Train Review Regarding a Possible Failure]”. original language: German. Bachelor’s Thesis. Technical University of Munich, Feb. 2015.

[S19] S. Schwimmbeck. “Elektrische Maschinen – Eine Übersicht der Entwicklung in Windenergieanlagen und im PKW [Electrical machines – An overview of the development in wind turbines and passenger cars]”. original language: German. Seminar Report. Technical University of Munich, Jan. 2016.

[S20] S. Schwimmbeck. “Modellbasierte Bewertung und Vergleich der Zuverlässigkeit von Asynchronmaschine und permanenterregter Synchronmaschine [Model-Based Grading and Comparison of the Synchronous Machine with Permanent Magnets and the Induction Machine Regarding Reliability]”. original language: German. Master’s Thesis. Technical University of Munich, Jan. 2016.

[S21] S. Schwimmbeck. “Topologievergleich von H-Brücke und 6-Puls-Brücke in spannungsgespeisten Wechselrichtern [Comparison of H-Bridge and Six-Pulse Bridge in a Voltage Source Converter]”. original language: German. Bachelor’s Thesis. Technical University of Munich, Sept. 2014.

[S22] S. Shaaban. “Systems Engineering and Product Development Methods”. Seminar Report. Technical University of Munich, July 2014.

[S23] L. Tippe. “Zwischenkreisauslegung in elektrischen Antriebssträngen [Intermediate Circuit Analysis for Electrical Drive Trains]”. original language: German. Bachelor’s Thesis. Technical University of Munich, Mar. 2015.

[S24] M. Tosi. “Rotary Transformer Design for Brushless Electrically Excited Synchronous Machines”. Master’s Thesis. Technical University of Munich, University of Padova, Feb. 2014.

[S25] M. Webersberger. “Entwurf einer rein elektrischen Steuerung für Helikopter am Beispiel des EC135 [Design of a purely electrical steering system for a helicopter through the example of the EC135]”. original language: German. Bachelor’s Thesis. Technical University of Munich, May 2015.

[S26] G. v. Zitzewitz. “Zuverlässigkeitsuntersuchung von permanenterregten Synchronmaschinen [Reliability analysis of permanent magnet synchronous machines]”. original language: German. Bachelor’s Thesis. Technical University of Munich, Mar. 2016.